Alma Mater Studiorum - Università di Bologna

DOTTORATO DI RICERCA IN

SCIENZE MEDICHE GENERALI E SCIENZE DEI SERVIZI

Ciclo 36

Settore Concorsuale: 05/G1 - FARMACOLOGIA, FARMACOLOGIA CLINICA E FARMACOGNOSIA

Settore Scientifico Disciplinare: BIO/14 - FARMACOLOGIA

CHARACTERIZING "EXPOSURE-PK/PD-BIOMARKER" RELATIONSHIPS IN PATIENTS WITH HEMATOLOGIC MALIGNANCIES

Presentata da: Chun Liu

Coordinatore Dottorato

Susi Pelotti

Supervisore

Federico Pea

Co-supervisore

Fabrizio De Ponti

Esame finale anno 2024

Alma Mater Studiorum - Università di Bologna

Department of Medical and Surgical Sciences
Ph.D Thesis
(01/11/2020 - 31/10/2023, 36th Cycle)

Characterizing "Exposure-PK/PD-Biomarker" Relationships in Patients with Hematologic Malignancies

Author: Chun Liu

Supervisor:
Prof. Federico Pea
federico.pea@unibo.it
University of Bologna, IT

Co-Supervisor:
Dr. Pier Giorgio Cojutti
piergiorgio.cojutti@unibo.it
University of Bologna, IT

TIPAT Coordinator & Co-Supervisor:
Dr. Coen van Hasselt
coen.vanhasselt@lacdr.leidenuniv.nl
Leiden University, NL

This Ph.D. research project is part of the European Commission-funded consortium Training for Innovative Personalized Antibiotic Therapies (TIPAT, www.tipat.eu) under the Marie Skłodowska-Curie grant agreement No. 861323.

Declaration and Authorization

I authorize the University of Bologna to lend this thesis to other institutions or individuals for the purpose of scholarly research. I further authorize the University of Bologna to reproduce the thesis by photocopying or by other means, in total or in part, at the request of other institutions or individuals for the purpose of scholarly research.

Chun Liu
January 25, 2024
Bologna, Italy

About This Thesis

Antimicrobial stewardship programs are gaining more and more relevance in optimizing anti-infective treatment and in preventing the emergence of antimicrobial resistance. Personalization of antimicrobial treatment based on real-time therapeutic drug morning (TDM) and dosing adaptation may represent an important tool in antimicrobial stewardship programs.

In this Ph.D project, we aim to focus on differences in pharmacokinetics (PK) for meropenem and piperacillin/tazobactam and host response biomarkers (e.g., C-reactive protein) in severe Gram-negative related infections occurring in oncohematologic patients. We are interested in identifying optimized model-based individualized dosing strategies for these antibiotics focusing on biomarkers-guided prediction of PK and pharmacodynamic (PD) parameters using population PK/PD modelling. We expect to identify optimal model-based dosing targets for these antibiotics for special populations for implementation in TDM routines, and mathematical models characterizing the relationship between biomarkers and outcomes in these populations.

Contents

List of Figures

List of Tables


NO THANKS.
I AM GOING TO GO GET SOME FRIES ON THE PIER, DO YOU JOIN ME?
I AM STRUGGLING WITH MANAGING INFECTIONS IN PATIENTS WITH HEMATOLOGIC MALIGNANCY.
WHAT HAPPENED?
THE EXPOSURE-RESPONSE RELATIONSHIP OF ANTIBIOTICS REMAINS UNCLEAR IN THIS POPULATION.
ALL ROADS LEAD TO ROME. MAYBE BIOMARKERS CAN HELP.
GOOD IDEA! I'M GONNA USE IT TO GET A PHD.
NOW DO YOU WANT TO GO GET SOME FRIES ON THE PIER?

Chapter 1

General Introduction and Research Scope

1.1 General Introduction

The cure of oncohematologic patients poses multifaceted challenges besides the malignancy itself, chief among them being the heightened susceptibility to post-treatment infections due to compromised immune systems[1]–[3]. Antibiotics have emerged as indispensable agents in this context, playing a pivotal role in safeguarding oncohematologic patients' well-being[4]. However, good anti-infection management remains tricky in this population. This thesis addresses the use of biomarkers and pharmacometric techniques for precision medicine in oncohematologic patients. We characterized the relationship between antibiotic exposure and its therapeutic outcomes via biomarkers and provided new insights into dose optimization in this special population.

1.1.1 Hematologic Malignancy and Anti-infection Management

Hematologic malignancies are defined as a highly heterogeneous set of blood and/or bone marrow diseases with noteworthy mortality. Approximately 1.2 million new cases, including but not limited to leukemia, lymphoma, and multiple myeloma, are reported each year worldwide. Over the past 40 years, therapies for hematologic malignancies have shown increased development. Combination chemotherapy was first established successfully at the beginning of the 1980s, followed by molecular targeted therapy 20 years later, and then with immunotherapy, e.g., Chimeric Antigen Receptor T Cell (CAR-T) therapy, currently[5]–[9]. Thanks to the development of therapeutic methods, the 5-year survival rates of some hematologic malignancies have increased to 80%[10]–[12]. These life-threatening diseases are no longer incurable.

Besides treatment approach, the survival rate of oncohematologic patients can be influenced by a variety of factors. One issue that deserves special attention is infection[13]–[17]. The hematologic malignancy itself, combined with treatment, alters the total number and/or composition of healthy immune cells and then impairs/disrupts the immune system[2]. These patients, with compromised immune systems, are particularly susceptible to acquiring healthcare-associated infections and experiencing infection transmission within hospital settings. Infectious complications contribute greatly to poor prognosis in oncohematologic patients by leading to persistent hyperthermia, sepsis/septic shock, multi-organ failure, and diffuse coagulation, especially those undergoing intensive chemotherapy or hematopoietic stem-cell transplantation[14], [15], [18]. Hence, good anti-infection management is crucial for targeting prevention and documented infection control.

Treatment of infection involves several key steps to ensure efficacy while avoiding adverse effects and antimicrobial resistance. Generally, there are rules/guidelines to follow. The first step is to identify pathogens by blood culture and sensitivity test, then appropriate antibiotics can be selected based on this fact and multiple patient-specific factors, for example, site/severity of infection, allergies,

organ function, age, weight or so[19]–[21]. The next consideration is to define the optimal treatment target. Probability of Target Attainment (PTA) is a crucial concept in antibiotic management to assess whether the antibiotic concentration is sufficient to effectively combat the pathogen. PTA considers both the pharmacokinetics/pharmacodynamics (PK/PD) properties of antibiotics, namely, how the patient handles antibiotics and how the antibiotic affects pathogens[22]. There are two different ways antibiotics exert their effects on pathogens: time-dependently and concentration-dependently. Time-dependent antibiotics, e.g., meropenem and piperacillin/tazobactam, work by continuously exposing the pathogen to a concentration that inhibits its growth for a period. The efficacy of this type of antibiotic can be predicted well by the fraction of time that antibiotic concentration maintains above the minimum inhibitory concentration (MIC) to a specific pathogen (%ft>MIC). As for concentration-dependent antibiotics, they work by killing the pathogen at a high concentration shortly after administration. The max concentration (C_{max}) or area under the curve (AUC) of the antibiotics are commonly used PK/PD indices, i.e., C_{max}/MIC and AUC/MIC. The specific PTA value is tailored to the unique circumstances of each clinical scenario. Generally, PTA>50-60% is considered sufficient to inhibit bacterial growth, while to achieve a bactericidal effect a higher PTA (e.g., >90%) is typically desired[22]–[24]. Joint use of the PK/PD indices mentioned above and therapeutic drug monitoring (TDM), especially for antibiotics with a narrow therapeutic window, allows real-time dose adjustment to maintain optimal therapeutic levels.

In some cases, empirical antibiotics can and should be started before identifying pathogens. For example, in patients with risk of life-threatening infections, or specific clinical scenarios like oncohematologic patients. Signs and symptoms of infection/inflammation are typically attenuated in oncohematologic patients. In a large number of cases, fever may be the only indication[25]. The Infection Disease Society of America, European Conference on Infections in Leukemia, and German Society of Hematology and Medical Oncology recommended therapy with a broad-spectrum anti-pseudomonal beta-lactam agent, e.g., piperacillin/tazobactam or meropenem as an escalation treatment, for high infection-risk patients as early as possible[4], [25], [26]. Other agents against Gram-positive pathogens, fungi, and viruses may be added if antimicrobial resistance is suspected or proven.

Unlike general populations, prescribing antibiotics in oncohematologic patients presents several challenges due to their unique characteristics. The rules we mentioned above cannot be applied here. Due to the urgency of treating/preventing infections, empirical therapy is often initiated before identifying a specific pathogen. Choosing the appropriate type of antibiotic while avoiding overdose/resistance is therefore a tough job due to the unavailability of MIC and pathogen features. Long treatment duration is another issue that deserves attention. It can increase the risk of adverse effects and contribute to resistance development when the dosing strategy is not adjusted in time.

Beyond the direct impact of hematologic malignancies on the hematopoietic system, these malignancies exert far-reaching effects on diverse aspects of patient physiology, for instance, PK features of drugs[27], [28]. The hypermetabolic state is a hematologic malignancy-induced phenomenon, it refers to an abnormal in-

crease in the body's metabolic rate. Disease-induced energy consumption elevation, cellular signal alteration, cachexia state, weight loss, etc. can change the metabolic procedure and disrupt organ function[29]. Meanwhile, these changes collectively influence antibiotics' absorption, distribution, metabolism, and excretion. For example, chronic inflammation, changes in plasma protein levels, and alterations in blood flow patterns significantly impact the distribution of antibiotics and then change the volume of distribution; renal impairment/augment can also lead to altered antibiotic clearance (CL). Recognizing/understanding the intricate interplay between hematologic malignancies and antibiotic PK is paramount for precision dosing and ultimately improving the survival rate.

1.1.2 The Role of Biomarkers in Oncohematologic Patients

Biomarkers play a crucial role in infection management by providing objective evidence of the body's response to antibiotic treatment. They can be detected before clinical symptoms become apparent and quantitatively reflect the body's inflammatory state. Elevated biomarker levels can support the decision of early antibiotic therapy initiation and antibiotic regimen adjustment. It can also assist in tailoring precision antibiotic therapy to a specific patient[30]. Appropriate antibiotic class, dose regimen, and length of treatment can be decided based on biomarkers, especially when clinical information is unavailable or good antibiotic exposure-response relationships cannot be guaranteed[30]–[33].

C-reactive protein (C-RP) is a commonly used biomarker in oncohematologic patients. It is synthesized by liver during the acute phase of inflammation, meaning its level increases rapidly in response to inflammatory conditions within a few hours therefore making it an early indicator of the inflammation process[34]–[36]. C-RP can be elevated in various conditions of inflammation, including bacterial infection-, surgery-, tissue injury-, and certain cancer-induced inflammation[35], [37]. Despite the less specificity to infection, C-RP is broadly used as an infection biomarker in clinical practice due to its rapid response advantage. As we have mentioned in the previous section, oncohematologic patients have a high susceptibility to infection whereas their infection symptoms/signs are typically attenuated, which challenges early diagnosis and good anti-infection management. In this circumstance C-RP is still sensitive to suggesting the presence of potential infectious processes, which is particularly important in this population.

In patients undergoing anti-infection treatment, C-RP can be monitored to support decision-making, e.g., post-surgery levels of C-RP have demonstrated the ability to forecast the risk of developing sepsis within a short time period in order to initiate antibiotics in time[38]. Meanwhile, it is also a good tool to assess the response to therapy. Decreasing C-RP level may indicate a positive response to treatment, while persistently elevated levels may raise concern for treatment failure or the presence of an ongoing infection. Both the absolute value and dynamic of C-RP can support clinical decision-making of antibiotic treatment[30]. For example, a study done in patients undergoing non-emergency abdominal surgery reported that those having C-RP>250mg/mL had less probability of success in anti-

infection treatment at 10 days compared with those having C-RP<250mg/mL[39]. Another study presented that the C-RP decline rate during the 5 days in the Intensive Care Unit is markedly associated with Community-Acquired Sepsis prognosis[40].

A noteworthy fact is that while C-RP is a valuable diagnosis tool in oncohematologic patients, the use of it remains controversial. Some studies reported that C-RP performs not superior to other biomarkers in reflecting infection[41], [42]. Besides, interpreting the C-RP level in oncohematologic patients is also an unclear task. Normal baseline C-RP levels in healthy individuals are quite scarce, however, it can vary depending on age, sex or so. A slightly elevated C-RP can be observed in oncohematologic patients due to disease-induced inflammation. Interpretation of C-RP levels should therefore be done case by case prudently. After initiating antibiotic treatment for a suspected infection, monitoring C-RP levels can help assess the patient's response. Currently, relying solely on C-RP maybe not be sufficient, a comprehensive assessment of patients is still recommended for accurate diagnosis. In this study, we aim to figure out how to use C-RP to warrant good anti-infective management in oncohematologic patients.

1.1.3 Individualized Dosing Strategy: Model-Informed Precision Dosing

Model-informed precision dosing (MIPD) represents a cutting-edge approach to therapeutic drug management. Rooted in pharmacometrics/mathematical models, MIPD combines PK/PD principles with patients-specific features, e.g., real-time monitored drug concentrations/biomarkers and demographics, to guide dosing regimens optimization[43], [44]. Over the past decade, the MIPD approach has been broadly adopted at the point of care to complement traditional TDM by providing model-based predictions of drug concentrations at various time points and populations. This enhances the TDM and enables pharmacists/clinicians to anticipate future dosing needs and then make proactive adjustments.

In the previous section, we discussed the significant antibiotic PK/PD variability in oncohematologic patients[27], [28]. Hematologic malignancy type, concomitant medications, organ dysfunction, and genetic polymorphisms cause difficulties in antibiotic management. MIPD acknowledges this heterogeneity and provides a framework for individualized dosing regimens accordingly. Complexity in empirical antibiotic prescription is another critical consideration of using MIPD in oncohematologic patients. Due to the frequent absence of detailed pathogen information, empirical antibiotic treatment is common in this population. MIPD overcomes this limitation by utilizing pharmacometrics and/or mathematical models that integrate patient-specific data to guide decision-making.

The application of MIPD in supporting antibiotic use in oncohematologic patients represents a pivotal advancement in therapeutic drug management[45], [46]. By counting patient-specific, drug-specific, and treatment-related factors, MIPD offers a refined approach to optimize anti-infection treatment strategies. This not

only enhances the antibiotic efficacy but also safeguards against potential adverse effects, ultimately improving the overall quality of anti-infection care for oncohematologic patients.

1.1.4 Machine Learning Techniques in Supporting Precision Dosing

In the previous sections, we have discussed the role of biomarkers and pharmacometrics models in improving precision medicine from a population perspective. However, tailoring antibiotic treatment to individual patients can still be a complex task. The emergence of machine learning (ML) offers a promising avenue to revolutionize this situation, providing a data-driven approach to tailor dosing regimens to individual patients.

ML is a subset of artificial intelligence that focuses on enabling computer systems to learn from large datasets and then make predictions without being explicitly programmed for each task. The mathematical algorithm enables the machine to identify dataset patterns and/or relationships[47], [48]. In the training stage, the machine is exposed to labeled data, meaning that ideal answers have been provided. Then a trained model is outputted from the training data. This model generalizes the pattern from the training data to make accurate predictions on new instances. The predictions themselves can be used as feedback to refine the model further. In the aspect of anti-infection management, ML can be integrated into TDM software to improve personalized dosage plans[49]–[52]. It helps select the most appropriate PK models of antibiotics used for prediction and provides real-time assessment of antibiotic concentrations and/or biomarkers. In other words, the learning algorithms can be trained by a vast dataset encompassing patient features, e.g., demographics, PK, laboratory measurements, TDM concentration, and infected pathogens, and then generate personalized dosing strategies with reference to those individual-specific features.

While ML holds great promise in enhancing precision dosing, it is important to acknowledge its limitations. First and foremost, ML models heavily rely on the size and quality of the training dataset. Whereas real-world clinical data is usually biased with unexpected noise, which can lead to an inaccurate model[53], [54]. Second, ML models are built in a highly data-driven pattern. It cannot handle sophisticated physiological interactions that may impact antibiotic response[55]. Over or under fitting is also a consideration. It usually occurs when the data size and model complexity do not match, especially in the early stages of model building. Besides, ML models can struggle to accurately capture/predict rare events, for example, outlier drug concentrations and rare adverse events. Understanding these limitations is crucial for implementing/improving ML models.

Despite the immaturity of this approach, ML still represents a significant advancement in the field of individualized precision medicine. By combining the power of ML with TDM software and clinical expertise, pharmacists/clinicians can optimize antibiotic dose regimens for individual patients, leading to an optimal outcome.

1.2 Research Scope

This multifaceted research encompasses a comprehensive approach to precision antibiotic dosing in oncohematologic patients. The study unfolds in three distinct but interconnected parts, each designed to address specific challenges encountered in antibiotic therapy within this patient population (Figure 1.1). Part I (chapter 2) provides crucial insights into the impact of CAR-T therapy on absolute biomarkers levels and antibiotics CL, facilitating refined anti-infection management strategies for this population. Part II (chapter 3) establishes a quantitative framework through (A) pharmacometrics and (B) mathematical modeling, unraveling the intricate interplay between meropenem exposure, C-RP dynamics, and therapeutic outcomes. Lastly, part III (chapter 4) introduces an innovative approach utilizing ML to recommend precise vancomycin dose regimens, particularly in scenarios where conventional PK models encounter challenges.

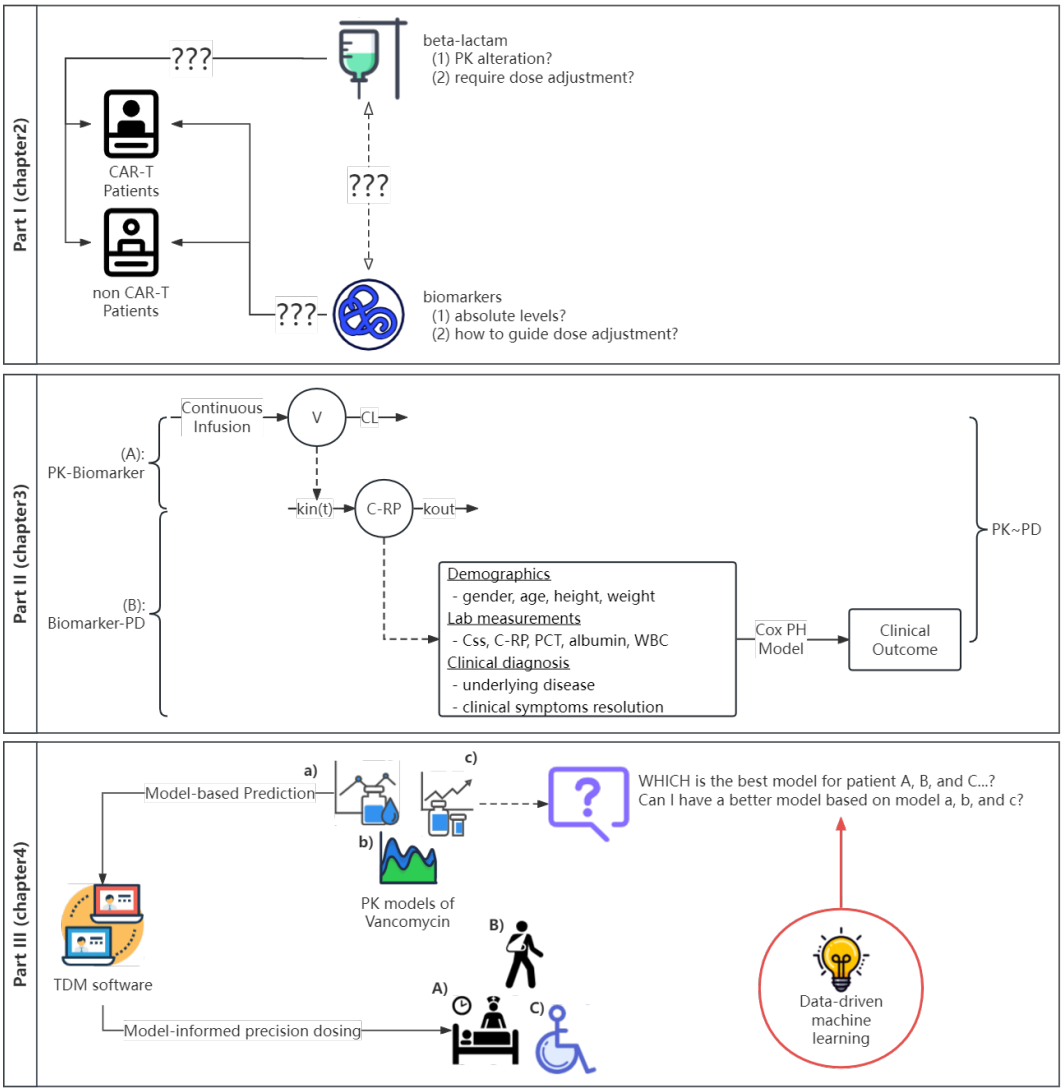

Figure 1.1: Overview of research scope.

1.2.1 Chapter 2: Does CAR-T Cell Treatment Have an Impact on The Pharmacokinetics of Meropenem and Piperacillin/Tazobactam in Oncohematologic Patients? Findings From an Observational Case-Control Study

In this chapter, our exploration seeks to discern whether adjustments in beta-lactam dosing strategies are warranted for patients undergoing CAR-T therapy by patient- and drug-specific biomarkers/features.

CAR-T immunotherapy is a novel targeted therapy for hematologic malignancies. Treatment-related cytokine storms may significantly alter the PK of beta-lactams which are the mainstay of treatment in febrile neutropenic CAR-T patients. This study embarks on a comparative analysis, meticulously examining the biomarker profiles and beta-lactam CL between patients receiving CAR-T therapy and their counterparts with general treatment conditions. Our aim was to explore the PK changes of beta-lactams in relation to cytokine burden trends in CAR-T patients.

1.2.2 Chapter 3: The Role of Pharmacometrics/Mathematical Models in Precision Dosing

This chapter focuses on unraveling the "exposure-PK/PD-response" relationships of meropenem via C-RP as a biomarker, in order to forecast/enhance therapeutic outcomes of anti-infection treatment. Overall, this research offers a crucial framework for optimizing antibiotic therapy in the context of microbiological data absence.

In the absence of microbiological data, which is commonplace in empirical antibiotic treatment for oncohematologic patients, establishing a direct antibiotic exposure-response relationship can be a formidable challenge. This study comprehensively characterizes the relationship between meropenem and its clinical outcomes via biomarkers. In the first part, we clarified the efficacy of meropenem on the C-RP trend quantitively by means of a population PK/PD model. In the second part, C-RP and other possible biomarkers/features were implemented into a Cox proportional hazard model for predicting the therapeutic outcomes of meropenem and piperacillin/tazobactam.

1.2.2.1 Part A - Population Pharmacokinetics/Pharmacodynamics of Meropenem and C-Reactive Protein in Oncohematologic Patients

Oncohematologic patients with febrile neutropenia (FN) are at high risk of developing severe infections due to multidrug-resistant Gram-negative pathogens. Meropenem is a beta-lactam commonly used as a second-line antimicrobial for patients not responding to piperacillin/tazobactam. Although the use of 24h-continuous infusion (CI) administration coupled with TDM may optimize the ex-

posure of meropenem, patient's response to therapy is still difficult to predict, and the identification of clinical biomarkers of response may be highly beneficial. The aim of this study is to assess the PK/PD relationship between 24h-CI meropenem and C-RP in a cohort of oncohematologic patients with FN.

1.2.2.2 Part B - C-Reactive Protein as Predictor for Outcomes Of Beta-Lactam Therapies in Oncohematologic Patients

Oncohematologic patients are recognized for the high risk of developing the life-threatening infections. However, the difficulty in establishing good "exposure-response" relationships of beta-lactam due to undetectable pathogens remains a big challenge to good infection management in this population. This study explored the role of biomarkers, e.g., C-RP dynamic, in predicting antibiotic therapeutic outcomes in oncohematologic patients.

1.2.3 Chapter 4: Data-Driven Model Selection for Model-Informed Precision Dosing: A Machine Learning Case Study Of Vancomycin

This chapter endeavors to harness the power of ML to suggest tailored vancomycin dose regimens, particularly in instances where conventional PK models may face limitations.

A validated and reliable PK model serves as a cornerstone in TDM software for guiding antibiotic dosing decisions. However, instances arise where conventional models prove inadequate/inappropriate to a specific population/person. By employing an ML model trained on vancomycin TDM data from us hospitals that use TDM software (Insight Rx®, San Francisco, California, US) for dosing optimization, this section aims to figure out the appropriate PK model or, alternatively, perform model averaging for individual optimal dose recommendations.

Bibliography

[1] E. J. Ariza-Heredia and R. F. Chemaly, "Infection Control Practices in Patients With Hematological Malignancies and Multidrug-Resistant Organisms: Special Considerations and Challenges," Clinical Lymphoma Myeloma and Leukemia, vol. 14, pp. S104–S110, Sep. 2014, doi: 10.1016/j.clml.2014.06.021.

[2] A. J. Barrett and B. N. Savani, "Does chemotherapy modify the immune surveillance of hematological malignancies?," Leukemia, vol. 23, no. 1, pp. 53–58, Jan. 2009, doi: 10.1038/leu.2008.273.

[3] P. Tatarelli and M. Mikulska, "Multidrug-resistant bacteria in hematology patients: emerging threats," Future Microbiol, vol. 11, pp. 767–780, Jun. 2016, doi: 10.2217/fmb-2015-0014.

[4] A. G. Freifeld et al., "Clinical Practice Guideline for the Use of Antimicrobial Agents in Neutropenic Patients with Cancer: 2010 Update by the Infectious Diseases Society of America," Clinical Infectious Diseases, vol. 52, no. 4, pp. e56–e93, Feb. 2011, doi: 10.1093/cid/cir073.

[5] Y. D. Tseng and A. K. Ng, "Hematologic Malignancies," Hematology/Oncology Clinics of North America, vol. 34, no. 1, pp. 127–142, Feb. 2020, doi: 10.1016/j.hoc.2019.08.020.

[6] R. R. Kansara and C. Speziali, "Immunotherapy in hematologic malignancies," Curr Oncol, vol. 27, no. Suppl 2, pp. S124–S131, Apr. 2020, doi: 10.3747/co.27.5117.

[7] X. Zhang, L. Zhu, H. Zhang, S. Chen, and Y. Xiao, "CAR-T Cell Therapy in Hematological Malignancies: Current Opportunities and Challenges," Front Immunol, vol. 13, p. 927153, Jun. 2022, doi: 10.3389/fimmu.2022.927153.

[8] B. T. Emmer and D. Ginsburg, "Genome Editing and Hematologic Malignancy," Annu Rev Med, vol. 71, pp. 71–83, Jan. 2020, doi: 10.1146/annurev-med-052318-100741.

[9] A. Shimada, "Hematological malignancies and molecular targeting therapy," Eur J Pharmacol, vol. 862, p. 172641, Nov. 2019, doi: 10.1016/j.ejphar.2019.172641.

[10] D. Pulte, L. Jansen, F. A. Castro, and H. Brenner, "Changes in the survival of older patients with hematologic malignancies in the early 21st century," Cancer, vol. 122, no. 13, pp. 2031–2040, Jul. 2016, doi: 10.1002/cncr.30003.

[11] M. Sant et al., "Survival for haematological malignancies in Europe between 1997 and 2008 by region and age: results of EUROCARE-5, a population-based study," Lancet Oncol, vol. 15, no. 9, pp. 931–942, Aug. 2014, doi: 10.1016/S1470-2045(14)70282-7.

[12] K. Hemminki, J. Hemminki, A. Försti, and A. Sud, "Survival in hematological malignancies in the Nordic countries through a half century with correlation to treatment," Leukemia, vol. 37, no. 4, pp. 854–863, Apr. 2023, doi: 10.1038/s41375-023-01852-w.

[13] J. Tessier and C. D. Sifri, "Epidemiology and prevention of bacterial infections in patients with hematologic malignancies," Infect Disord Drug Targets, vol. 11, no. 1, pp. 11–17, Feb. 2011, doi: 10.2174/187152611794407728.

[14] D. J. Bays and G. R. Thompson, "Fungal Infections of the Stem Cell Transplant Recipient and Hematologic Malignancy Patients," Infect Dis Clin North Am, vol. 33, no. 2, pp. 545–566, Jun. 2019, doi: 10.1016/j.idc.2019.02.006.

[15] L. Fontana and L. Strasfeld, "Respiratory Virus Infections of the Stem Cell Transplant Recipient and the Hematologic Malignancy Patient," Infect Dis Clin North Am, vol. 33, no. 2, pp. 523–544, Jun. 2019, doi: 10.1016/j.idc.2019.02.004.

[16] D. Neofytos, "Antimicrobial Prophylaxis and Preemptive Approaches for the Prevention of Infections in the Stem Cell Transplant Recipient, with Analogies to the Hematologic Malignancy Patient," Infectious Disease Clinics of North America, vol. 33, no. 2, pp. 361–380, Jun. 2019, doi: 10.1016/j.idc.2019.02.002.

[17] R. Maglie et al., "Immune-Mediated Dermatoses in Patients with Haematological Malignancies: A Comprehensive Review," Am J Clin Dermatol, vol. 21, no. 6, pp. 833–854, 2020, doi: 10.1007/s40257-020-00553-9.

[18] N. Al-Bader and D. C. Sheppard, "Aspergillosis and stem cell transplantation: An overview of experimental pathogenesis studies," Virulence, vol. 7, no. 8, pp. 950–966, Nov. 2016, doi: 10.1080/21505594.2016.1231278.

[19] T. Lehrnbecher et al., "Guideline for the Management of Fever and Neutropenia in Pediatric Patients With Cancer and Hematopoietic Cell Transplantation Recipients: 2023 Update," J Clin Oncol, vol. 41, no. 9, pp. 1774–1785, Mar. 2023, doi: 10.1200/JCO.22.02224.

[20] M. Zeng et al., "Guidelines for the diagnosis, treatment, prevention and control of infections caused by carbapenem-resistant gram-negative bacilli," Journal of Microbiology, Immunology and Infection, vol. 56, no. 4, pp. 653–671, Aug. 2023, doi: 10.1016/j.jmii.2023.01.017.

[21] K. Wu, S.-Y. Choi, K. Bergman, and S. Seo, "Antimicrobial Dose Selection under the Animal Rule," Clin Pharmacol Ther, vol. 109, no. 4, pp. 971–976, Apr. 2021, doi: 10.1002/cpt.2201.

[22] F. Pea, Pharmacokinetics in Everyday Clinical Practice, 1st edition. SEEd Medical Publishers, 2012.

[23] R. F. Eyler and K. Shvets, "Clinical Pharmacology of Antibiotics," Clin J Am Soc Nephrol, vol. 14, no. 7, pp. 1080–1090, Jul. 2019, doi: 10.2215/CJN.08140718.

[24] N. Frimodt-Møller, "How predictive is PK/PD for antibacterial agents?," Int J Antimicrob Agents, vol. 19, no. 4, pp. 333–339, Apr. 2002, doi: 10.1016/s0924-8579(02)00029-8.

[25] W. J. Heinz et al., "Diagnosis and empirical treatment of fever of unknown origin (FUO) in adult neutropenic patients: guidelines of the Infectious Diseases Working Party (AGIHO) of the German Society of Hematology and Medical Oncology (DGHO)," Ann Hematol, vol. 96, no. 11, pp. 1775–1792, Nov. 2017, doi: 10.1007/s00277-017-3098-3.

[26] D. Averbuch et al., "European guidelines for empirical antibacterial therapy for febrile neutropenic patients in the era of growing resistance: summary of the 2011 4th European Conference on Infections in Leukemia," Haematologica, vol. 98, no. 12, pp. 1826–1835, Dec. 2013, doi: 10.3324/haematol.2013.091025.

[27] F. B. Sime et al., "Altered pharmacokinetics of piperacillin in febrile neutropenic patients with hematological malignancy," Antimicrob Agents Chemother, vol. 58, no. 6, pp. 3533–3537, Jun. 2014, doi: 10.1128/AAC.02340-14.

[28] J. C. Álvarez et al., "Pharmacokinetics of piperacillin/tazobactam in cancer patients with hematological malignancies and febrile neutropenia after chemotherapy," BMC Pharmacol Toxicol, vol. 14, p. 59, Nov. 2013, doi: 10.1186/2050-6511-14-59.

[29] M. Abramson and A. Mehdi, "Hematological Malignancies and the Kidney," Advances in Chronic Kidney Disease, vol. 29, no. 2, pp. 127-140.e1, Mar. 2022, doi: 10.1053/j.ackd.2022.02.003.

[30] L. B. S. Aulin, D. W. Lange, M. A. A. Saleh, P. H. Graaf, S. Völler, and J. G. C. Hasselt, "Biomarker-Guided Individualization of Antibiotic Therapy," Clin. Pharmacol. Ther., vol. 110, no. 2, pp. 346–360, Aug. 2021, doi: 10.1002/cpt.2194.

[31] A. Branche, O. Neeser, B. Mueller, and P. Schuetz, "Procalcitonin to guide antibiotic decision making," Curr Opin Infect Dis, vol. 32, no. 2, pp. 130–135, Apr. 2019, doi: 10.1097/QCO.0000000000000522.

[32] P. Schuetz et al., "Procalcitonin to initiate or discontinue antibiotics in acute respiratory tract infections," Cochrane Database Syst Rev, vol. 10, no. 10, p. CD007498, Oct. 2017, doi: 10.1002/14651858.CD007498.pub3.

[33] H. J. Prins et al., "CRP-guided antibiotic treatment in acute exacerbations of COPD in hospital admissions," Eur Respir J, vol. 53, no. 5, p. 1802014, May 2019, doi: 10.1183/13993003.02014-2018.

[34] Z. Yao, Y. Zhang, and H. Wu, "Regulation of C-reactive protein conformation in inflammation," Inflamm Res, vol. 68, no. 10, pp. 815–823, Oct. 2019, doi: 10.1007/s00011-019-01269-1.

[35] S. Black, I. Kushner, and D. Samols, "C-reactive Protein*," Journal of Biological Chemistry, vol. 279, no. 47, pp. 48487–48490, Nov. 2004, doi: 10.1074/jbc.R400025200.

[36] J. E. Volanakis, "Human C-reactive protein: expression, structure, and function," Mol Immunol, vol. 38, no. 2–3, pp. 189–197, Aug. 2001, doi: 10.1016/s0161-5890(01)00042-6.

[37] F. G. Hage, "C-reactive protein and hypertension," J Hum Hypertens, vol. 28, no. 7, pp. 410–415, Jul. 2014, doi: 10.1038/jhh.2013.111.

[38] H. Rao, S. Dutta, P. Menon, S. Attri, N. Sachdeva, and M. Malik, "Procalcitonin and C-reactive protein for diagnosing post-operative sepsis in neonates," J Paediatr Child Health, vol. 58, no. 4, pp. 593–599, Apr. 2022, doi: 10.1111/jpc.15774.

[39] A. Perrella et al., "C-reactive protein but not procalcitonin may predict antibiotic response and outcome in infections following major abdominal surgery," Updates Surg, vol. 74, no. 2, pp. 765–771, Apr. 2022, doi: 10.1007/s13304-021-01172-7.

[40] P. P, T.-P. Am, and C. Ah, "C-reactive protein, an early marker of community-acquired sepsis resolution: a multi-center prospective observational study," Critical care (London, England), vol. 15, no. 4, Jul. 2011, doi: 10.1186/cc10313.

[41] C. Pierrakos, D. Velissaris, M. Bisdorff, J. C. Marshall, and J.-L. Vincent, "Biomarkers of sepsis: time for a reappraisal," Crit Care, vol. 24, no. 1, p. 287, Jun. 2020, doi: 10.1186/s13054-020-02993-5.

[42] A. Luzzani, E. Polati, R. Dorizzi, A. Rungatscher, R. Pavan, and A. Merlini, "Comparison of procalcitonin and C-reactive protein as markers of sepsis," Crit Care Med, vol. 31, no. 6, pp. 1737–1741, Jun. 2003, doi: 10.1097/01.CCM.0000063440.19188.ED.

[43] G. G. Rao and C. B. Landersdorfer, "Antibiotic pharmacokinetic/pharmacodynamic modelling: MIC, pharmacodynamic indices and beyond," Int J Antimicrob Agents, vol. 58, no. 2, p. 106368, Aug. 2021, doi: 10.1016/j.ijantimicag.2021.106368.

[44] S. G. Wicha et al., "From Therapeutic Drug Monitoring to Model-Informed Precision Dosing for Antibiotics," Clin Pharmacol Ther, vol. 109, no. 4, pp. 928–941, Apr. 2021, doi: 10.1002/cpt.2202.

[45] P. Del Valle-Moreno et al., "Model-Informed Precision Dosing Software Tools for Dosage Regimen Individualization: A Scoping Review," Pharmaceutics, vol. 15, no. 7, p. 1859, Jul. 2023, doi: 10.3390/pharmaceutics15071859.

[46] E. Wallenburg, R. ter Heine, J. A. Schouten, and R. J. M. Brüggemann, "Personalised antimicrobial dosing: standing on the shoulders of giants," International Journal of Antimicrobial Agents, vol. 56, no. 3, p. 106062, Sep. 2020, doi: 10.1016/j.ijantimicag.2020.106062.

[47] R. Y. Choi, A. S. Coyner, J. Kalpathy-Cramer, M. F. Chiang, and J. P. Campbell, "Introduction to Machine Learning, Neural Networks, and Deep Learning," Transl Vis Sci Technol, vol. 9, no. 2, p. 14, Feb. 2020, doi: 10.1167/tvst.9.2.14.

[48] J. G. Greener, S. M. Kandathil, L. Moffat, and D. T. Jones, "A guide to machine learning for biologists," Nat Rev Mol Cell Biol, vol. 23, no. 1, pp. 40–55, Jan. 2022, doi: 10.1038/s41580-021-00407-0.

[49] J. H. Hughes and R. J. Keizer, "A hybrid machine learning/pharmacokinetic approach outperforms maximum a posteriori Bayesian estimation by selectively flattening model priors," CPT Pharmacometrics Syst Pharmacol, vol. 10, no. 10, pp. 1150–1160, Oct. 2021, doi: 10.1002/psp4.12684.

[50] D. W. Uster et al., "A Model Averaging/Selection Approach Improves the Predictive Performance of Model-Informed Precision Dosing: Vancomycin as a Case Study," Clin Pharmacol Ther, vol. 109, no. 1, pp. 175–183, Jan. 2021, doi: 10.1002/cpt.2065.

[51] R. Faelens, N. Luyckx, D. Kuypers, T. Bouillon, and P. Annaert, "Predicting model-informed precision dosing: A test-case in tacrolimus dose adaptation for kidney transplant recipients," CPT Pharmacometrics Syst Pharmacol, vol. 11, no. 3, pp. 348–361, Mar. 2022, doi: 10.1002/psp4.12758.

[52] A. Heus et al., "Model-informed precision dosing of vancomycin via continuous infusion: a clinical fit-for-purpose evaluation of published PK models," Int J Antimicrob Agents, vol. 59, no. 5, p. 106579, May 2022, doi: 10.1016/j.ijantimicag.2022.106579.

[53] N. Peiffer-Smadja et al., "Machine learning for clinical decision support in infectious diseases: a narrative review of current applications," Clinical Microbiology and Infection, vol. 26, no. 5, pp. 584–595, May 2020, doi: 10.1016/j.cmi.2019.09.009.

[54] R. Tang, R. Luo, S. Tang, H. Song, and X. Chen, "Machine learning in predicting antimicrobial resistance: a systematic review and meta-analysis," Int J Antimicrob Agents, vol. 60, no. 5–6, p. 106684, 2022, doi: 10.1016/j.ijantimicag.2022.106684.

[55] J. I. Kim et al., "Machine Learning for Antimicrobial Resistance Prediction: Current Practice, Limitations, and Clinical Perspective," Clin Microbiol Rev, vol. 35, no. 3, p. e0017921, Sep. 2022, doi: 10.1128/cmr.00179-21.

Chapter 2

Does Cytokine-Release Syndrome Induced by CAR-T Cell Treatment Have an Impact on the Pharmacokinetics of Meropenem and Piperacillin/Tazobactam in Patients with Hematologic Malignancies? Findings from an Observational Case-Control Study

Authors:
Chun Liu
Pier Giorgio Cojutti
Maddalena Giannella
Marcello Roberto
Beatrice Casadei
Gianluca Cristiano
Cristina Papayannidis
Nicola Vianelli
Pier Luigi Zinzani
Pierluigi Viale
Francesca Bonifazi
Federico Pea*

Pharmaceutics 2023, 15, 1022. https://doi.org/10.3390/pharmaceutics15031022

Abstract

Chimeric Antigen Receptor T (CAR-T) cell therapy is a promising approach for some relapse/refractory hematologic B-cell malignancies; however, in most patients, cytokine release syndrome (CRS) may occur. CRS is associated with acute kidney injury (AKI) that may affect the pharmacokinetics of some beta-lactams. The aim of this study was to assess whether the pharmacokinetics of meropenem and piperacillin may be affected by CAR-T cell treatment. The study included CAR-T cell treated patients (cases) and oncohematologic patients (controls), who were administered 24h continuous infusion (CI) meropenem or piperacillin/tazobactam, optimized by therapeutic drug monitoring, over a 2-year period. Patients' data were retrospectively retrieved and matched on a 1:2 ratio. Beta-lactam clearance (CL) was calculated as CL=DailyDose/InfusionRate. A total of 38 cases (of whom 14 and 24 were treated with meropenem and piperacillin/tazobactam, respectively) was matched with 76 controls. CRS occurred in 85.7% (12/14) and 95.8% (23/24) of patients treated with meropenem and piperacillin/tazobactam, respectively. CRS-induced AKI was observed in only 1 patient. CL did not differ between cases and controls for both meropenem (11.1 vs. 11.7 L/h, p=0.835) and piperacillin (14.0 vs. 10.4 L/h, p=0.074). Our findings suggest that 24h-CI meropenem and piperacillin dosages should not be reduced a priori in CAR-T cell patients experiencing CRS.

Keywords: CAR-T cell therapy; meropenem; piperacillin/tazobactam; cytokine release syndrome; therapeutic drug monitoring.

2.1 Introduction

Chimeric Antigen Receptor T (CAR-T) cell therapies have remarkably changed the treatment of some relapsed or refractory hematologic B-cell malignancies [1]. This complex immunotherapy consists of infusing the patient's own T-cells after previously genetically modifying these to express CAR for targeting tumor cells. Approved indications include relapse/refractory acute lymphoblastic leukemia, some B-cell lymphomas (diffuse large B cell, primary mediastinal, high-grade, follicular, or mantle cell lymphoma) and, ultimately, multiple myeloma [2–4].

CAR-T cell treatment may be associated with cytokine release syndrome (CRS), an adverse effect that may occur in approximately 80% of patients [5]. CRS is characterized by high fever, hypotension, hypoxia, and ongoing injury that mimics sepsis. It usually appears within 14–21 days from CAR-T cell infusion [5,6]. Other complications occurring in the post-infusion period may be immune effector cell-associated neurologic syndrome (ICANS) and acute kidney injury (AKI) following vasodilatory shock [5,7].

CAR-T cell patients are at high risk of infection due to cytokine-mediated cytopenias, myelosuppression related to chemotherapy, and CRS treatment with high-dose corticosteroids and/or IL-6 inhibitors, such as tocilizumab [8]. The

prevalence of infection in CAR-T cell patients may be 27–36%, with bacteremia, pneumonia, and skin and soft tissue infections being the most prevalent [8].

In general, all patients with hematologic malignancies with febrile neutropenia (FN), including CAR-T cell patients, are at high risk of bacterial infection complications. Bloodstream infections caused by Gram-negative pathogens have a prevalence rate of 11–38% in these populations [9]. Among the most common Gram-negative pathogens are *Klebsiella pneumoniae*, *Escherichia coli*, *Enterobacter cloacae*, and *Pseudomonas aeruginosa*. The management of infections caused by these pathogens is challenged by the reduced antimicrobial susceptibility to beta-lactams in these patients. In particular, in oncohematologic patients, the susceptibility rate of piperacillin/tazobactam and meropenem has been reported to be 79.1% and 63.1%, respectively [10].

Current guidelines recommend an antipseudomonal beta-lactam, e.g., piperacillin/tazobactam, cefepime, or ceftazidime as the first-line choice for the empirical treatment of FN in patients with hematologic malignancies. These beta-lactams are preferred in clinically stable febrile neutropenic patients who have not had previous infections and/or colonization caused by multi-drug resistant (MDR) Gram-negative bacteria. In the absence of a positive clinical response within 2–3 days, escalation to meropenem is suggested [11,12].

Beta-lactams have a time-dependent pharmacodynamic activity, whose efficacy is related to the percentage of time that free plasma concentrations are maintained above the minimum inhibitory concentration (MIC) of the bacterial pathogen (% fT>MIC) during the dosing interval. Pre-clinical data indicate that the required threshold to achieve bactericidal activity with beta-lactams is 40–70% fT>MIC [13]. However, clinical evidence suggests that more aggressive pharmacokinetic/pharmacodynamic (PK/PD) targets, namely, 100% $fT>_{4\text{-}6\ folds}MIC$, should be adopted to ensure better outcomes in clinical contexts characterized by high inter-individual variability, such as critically ill patients [14,15].

Administration of beta-lactams by 24h continuous infusion (CI) maximizes the attainment of such a high PK/PD threshold during the entire dosing interval. Moreover, optimizing beta-lactam exposure by means of real-time therapeutic drug monitoring (TDM) has been proven effective in improving treatment outcomes with beta-lactams [13,14].

For the treatment of severe infections, high-dosing regimens of meropenem administered by 24h-CI has been advocated in different clinical settings [16,17]. Specifically, in order to maximize empirical treatment of *Enterobacterales* and *Pseudomonas aeruginosa* in FN patients with hematologic malignancies, Monte Carlo simulations suggest the use of meropenem dosages ranging from 3 to 5 g daily by 24h-CI in relation to patient renal function.

Considering that up to 30% of CAR-T cell patients may develop AKI [7] and that beta-lactams are eliminated mainly by the renal route, it might be expected that the PK of these agents may be altered in oncohematologic patients undergoing CAR-T compared with those who are not.

The aim of this case-control study was to assess whether the pharmacokinetics of meropenem and/or piperacillin/tazobactam administered by continuous infusion were changed in oncohematologic patients who received anti-CD19 CAR-T cell therapy compared with those who did not.

2.2 Materials and Methods

2.2.1 Study Design

This evaluation retrospectively included CAR-T cell patients (case group) and oncohematologic patients (control group) who underwent TDM-guided adaptive dosage of continuous infusion meropenem and/or piperpacillin/tazobactam for the empirical treatment of FN. The evaluation was conducted at the IRCCS Azienda Ospedaliero-Universitaria di Bologna from January 2020 to January 2023. The ratio of the case group vs. the control group was set at 1:2 for statistical empowerment.

All patients were treated with beta-lactam monotherapy at a standard initial dose (meropenem: 2g loading over 1h followed by 1g q6h over 6h [namely, 4g/daily by CI]; piperacillin/tazobactam: 8/1g loading over 1h followed by 16/2g over 24h by CI).

TDM was performed after at least 48h from starting therapy, by assessing the meropenem or piperacillin plasma steady-state concentration (C_{ss}). At our centre, all oncohematologic patients who received an antipseudomonal agent underwent a program of dosing optimization that included the assessment of drug concentration, along with a clinical pharmacological interpretation of the results. This program is conducted from Monday to Friday, as described elsewhere[18]. Briefly, in the pre-analytical phase, clinicians fill in an electronic form with patient demographics (age, weight, and height), patient clinical data (diagnosis and co-medications), and drug-related information (date of starting therapy, current dosing regimen, and time of the last dose). Blood samples are collected shortly before drug administration to assess trough concentration or at any time during infusion for drugs administered by 24h-CI. After collection, the blood samples are immediately sent to the lab where they are analyzed within 1-3 h from sample delivery. The TDM results are then published on the hospital intranet early in the afternoon. The post-analytical phase starts once the TDM results are made available. Each patient request is managed by a clinical pharmacologist. Written expert clinical pharmacological advice for dose adjustments is then published on the hospital intranet before 5 p.m.

Dosing adaptation seeks to obtain maximal effectiveness of the empirical treatment of FN. Therefore, a desired PK target of 100% $fT_{>4\text{-}8\ folds}MIC$[19,20] was set for all susceptible pathogens. This was achieved by considering as the MIC value the EUCAST clinical breakpoint of meropenem and piperacillin/tazobactam against *Pseudomonas aeruginosa* (namely, 2 and 8 mg/L, respectively) [21]. Consequently,

meropenem C_{ss} was targeted at 8-16 mg/L and piperacillin C_{ss} at 32-64 mg/L.

2.2.2 Drug Analysis

Meropenem and piperacillin were both measured using the validated high performance liquid chromatography tandem mass spectrometry (LC-MS/MS) method, as described below.

2.2.2.1 Sample Pre-Treatment

Blood samples were centrifuged for 10min at 9000×g. An aliquot of 50 µL of patient plasma was added, together with a 1.25 µL solution of internal standard (final concentration 5 µg/mL). Liquid-liquid extraction was carried out using the MassTox®TDM Series A basic kit from Chromsystems Instruments & Chemicals GmbH, Munich, Germany. According to the manufacturer's recommendation, an extraction buffer (25 µL) and a precipitation buffer (250 µL) were added to each sample. This solution was centrifuged for 10 min at 15,000×g, and an equal volume of the dilution buffer was added to the supernatant. Plasma samples used for the calibration curve and quality controls underwent the same procedure. Subsequently, using an autosampler vial in which 5 µL of the supernatant was transferred, a volume of 3 µL was injected into the LC-MS/MS system.

2.2.2.2 Conditions of Liquid Chromatography and Mass Spectrometry

Chromatographic separation was conducted at 25°C on a C18 column provided by the MassTox®TDM Series A basic kit from Chromsystems Instruments & Chemicals GmbH, Munich, Germany. The column was eluted with a gradient elution set at 0.5 mL/min using mobile phase A (0.1% formic acid in water) and mobile phase B (0.1% formic acid in methanol).

The Shimadzu UPLC system was coupled with the Sciex API 5500 Qtrap mass spectrometer with an electrospray ionization source set in positive ionization mode. Optimization of ionization conditions were performed by directly injecting drug solutions dissolved in a 50:50 volume mixture of mobile phases A and B. Mass spectrometer parameters were set as follows: medium for collision gas, 30 units for curtain gas, 5500 V for ionspray voltage, 500°C for probe temperature, and 50 ms for dwell time. A multiple reaction monitoring-based quantitation method technique was used. Specifically, analytes were monitored at two different transitions, namely, the quantifier ions for identification and the qualifier ions for confirmation. The Analyst 1.6 and Multiquant software Version 2.0, both provided by the spectrometer manufacturer, were used for chromatographic data acquisition, peak integration, and quantification.

2.2.2.3 Calibration Curve and Quality Controls

The meropenem and piperacillin/tazobactam stock solution was prepared in MilliQ water at a concentration of 10 mg/mL. The calibration standards for meropenem were prepared at 0, 3, 25, and 85 mg/L, while those for piperacillin/tazobactam were prepared at 0, 8, 50, and 195 mg/L. The calibration ranges were based on plasma concentration usually observed using approved drug dosages in clinical practice, namely, 0–100 mg/L for meropenem and 0–200 mg/L for piperacillin. The quality controls were prepared at two concentrations, namely, the low concentration (13 and 20 mg/L for meropenem and piperacillin/tazobactam, respectively) and the high concentration (43 and 97 mg/L for meropenem and piperacillin/tazobactam, respectively).

2.2.2.4 Chemical and Reagents

Meropenem, piperacillin/tazobactam sodium salt, and their isotopically labeled counterparts, 2H6-Meropenem and 2H5-Piperacillin/tazobactam, were purchased from Alsachim (Illkirch, France). Formic acid and methanol for LC-MS/MS mobile phases were purchased from CHROMASOLV (Thermofisher Scientific, Milan, Italy). A Milli-Q Direct system (Millipore Merck-Darmstadt, Germany) was used for LC-MS/MS grade water. Blank plasma was supplied for control purposes by the IRCCS Azienda Ospedaliero-Universitaria di Bologna (Bologna, Italy). Primary stock solutions for analytes and internal standards, obtained by dissolving the powder in water or dimethyl sulfoxide, were prepared to a final concentration of 10.0 and 1.0 mg/mL, respectively. All chemicals were stored at -80°C.

2.2.2.5 Accuracy, Precision and Limit of Quantification

The intra-day and inter-day precision and accuracy, expressed as the coefficient of variation (CV%) for the low- and high-quality controls, were <10% for both meropenem and piperacillin/tazobactam. The limits of quantification (LOQ) were 0.3 and 1.0 mg/L for meropenem and piperacillin/tazobactam, respectively.

2.2.3 Patient Clinical Data and Pharmacokinetic Analysis

Demographic, pharmacologic, and laboratory data were retrieved for each patient. Serum creatinine, serum albumin, C-reactive protein (C-RP), procalcitonin, interleukin-6 (IL-6), and interleukin-8 (IL-8) were collected on the days of each TDM assessment. The estimated glomerular filtration rate (eGFR) was calculated using the CKD-EPI formula[22]. Meropenem and piperacillin clearances (CL) were calculated using the following formula:

$$CL\ (L/h) = \frac{Dose\ (mg)}{C_{\mathrm{ss}}\ (mg/L) \times 24\ (h)}$$

where C_{ss} is the meropenem or piperacillin steady state concentration.

Descriptive statistics were reported as the median and interquartile range (IQR) for continuous data and numbers with percentages for categorical data. The inter-individual variability of meropenem or piperacillin/tazobactam CL was assessed by calculating the CV% of all the CL values obtained at each TDM assessment in each patient.

The relationship between meropenem or piperacillin/tazobactam CL and eGFR was expressed using the Spearman rank correlation coefficient (ρ). Categorical variables were compared using the $\chi 2$ test or Fisher's exact test, while continuous variables were compared using the Student t-test or the Mann–Whitney test. A p-value of <0.05 was required to achieve statistical significance. All statistical analysis and plotting was performed using R version 3.4.4 (R Foundation for Statistical Computing, Vienna, Austria).

2.3 Results

The patient inclusion criteria in the study are reported in Figure 2.1. First, patients with hematologic malignancies who underwent CAR-T cell during the study period (n=80) were retrospectively identified. Of these, only those who were administered 24h-CI meropenem or piperacillin/tazobactam and whose therapy was optimized by TDM were included (n=38). This group consisted of 14 patients treated with 24h-CI meropenem and 24 patients treated with 24h-CI piperacillin/tazobactam. These two groups were then matched at a 1:2 ratio to general oncohematologic patients treated with 24h-CI meropenem (n=28) or piperacillin/tazobactam (n=48) for FN but who did not receive CAR-T cell treatment. At the end, a total of 38 CAR-T cell patients was matched to 76 oncohematologic patients.

The CAR-T cell population included patients with relapse/refractory lymphomas (3 median lines of previous therapy) who were histologically grouped as follows: diffuse large B-cell lymphoma (n=21), mantle cell lymphoma (n=7), primary mediastinal B-cell lymphoma (n=5), follicular lymphoma (n=4), and high grade B-cell lymphoma (n=1). The patients were admitted for the infusion of anti-CD19 CAR-T after lymphodepleting chemotherapy. The comparator cohort included patients with different oncohematologic diagnoses: acute myeloid leukemia (n=31), lymphoma (n=29), acute lymphoblastic leukemia (n=6), myeloproliferative neoplasm (n=4), myelodysplastic syndrome (n=4), and plasma-cell dyscrasia (n=2). All these patients had undergone chemotherapy respective to the diagnosis and phase.

Table 2.1 reports the demographic and clinical characteristics of the case and the control patients treated with 24h-CI meropenem (n=14 and n=28, respectively). The CAR-T cell patients had a significantly lower eGFR compared with the control group (median eGFR of 63.5 vs. 94.5 mL/min/1.73m^2, p=0.005).

CRS occurred in 85.7% (12/14) of CAR-T cell patients, after a median (IQR) number of days from cell infusion of 4.0 (2.5–4.5). Meropenem was started after a median (IQR) number of days from cell infusion of 4.0 (1.25–4.75). During meropenem treatment, the median (IQR) range of IL-6 and IL-8 was 237.3 (49.2–2201.2) pg/mL and 46.0 (32.0–79.0) pg/mL, respectively. No patient developed AKI during treatment. The median meropenem CL in CAR-T cell patients was similar to that observed in oncohematologic patients (11.1 vs. 11.7 L/h, respectively, p=0.835), even if the inter-individual variability was quite high (CV% of 5% and 69.7%, respectively).

At the first TDM assessment, the distribution of C_{ss} was similar among CAR-T cell and non-CAR-T cell treated patients (median C_{ss} of 13.5 vs. 10.85 mg/L, respectively, p=0.858, Figure 2.2). A similar proportion of patients with C_{ss} outside the desired range [28.6% (4/14) vs. 21.4% (6/28), respectively, p=0.707] was observed.

Table 2.2 reports the demographic and clinical characteristics of the case and control patients treated with 24h-CI piperacillin/tazobactam (n=24 and n=48, respectively). No statistically significant difference was observed in any of the parameters between the CAR-T cell and the non-CAR-T cell patients.

CRS was observed in 95.8% (23/24) of CAR-T cell patients, after a median (IQR) number of days from cell infusion of 3.0 (2.0–4.0). Piperacillin/tazobactam was started after a median (IQR) number of days from cell infusion of 2.0 (0.0–4.00). During piperacillin/tazobactam treatment, the median (IQR) range of IL-6 and IL-8 was 69.4 (29.4–561.8) pg/mL and 56.0 (29.0–110.0) pg/mL, respectively. AKI occurred only in one CAR-T cell patient between day 3 and day 6 (median creatinine clearance value of 27 mL/min/1.73m^2), and renal function gradually recovered from day seven onward. In this patient, IL-6 levels and piperacillin CL were 4899 pg/mL and 3.78 L/h, respectively, during the AKI phase. Then, piperacillin CL increased up to 16.21 L/h when creatinine clearance returned to normal values (102 mL/min/1.73m^2). Median piperacillin CL was similar between the CAR-T cell and oncohematologic patients (CL of 14.0 vs. 10.4 L/h, respectively, p=0.074), but with very high inter-individual variability (CV% of 92.6% and 112.4%, respectively).

At the first TDM assessment, the distribution of piperacillin C_{ss} was similar between CAR-T cell and non-CAR-T cell treated patients (median C_{ss} of 42.8 vs. 57.3 mg/L, respectively, p=0.153, Figure 2.3). A similar proportion of patients with piperacillin C_{ss} out of the desired range (25.0% [6/24] vs. 16.7% [8/48], respectively, p=0.529) was observed.

2.4 Discussion

This investigation first reported the comparative PK of 24h-CI meropenem and piperacillin/tazobactam in CAR-T cell vs. non-CAR-T cell patients. Our findings suggest that the CL of both these beta-lactams should not be affected by CAR-T

cell treatment.

Indeed, almost all of the CAR-T cell patients experienced CRS, as evidenced by the high levels of both IL-6 and IL-8, and according to previously reported data [23–25]. CRS is an excessive and dysregulated immune response with increased secretion of proinflammatory cytokines, such as IL-2, IL-6, IL-10, and TNF-α [5]. This response is commonly associated with CAR-T cell therapy [5,26]. Among these cytokines, IL-6 appears to be a key driver of CRS. IL-6 is a pleiotropic cytokine that has been described as having both pro- and anti-inflammatory properties. IL-6 is produced directly by CAR-T cells after infusion, but it is also released by endothelial cells in response to pro-inflammatory signals, including TNF-α and hypoxia, and in response to tissue injury and organ failure. On target cells, IL-6 acts by binding to its receptor. This triggers gp130 and activates the Jak/STAT signaling pathway, which, in turn, activates STAT3 [27]. CRS was already associated with a downregulation of the CYP3A4-mediated drug biotransformation [28,29]. Additionally, CRS is closely associated with both AKI and chronic kidney disease [7,30,31]. It is likely that IL-6 plays a major role in kidney injury by causing acute tubular injury [32,33]. Pre-clinical models show that in nephrotoxin-induced AKI, IL-6 expression is enhanced more than a hundred-fold in the kidneys, mainly in the renal tubular epithelial cells; it is also strongly correlated with kidney damage [32]. However, mice with IL-6 deficiency and with reduced migration of neutrophil cells did not suffer from the consequences of kidney insult. This reinforces the role of IL-6-mediated neutrophil activation as one of the main mechanisms involved in AKI. Moreover, it has also been shown that IL-6 reduces endothelial nitric oxide production and adiponectin expression, thus suggesting the role of IL-6 also in patients with chronic kidney disease by inducing chronic vascular disease. Interestingly, a retrospective study conducted on 646 critically ill Japanese patients whose IL-6 levels were measured at ICU admission, showed that patients with higher levels of IL-6 (1189–2,346,310 pg/mL) had significantly higher in-hospital 90-day mortality, lower urine output, and increased probability of persistent anuria for 12 h compared with patients with lower IL-6 levels (1.5–150.2 pg/mL) [34].

On these bases, it could be expected that the elimination of meropenem and piperacillin/ tazobactam would be affected after CAR-T cell treatment of oncohematologic patients. However, this was not the case as the CAR-T cell patients had both meropenem and piperacillin CL similar to the control group, with values even higher than observed in other patient populations. Population PK studies of CI meropenem carried out in critically ill and oncohematologic patients showed meropenem CL ranging from 5.3 to 13.04 L/h [16,35–39]. For piperacillin, four population PK studies and one observational PK study showed drug CL ranging from 5.6 to 13.8 L/h [17,40–42]. Overall, these observations may be explained considering that most of our patients (83/114, 72.8%) had median eGFR>60 mL/min/1.73m^2 and the occurrence of transient AKI was observed in only one patient. It should be noted that this patient showed high values of IL-6 and a low value of piperacillin CL, suggesting that CRS-induced AKI may reduce the CL of drugs eliminated by the kidneys. We are aware that the low incidence of AKI in our population may be due to the lower levels of IL-6 that we observed in

our CAR-T cell patients compared with the values reported by [30]. Moreover, we also cannot exclude that the prompt administration of tocilizumab, a recombinant humanized anti-IL-6 receptor monoclonal antibody, to most of our patients may have attenuated the rise of IL-6.

With regard to achieving the desired efficacy targets, no difference was observed between the CAR-T cell and non-CAR-T cell treated patients. However, it is worth noting that up to 28.6% and 25% of patients treated with CI meropenem and piperacillin/tazobactam, respectively, did not attain the desired C_{ss} at the first TDM assessment.

Surprisingly, the relationship between beta-lactam CL and eGFR was only mild for meropenem in the CAR-T cell patients, and absent for piperacillin in the CAR-T cell patients and for both meropenem and piperacillin in the oncohematologic patients. This finding is in contrast to expectations based on previous data, which shows that eGFR is a significant covariate on both meropenem and piperacillin/tazobactam CL in different patient populations, including oncohematologic patients [16,17]. However, eGFR was recently reported to account for no more than 54% of the variability of meropenem elimination in critically ill patients [43], as this antibiotic is also eliminated by tubular secretion [44]. With regard to piperacillin CL, several studies show saturative elimination occurs at therapeutic dosages, which makes drug exposure unpredictable and uncorrelated to eGFR [17]. In any case, it has already been documented how the PK of antibiotics predominantly cleared by the renal route may be greatly modified in patients with oncohematologic malignancies [45,46]. Given that up to 25–30% of treated patients do not attain the desired target concentration at the first TDM assessment, and given the unreliability of eGFR in guiding dose adjustments both in CAR-T cell patients and in oncohematologic patients, TDM may be beneficial for dosage adjustments in both CAR-T cell treated patients and oncohematologic patients, similarly to what has been observed in critically ill patients [47].

Moreover, beta-lactam optimization by means of TDM may acquire special relevance for patients with augmented renal function, a condition that often occurs in oncohematologic patients [48]. In this patient population, dose adjustments should be based on measured rather than estimated renal function, as eGFR has been reported to either underestimate or overestimate measured creatinine clearance in different studies [49,50].

We recognize that our study has some limitations. The limited sample size and the estimation rather than measurement of creatinine CL must be acknowledged. Moreover, as only one patient experienced CRS-induced AKI in our cohort, it is difficult to draw definitive conclusions about the effect of CAR-T cell treatment on beta-lactam disposition. However, we believe that this study may be of interest to clinicians since our findings suggest that the treatment of FN with 24h-CI piperacillin/tazobactam or meropenem in CAR-T cell patients should be based on the same dosing regimens used for non-CAR-T cell patients.

In conclusion, our preliminary findings suggest the fact that 24h-CI meropenem and piperacillin dosages should not be reduced a priori in CAR-T cell treated

patients experiencing CRS, as CRS-induced AKI occurs rarely in CAR-T cell treated patients. However, clinicians should carefully monitor renal function in these patients, as drug accumulation may occur as soon as AKI develops. Large prospective studies are warranted to confirm these findings.

Table 2.1: Demographic and clinical characteristics of CAR-T cell patients and oncohematologic patients receiving 24h-CI meropenem (n=42).

Variable	CAR-T Cell Treated Patients	Oncohematologic Patients	p-Value
Number of patients (n)	14	28	-
Age (year)	61.5 (49–65)	62.5 (55–69.5)	0.371
Gender (male/female)	9/5	21/7	0.491
Weight (kg)	88.8 (71.0–97.0)	73.4 (63.0–80.0)	0.016
Height (m)	1.75 (1.64–1.80)	1.70 (1.64–1.75)	0.926
Creatinine (mg/dL)	1.08 (0.85–1.31)	0.69 (0.49–0.94)	¡0.001
eGFR (mL/min/1.73m^2)	63.5 (54.0–90.5)	94.5 (78.8–117.3)	0.005
Reasons for meropenem			
FN (n, %)	11 (78.7)	21 (75.0)	1.000
BSI (n, %)	1 (7.1)	5 (17.9)	0.645
HAP(n,%)	1 (7.1)	2 (7.1)	1.000
UTI (n, %)	1 (7.1)	0 (0)	0.333
Meropenem treatment			
Drug daily dose (g)	4.0 (4.0–4.0)	4.0 (4.0–4.0)	0.476
Treatment duration (day)	9.0 (7.0–11.8)	13.0 (8.0–17.0)	0.101
C_{ss} (mg/L)	11.0 (7.0–15.1)	12.0 (6.7–17.5)	0.852
CL (L/h)	11.1 (7.9–21.2)	11.7 (8.2–20.1)	0.835

Abbreviations: eGFR, estimated glomerular filtration rate; FN, febrile neutropenia; BSI, bloodstream infection; HAP, hospital-acquired pneumonia; UTI, urinary tract infection; C_{ss}, steady-state concentration; CL, clearance.

Data are presented as median (IQR) for continuous variables and as a number (%) for categorical variables.

Table 2.2: Demographic and clinical characteristics of CAR-T cell patients and oncohematologic patients receiving 24h-CI piperacillin/tazobactam (n=72).

Variable	CAR-T Cell Treated Patients	Oncohematologic Patients	p-Value
Number of patients (n)	24	48	-
Age (year)	61 (52–64)	64.5 (47–74)	0.187
Gender (male/female)	14/10	29/19	1.000
Weight (kg)	70 (61.5–82.3)	70.0 (60–80)	0.236
Height (m)	1.70 (1.63–1.76)	1.70 (1.64–1.76)	0.556
Creatinine (mg/dL)	0.99 (0.81–1.18)	0.81 (0.69–1.13)	0.153
eGFR (mL/min/1.73m^2)	76.5 (60.0–96.2)	95.5 (59.8–105.3)	0.186
Reasons for piperacillin/tazobactam			
FN (n, %)	20 (83.3)	35 (72.9)	0.390
BSI (n, %)	2 (8.3)	10 (20.8)	0.314
HAP(n,%)	1 (4.2)	2 (4.2)	1.000
UTI (n, %)	1 (4.2)	1 (2.1)	1.000
Piperacillin/tazobactam treatment			
Drug daily dose (g)	18.0 (13.5–18.0)	18.0 (13.5–18.0)	0.522
Treatment duration (day)	6.0 (5.0–14.0)	9.0 (7.0–12.0)	0.394
C_{ss} (mg/L)	43.7 (34.6–65.3)	58.4 (34.8–90.1)	0.058
CL (L/h)	14.0 (9.0–19.3)	10.40 (6.38–17.2)	0.074

Abbreviations: eGFR, estimated glomerular filtration rate; FN, febrile neutropenia; BSI, bloodstream infection; HAP, hospital-acquired pneumonia; UTI, urinary tract infection; C_{ss}, steady-state concentration; CL, clearance.

Data are presented as median (IQR) for continuous variables and as a number (%) for categorical variables.

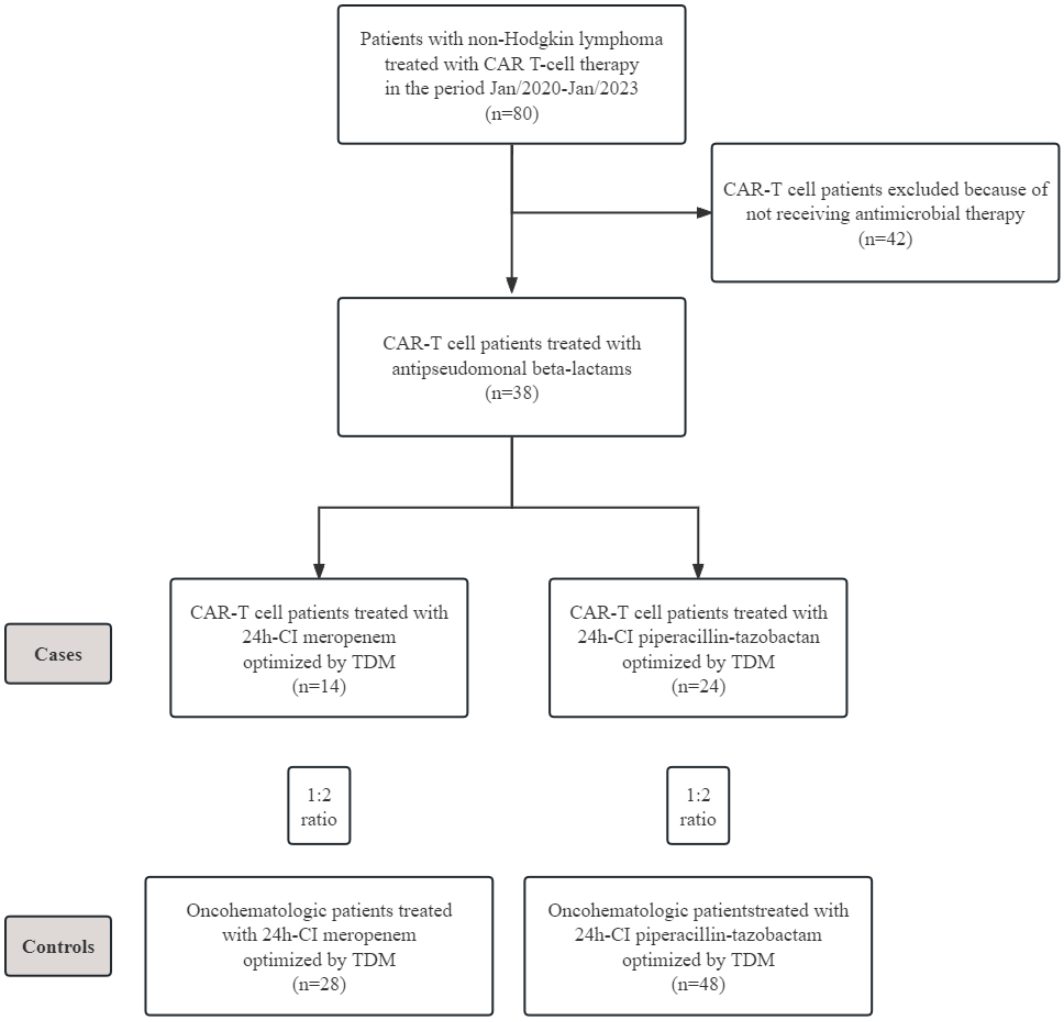

Figure 2.1: Flowchart of patient inclusion criteria in the study.

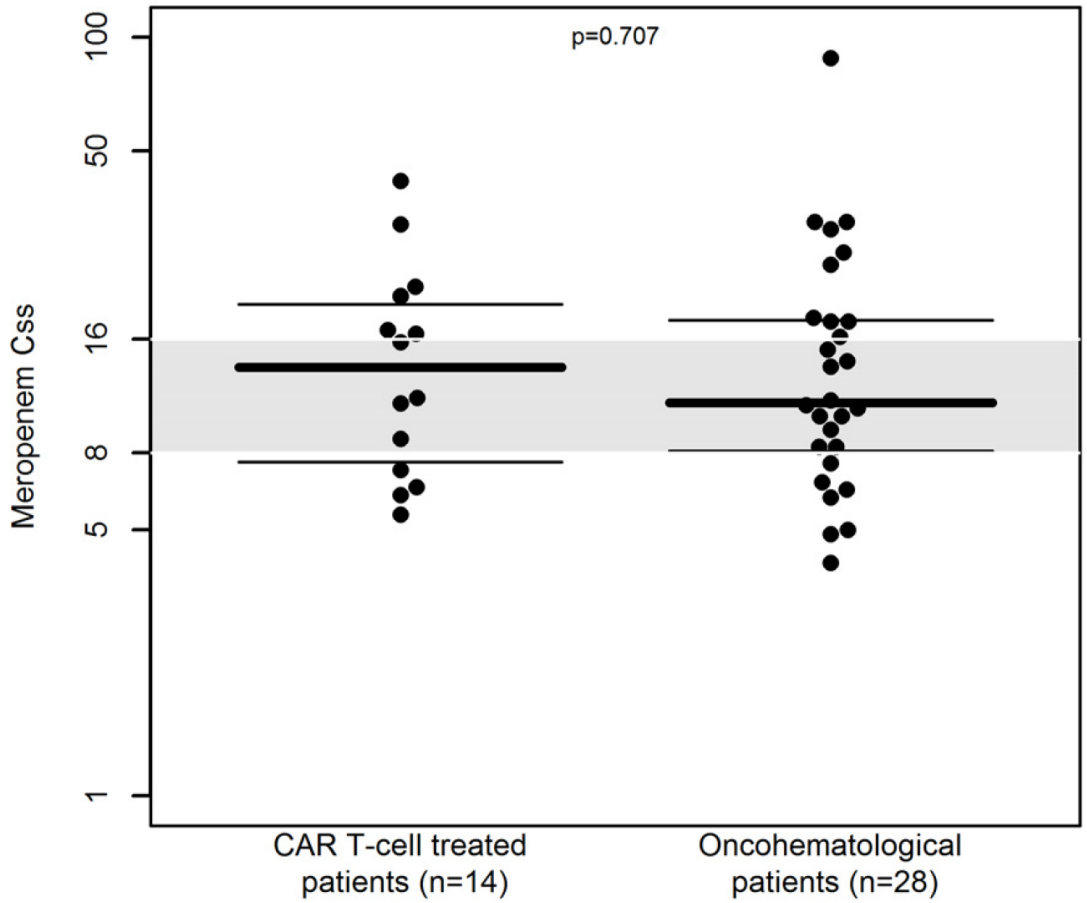

Figure 2.2: Beeswarm plot of distribution of C_{ss} of 24h-CI meropenem (n=42) in CAR-T cell treated patients and in oncohematologic patients at first TDM assessment. The gray shaded area represents the desired therapeutic range (C_{ss} of 8–16 mg/L). The dashed line is the median. The dotted lines represent the 25^{th} and 75^{th} percentiles.

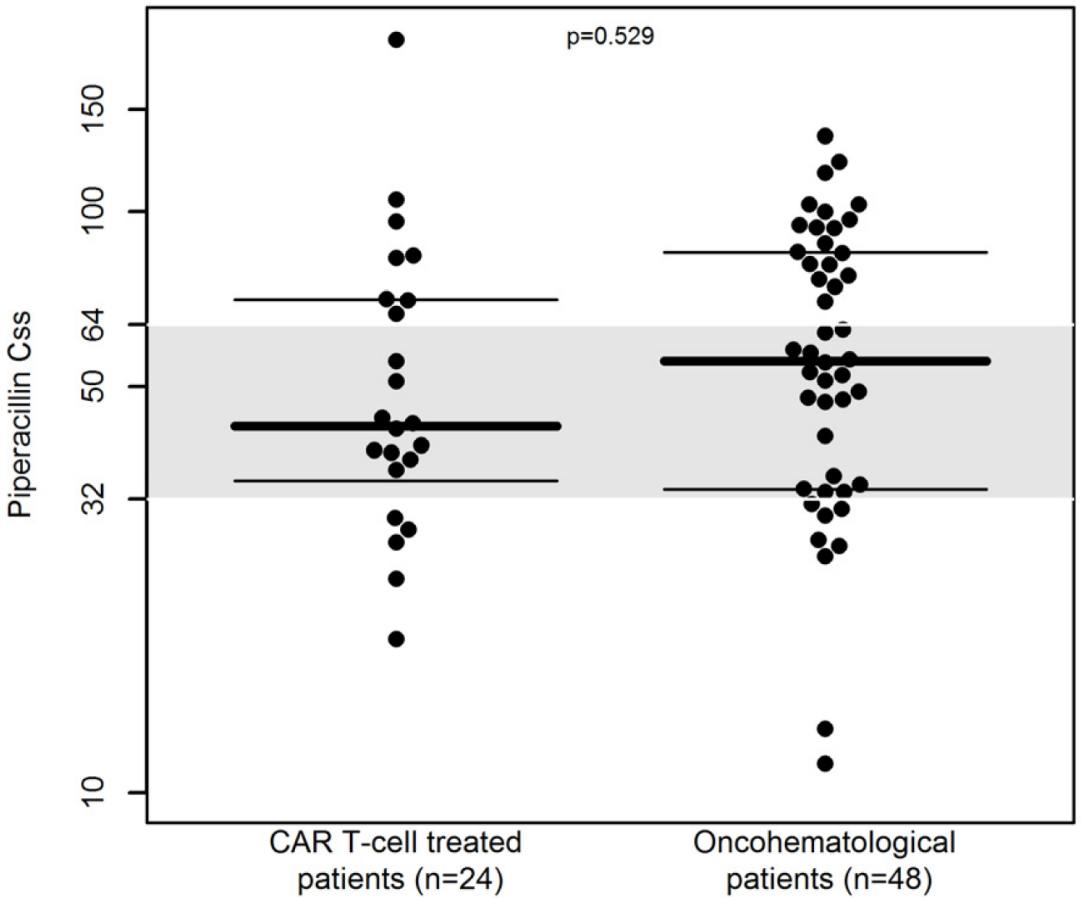

Figure 2.3: Beeswarm plot of distribution of C_{ss} of 24h-CI piperacillin/tazobactam (n=72) in CAR-T cell treated patients and in oncohematologic patients at first TDM assessment. The gray shaded area represents the desired therapeutic range (C_{ss} of 32–64 mg/L). The dashed line is the median. The dotted lines represent the 25^{th} and 75^{th} percentiles.

Bibliography

[1] Hernandez-Lopez, A.; Tellez-Gonzalez, M.A.; Mondragon-Teran, P.; Meneses-Acosta, A. Chimeric Antigen Receptor-T Cells: A Pharmaceutical Scope. Front. Pharmacol. 2021, 12, 720692.

[2] Roschewski, M.; Longo, D.L.; Wilson, W.H. CAR T-Cell Therapy for Large B-Cell Lymphoma—Who, When, and How? N. Engl. J. Med. 2022, 386, 692–696.

[3] Teoh, P.J.; Chng, W.J. CAR T-cell therapy in multiple myeloma: More room for improvement. Blood Cancer J. 2021, 11, 84.

[4] Hao, F.; Sholy, C.; Wang, C.; Cao, M.; Kang, X. The Role of T Cell Immunotherapy in Acute Myeloid Leukemia. Cells 2021, 10, 3376.

[5] Fajgenbaum, D.C.; June, C.H. Cytokine Storm. N. Engl. J. Med. 2020, 383, 2255–2273.

[6] Davila, M.L.; Riviere, I.; Wang, X.; Bartido, S.; Park, J.; Curran, K.; Chung, S.S.; Stefanski, J.; Borquez-Ojeda, O.; Olszewska, M.; et al. Efficacy and toxicity management of 19-28z CAR T cell therapy in B cell acute lymphoblastic leukemia. Sci. Transl. Med. 2014, 6, 224ra225.

[7] Gutgarts, V.; Jain, T.; Zheng, J.; Maloy, M.A.; Ruiz, J.D.; Pennisi, M.; Jaimes, E.A.; Perales, M.A.; Sathick, J. Acute Kidney Injury after CAR-T Cell Therapy: Low Incidence and Rapid Recovery. Biol. Blood Marrow Transplant. J. Am. Soc. Blood Marrow Transplant. 2020, 26, 1071–1076.

[8] Stewart, A.G.; Henden, A.S. Infectious complications of CAR T-cell therapy: A clinical update. Ther. Adv. Infect. Dis. 2021, 8, 20499361211036773.

[9] Tumbarello, M.; Trecarichi, E.M.; Caira, M.; Candoni, A.; Pastore, D.; Cattaneo, C.; Fanci, R.; Nosari, A.; Spadea, A.; Busca, A.; et al. Derivation and validation of a scoring system to identify patients with bacteremia and hematological malignancies at higher risk for mortality. PLoS ONE 2012, 7, e51612.

[10] Trecarichi, E.M.; Pagano, L.; Candoni, A.; Pastore, D.; Cattaneo, C.; Fanci, R.; Nosari, A.; Caira, M.; Spadea, A.; Busca, A.; et al. Current epidemiology and antimicrobial resistance data for bacterial bloodstream infections in patients with hematologic malignancies: An Italian multicentre prospective survey. Clin. Microbiol. Infect. Off. Publ. Eur. Soc. Clin. Microbiol. Infect. Dis. 2015, 21, 337–343.

[11] Heinz, W.J.; Buchheidt, D.; Christopeit, M.; von Lilienfeld-Toal, M.; Cornely, O.A.; Einsele, H.; Karthaus, M.; Link, H.; Mahlberg, R.; Neumann, S.; et al. Diagnosis and empirical treatment of fever of unknown origin (FUO) in adult neutropenic

patients: Guidelines of the Infectious Diseases Working Party (AGIHO) of the German Society of Hematology and Medical Oncology (DGHO). Ann. Hematol. 2017, 96, 1775–1792.

[12] Schmidt-Hieber, M.; Teschner, D.; Maschmeyer, G.; Schalk, E. Management of febrile neutropenia in the perspective of antimicro- bial de-escalation and discontinuation. Expert Rev. Anti-Infect. Ther. 2019, 17, 983–995.

[13] Craig, W.A. Pharmacokinetic/pharmacodynamic parameters: Rationale for antibacterial dosing of mice and men. Clin. Infect. Dis. Off. Publ. Infect. Dis. Soc. Am. 1998, 26, 1–10.

[14] Roberts, J.A.; Paul, S.K.; Akova, M.; Bassetti, M.; De Waele, J.J.; Dimopoulos, G.; Kaukonen, K.M.; Koulenti, D.; Martin, C.; Montravers, P.; et al. DALI: Defining antibiotic levels in intensive care unit patients: Are current beta-lactam antibiotic doses sufficient for critically ill patients? Clin. Infect. Dis. Off. Publ. Infect. Dis. Soc. Am. 2014, 58, 1072–1083.

[15] Yu, Z.; Pang, X.; Wu, X.; Shan, C.; Jiang, S. Clinical outcomes of prolonged infusion (extended infusion or continuous infusion) versus intermittent bolus of meropenem in severe infection: A meta-analysis. PLoS ONE 2018, 13, e0201667.

[16] Cojutti, P.G.; Candoni, A.; Lazzarotto, D.; Fili, C.; Zannier, M.; Fanin, R.; Pea, F. Population Pharmacokinetics of Continuous- Infusion Meropenem in Febrile Neutropenic Patients with Hematologic Malignancies: Dosing Strategies for Optimizing Empirical Treatment against Enterobacterales and P. aeruginosa. Pharmaceutics 2020, 12, 785.

[17] Cojutti, P.G.; Morandin, E.; Baraldo, M.; Pea, F. Population pharmacokinetics of continuous infusion of piperacillin/tazobactam in very elderly hospitalized patients and considerations for target attainment against Enterobacterales and Pseudomonas aeruginosa. Int. J. Antimicrob. Agents 2021, 58, 106408.

[18] Gatti, M.; Cojutti, P.G.; Bartoletti, M.; Tonetti, T.; Bianchini, A.; Ramirez, S.; Pizzilli, G.; Ambretti, S.; Giannella, M.; Mancini, R.; et al. Expert clinical pharmacological advice may make an antimicrobial TDM program for emerging candidates more clinically useful in tailoring therapy of critically ill patients. Crit. Care 2022, 26, 178.

[19] Gatti, M.; Cojutti, P.G.; Pascale, R.; Tonetti, T.; Laici, C.; Dell'Olio, A.; Siniscalchi, A.; Giannella, M.; Viale, P.; Pea, F. Assessment of a PK/PD Target of Continuous Infusion Beta-Lactams Useful for Preventing Microbiological Failure and/or Resistance Development in Critically Ill Patients Affected by Documented Gram-Negative Infections. Antibiotics 2021, 10, 1311.

[20] Cojutti, P.G.; Gatti, M.; Rinaldi, M.; Tonetti, T.; Laici, C.; Mega, C.; Siniscalchi, A.; Giannella, M.; Viale, P.; Pea, F. Impact of Maximizing Css/MIC Ratio on Efficacy of Continuous Infusion Meropenem Against Documented Gram-Negative Infections in Critically Ill Patients and Population Pharmacokinetic/Pharmacodynamic Analysis to Support Treatment Optimization. Front. Pharmacol. 2021, 12, 781892.

[21] The European Committee on Antimicrobial Susceptibility Testing. Breakpoint Tables for Interpretation of MICs and Zone Diameters, Version 11.0. 2021. Available online: http://www.eucast.org (accessed on 24 February 2023).

[22] Levey, A.S.; Stevens, L.A.; Schmid, C.H.; Zhang, Y.L.; Castro, A.F., 3rd; Feldman, H.I.; Kusek, J.W.; Eggers, P.; Van Lente, F.; Greene, T.; et al. A new equation to estimate glomerular filtration rate. Ann. Intern. Med. 2009, 150, 604–612.

[23] Santomasso, B.; Bachier, C.; Westin, J.; Rezvani, K.; Shpall, E.J. The Other Side of CAR T-Cell Therapy: Cytokine Release Syndrome, Neurologic Toxicity, and Financial Burden. Am. Soc. Clin. Oncol. Educ. Book. Am. Soc. Clin. Oncol. Annu. Meet. 2019, 39, 433–444.

[24] Neelapu, S.S.; Locke, F.L.; Bartlett, N.L.; Lekakis, L.J.; Miklos, D.B.; Jacobson, C.A.; Braunschweig, I.; Oluwole, O.O.; Siddiqi, T.; Lin, Y.; et al. Axicabtagene Ciloleucel CAR T-Cell Therapy in ref2ractory Large B-Cell Lymphoma. N. Engl. J. Med. 2017, 377, 2531–2544.

[25] O'Leary, M.C.; Lu, X.; Huang, Y.; Lin, X.; Mahmood, I.; Przepiorka, D.; Gavin, D.; Lee, S.; Liu, K.; George, B.; et al. FDA Approval Summary: Tisagenlecleucel for Treatment of Patients with Relapsed or ref2ractory B-cell Precursor Acute Lymphoblastic Leukemia. Clin. Cancer Res. Off. J. Am. Assoc. Cancer Res. 2019, 25, 1142–1146.

[26] Hong, R.; Zhao, H.; Wang, Y.; Chen, Y.; Cai, H.; Hu, Y.; Wei, G.; Huang, H. Clinical characterization and risk factors associated with cytokine release syndrome induced by COVID-19 and chimeric antigen receptor T-cell therapy. Bone Marrow Transplant. 2021, 56, 570–580.

[27] Kang, L.; Tang, X.; Zhang, J.; Li, M.; Xu, N.; Qi, W.; Tan, J.; Lou, X.; Yu, Z.; Sun, J.; et al. Interleukin-6-knockdown of chimeric antigen receptor-modified T cells significantly reduces IL-6 release from monocytes. Exp. Hematol. Oncol. 2020, 9, 11.

[28] Cojutti, P.G.; Londero, A.; Della Siega, P.; Givone, F.; Fabris, M.; Biasizzo, J.; Tascini, C.; Pea, F. Comparative Population Pharmacokinetics of Darunavir in SARS-CoV-2 Patients vs. HIV Patients: The Role of Interleukin-6. Clin. Pharmacokinet. 2020, 59, 1251–1260.

[29] Machavaram, K.K.; Almond, L.M.; Rostami-Hodjegan, A.; Gardner, I.; Jamei, M.; Tay, S.; Wong, S.; Joshi, A.; Kenny, J.R. A physiologically based pharmacokinetic modeling approach to predict disease-drug interactions: Suppression of CYP3A by IL-6. Clin. Pharmacol. Ther. 2013, 94, 260–268.

[30] Kanduri, S.R.; Cheungpasitporn, W.; Thongprayoon, C.; Petnak, T.; Lin, Y.; Kovvuru, K.; Manohar, S.; Kashani, K.; Herrmann, S.M. Systematic Review of Risk factors and Incidence of Acute Kidney Injury Among Patients Treated with CAR-T Cell Therapies. Kidney Int. Rep. 2021, 6, 1416–1422.

[31] Gupta, S.; Seethapathy, H.; Strohbehn, I.A.; Frigault, M.J.; O'Donnell, E.K.; Jacobson, C.A.; Motwani, S.S.; Parikh, S.M.; Curhan, G.C.; Reynolds, K.L.; et al. Acute Kidney Injury and Electrolyte Abnormalities After Chimeric Antigen Receptor T-Cell (CAR-T) Therapy for Diffuse Large B-Cell Lymphoma. Am. J. Kidney Dis. Off. J. Natl. Kidney Found. 2020, 76, 63–71.

[32] Nechemia-Arbely, Y.; Barkan, D.; Pizov, G.; Shriki, A.; Rose-John, S.; Galun, E.; Axelrod, J.H. IL-6/IL-6R axis plays a critical role in acute kidney injury. J. Am. Soc. Nephrol. JASN 2008, 19, 1106–1115.

[33] Su, H.; Lei, C.T.; Zhang, C. Interleukin-6 Signaling Pathway and Its Role in Kidney Disease: An Update. Front. Immunol. 2017, 8, 405.

[34] Shimazui, T.; Nakada, T.A.; Tateishi, Y.; Oshima, T.; Aizimu, T.; Oda, S. Association between serum levels of interleukin-6 on ICU admission and subsequent outcomes in critically ill patients with acute kidney injury. BMC Nephrol. 2019, 20, 74.

[35] Pai, M.P.; Cojutti, P.; Pea, F. Pharmacokinetics and pharmacodynamics of continuous infusion meropenem in overweight, obese, and morbidly obese patients with stable and unstable kidney function: A step toward dose optimization for the treatment of severe gram-negative bacterial infections. Clin. Pharmacokinet. 2015, 54, 933–941.

[36] Kees, M.G.; Minichmayr, I.K.; Moritz, S.; Beck, S.; Wicha, S.G.; Kees, F.; Kloft, C.; Steinke, T. Population pharmacokinetics of meropenem during continuous infusion in surgical ICU patients. J. Clin. Pharmacol. 2016, 56, 307–315.

[37] Usman, M.; Frey, O.R.; Hempel, G. Population pharmacokinetics of meropenem in elderly patients: Dosing simulations based on renal function. Eur. J. Clin. Pharmacol. 2017, 73, 333–342.

[38] Minichmayr, I.K.; Roberts, J.A.; Frey, O.R.; Roehr, A.C.; Kloft, C.; Brinkmann, A. Development of a dosing nomogram for continuous-infusion meropenem in critically ill patients based on a validated population pharmacokinetic model. J. Antimicrob. Chemother. 2018, 73, 1330–1339.

[39] Dhaese, S.A.M.; Farkas, A.; Colin, P.; Lipman, J.; Stove, V.; Verstraete, A.G.; Roberts, J.A.; De Waele, J.J. Population pharmacoki- netics and evaluation of the predictive performance of pharmacokinetic models in critically ill patients receiving continuous infusion meropenem: A comparison of eight pharmacokinetic models. J. Antimicrob. Chemother. 2019, 74, 432–441.

[40] Li, C.; Kuti, J.L.; Nightingale, C.H.; Mansfield, D.L.; Dana, A.; Nicolau, D.P. Population pharmacokinetics and pharmacodynamics of piperacillin/tazobactam in patients with complicated intra-abdominal infection. J. Antimicrob. Chemother. 2005, 56, 388–395.

[41] Dhaese, S.A.M.; Roberts, J.A.; Carlier, M.; Verstraete, A.G.; Stove, V.; De Waele, J.J. Population pharmacokinetics of continuous infusion of piperacillin in critically ill patients. Int. J. Antimicrob. Agents 2018, 51, 594–600.

[42] Richter, D.C.; Frey, O.; Rohr, A.; Roberts, J.A.; Koberer, A.; Fuchs, T.; Papadimas, N.; Heinzel-Gutenbrunner, M.; Brenner, T.; Lichtenstern, C.; et al. Therapeutic drug monitoring-guided continuous infusion of piperacillin/tazobactam significantly improves pharmacokinetic target attainment in critically ill patients: A retrospective analysis of four years of clinical experience. Infection 2019, 47, 1001–1011.

[43] Trosi, C.; Cojutti, P.; Rinaldi, M.; Laici, C.; Siniscalchi, A.; Viale, P.; Pea, F. Measuring Creatinine Clearance Is the Most AccurateWay for Calculating the Proper Continuous Infusion Meropenem Dose for Empirical Treatment of Severe Gram-Negative Infections among Critically Ill Patients. Pharmaceutics 2023, 15, 551.

[44] Dong, J.; Liu, Y.; Li, L.; Ding, Y.; Qian, J.; Jiao, Z. Interactions Between Meropenem and Renal Drug Transporters. Curr. Drug Metab. 2022, 23, 423–431.

[45] Daenen, S.; Erjavec, Z.; Uges, D.R.; De Vries-Hospers, H.G.; De Jonge, P.; Halie, M.R. Continuous infusion of ceftazidime in febrile neutropenic patients with acute myeloid leukemia. Eur. J. Clin. Microbiol. Infect. Dis. Off. Publ. Eur. Soc. Clin. Microbiol. 1995, 14, 188–192.

[46] Cojutti, P.G.; Candoni, A.; Ramos-Martin, V.; Lazzarotto, D.; Zannier, M.E.; Fanin, R.; Hope, W.; Pea, F. Population pharmacoki- netics and dosing considerations for the use of daptomycin in adult patients with haematological malignancies. J. Antimicrob. Chemother. 2017, 72, 2342–2350.

[47] Abdul-Aziz, M.H.; Alffenaar, J.C.; Bassetti, M.; Bracht, H.; Dimopoulos, G.; Marriott, D.; Neely, M.N.; Paiva, J.A.; Pea, F.; Sjovall, F.; et al. Antimicrobial therapeutic drug monitoring in critically ill adult patients: A Position Paper. Intensive Care Med. 2020, 46, 1127–1153.

[48] Hirai, K.; Ishii, H.; Shimoshikiryo, T.; Shimomura, T.; Tsuji, D.; Inoue, K.; Kadoiri, T.; Itoh, K. Augmented Renal Clearance in Patients With Febrile Neutropenia is Associated With Increased Risk for Subtherapeutic Concentrations of Vancomycin. Ther. Drug Monit. 2016, 38, 706–710.

[49] Gijsen, M.; Wilmer, A.; Meyfroidt, G.; Wauters, J.; Spriet, I. Can augmented renal clearance be detected using estimators of glomerular filtration rate? Crit. Care 2020, 24, 359.

[50] Declercq, P.; Gijsen, M.; Meijers, B.; Schetz, M.; Nijs, S.; D'Hoore, A.; Wauters, J.; Spriet, I. Reliability of serum creatinine-based formulae estimating renal function in non-critically ill surgery patients: Focus on augmented renal clearance. J. Clin. Pharm. Ther. 2018, 43, 695–706.

Chapter 3

The Role of The Pharmacometrics/Mathematical Models in Precision Dosing

Part A: Population Pharmacokinetics/Pharmacodynamics of Meropenem and C-Reactive Protein in Oncohematologic Patients

Abstract

Background: Oncohematologic patients with febrile neutropenia (FN) are at high risk of developing severe infections due to multidrug-resistant Gram-negative pathogens. Meropenem is a beta-lactam commonly used as a second-line antimicrobial in those patients. Although the use of 24h continuous infusion (CI) administration coupled with therapeutic drug monitoring may optimize meropenem exposure, patient response to therapy is still difficult to predict, and the identification of clinical biomarkers of response may be highly beneficial. The aim of this study was to assess the pharmacokinetic/pharmacodynamic (PK/PD) relationship between 24h-CI meropenem and C-reactive protein (C-RP) in a cohort of oncohematologic patients with FN.

Methods: All patients included were administered 24h-CI meropenem for the treatment of FN. Meropenem steady-state concentrations (C_{ss}) and C-RP measurements were collected during therapy, along with demographics and clinical data. A joint population PK/PD model was adopted to fit meropenem C_{ss} and C-RP values by means of Monolix® software. PK/PD analysis evaluated diverse indirect PK/PD models linking C-RP and meropenem concentrations. Monte Carlo simulations were generated to obtain C-RP concentrations-vs-time profiles according to different meropenem dosages optimized for renal function. The probability of target attainment (PTA) was defined as the proportion of patients having a 25%, 50%, and 75% reduction of C-RP levels from baseline in each simulated scenario at days 3, 5, and 7 from starting therapy.

Results: Totally, 141 oncohematologic patients (59.57% males, 84/141), who provided 283 meropenem C_{ss} and 1373 C-RP concentrations, were enrolled. Among those patients, 82 (58.2%, 82/141) received meropenem plus an anti-Gram-positive agent plus an antifungal agent, and 52 (36.9, 52/141) received meropenem plus an antifungal agent. A one-compartment model that included estimated glomerular filtration rate as a covariate on meropenem clearance was built based on all the patients (n=141). The population estimate of meropenem CL was 13.3 L/h. The PD model was based on data coming from patients receiving both meropenem and antifungal agents (n=134). C-RP profiles were best described by a turnover full inhibition of the production model. No significant covariates were identified on any PD parameters. The IC50 was 41.5 mg/L. Monte Carlo simulations showed that PTA of 50% C-RP reduction from baseline assessed at days 3, 5, and 7 and associated with the dose of 1 g q8h by CI were 23.9%, 42.1%, and 56.3%, respectively; those associated with the dose of 1g q6h by CI were of 24.1%, 41.6%, and 55.6%, respectively; and those associated with the dose of 1.25g q6h by CI were of 22.5%, 39.9%, and 54.4%, respectively.

Conclusion: The decrease of C-RP in oncohematologic patients treated with meropenem for FN is slow during the first two weeks of therapy. C-RP does not represent a reliable biomarker of quick response to meropenem therapy.

Keywords: population PK/PD, C-Reactive Protein, Meropenem, Oncohematologic patients

3.1 Introduction

Oncohematologic patients undergoing induction chemotherapy or conditioning regimens for stem cell transplantation are vulnerable to developing infectious complications. Bloodstream infection caused by Gram-negative pathogens is the most common infection in this population, with a prevalence rate of 11-38%[1]. Antimicrobial agents that are conventionally used in onchohematologic patients should target *Enterobacterales*, such as *Escherichia coli*, *Klebsiella pneumoniae*, *Enterobacter cloacae*, and non-fermenting pathogens such as *Pseudomonas aeruginosa*[2].

International guidelines recommend antipseudomonal beta-lactams, e.g., ceftazidime, piperacillin/tazobactam, or cefepime as first-line agents for the treatment of febrile neutropenia (FN) in oncohematologic patients[3], [4]. Escalation to meropenem is suggested in case of no response within the next 48-72h.

The pharmacodynamic (PK) activity of meropenem is maximized when its plasma concentration is maintained 4-6 folds higher than pathogen minimum inhibitory concentration (MIC) for 100% of the dosing interval (100% $fT_{>4\text{-}6\ folds}MIC$)[5], [6]. Administration of meropenem by 24h continuous infusion (CI) and therapeutic drug monitoring (TDM) may be highly beneficial for attaining this optimal PK/pharmacodynamic (PK/PD) target of efficacy[7], [8].

In this population, measurement of correct antibiotic exposure, clinical judgment of the evolution of signs and/or symptoms of infection, and measurement of inflammatory biomarkers such as C-reactive protein (C-RP) are used to assess the response to therapy[9], [10]. C-RP is an acute-phase protein that is extensively used in diagnosing and managing bacterial infectious diseases[11], [12]. However, few studies have investigated the relationship between antimicrobial exposure and C-RP dynamics.

The aim of this study was to develop a population PK/PD model to describe the C-RP dynamics in relation to meropenem exposure over time in a cohort of oncohematologic patients treated for FN and to simulate the attainment of both C-RP halving from baseline and C-RP negativization.

3.2 Materials and Methods

3.2.1 Study Design

This was a retrospective single-center clinical study that included all consecutive adult oncohematologic patients who were admitted to the Division of Hematology of the IRCCS Azienda Ospedaliero-Universitaria di Bologna, Italy, between January 2021 and August 2023 and who were treated with 24h-CI meropenem as a second-line single-agent therapy for FN. This study was approved by the ethics committee of the study hospital (No. 308/2021/Oss/AOUBo). Written informed consent was waived due to the retrospective nature of this investigation.

Meropenem dose was initiated in all the patients with a loading dose of 1g over 30min followed by a maintenance dose of 1g q8h CI over 8h if the estimated glomerular filtra-

tion rate (eGFR)<90 mL/min/1.73m^2 or 1g q6h CI over 6h if eGFR between 90-130 mL/min/1.73m^2 or 1.25g q6h CI over 6h if eGFR>130 mL/min/1.73m^2. Stability of 24h-CI meropenem was granted by reconstituting each solution every 6-8 h with infusions of 6-8h. Real-time TDM-based clinical pharmacological advice was applied for guiding meropenem dosages, with the intent of targeting meropenem steady-state concentration (C_{ss}) over MIC ratio (C_{ss}/MIC) between 4-8 folds of the EUCAST clinical breakpoint of 2 mg/L against *Enterobacterales* and *Pseudomonas aeruginosa*, finalized at achieving meropenem C_{ss} at 8-16 mg/L. TDM was first assessed after at least 48 hours from starting therapy and then reassessed every 48-72h until the end of treatment. At each TDM assessment, 3 mL of peripheral blood samples were collected and meropenem concentrations were analyzed by means of a validated liquid chromatography-tandem mass spectrometry (LC-MS/MS) commercially available method (Chromsystems Instruments & Chemicals GmbH, Munich, Germany). The lower limit of detection was 0.3 mg/L.

Meropenem C_{ss} and C-RP concentrations were collected during therapy, along with the following demographics and clinical data from each patient's medical record: age, gender, weight, height, serum creatinine, eGFR, type and site of infection, and microbiological isolates with meropenem MIC. The Chronic Kidney Disease Epidemiology (CKD-EPI) formula was used for eGFR calculation[13].

To adequately assess the relationship between meropenem exposure and C-RP dynamics, the patients were divided into the following groups: (a) patients receiving meropenem, anti-fungal agents, and anti-Gram-positive agents; (b) patients receiving meropenem and anti-fungal agents; (c) patients receive meropenem and anti-Gram-positive agents; (d) patients receive meropenem alone.

3.2.2 Population Pharmacokinetic/Pharmacodynamic Analysis

A PK/PD model based on the stochastic approximation of the standard expectation maximization (SAEM) algorithm was implemented in Monolix® (version 2023R1, Lixoft, Antony, France). To overcome initial model instability and biases when simultaneously fitting sparse clinical PK and PD data, an intermediate PK/PD approach was used for model building. This approach consisted in building at first a PK model. Then, the median Bayesian posterior estimates of the PK parameters were fixed and integrated into a PK model which was built to fit the individual C-RP concentration over time. Different PD models were tested on C-RP production and degradation. Diverse covariates, i.e., eGFR, weight, height, age, and gender, were tested on each PK/PD parameter. Exponential random effects were assumed to describe between-subject variability. Correlations between random effects were tested in the variance-covariance matrix and implemented into the structural model accordingly. Constant, proportional, or combined error models were tested to describe the residual variability.

Since all meropenem concentrations were collected during 24h-CI administration, modeling was built according to the one-compartment pharmacokinetic model develop in oncohematologic patients by Cojutti et al.[8], which included only eGFR as a covariate of meropenem total clearance. As the adoption of the one-compartment model and the 24-CI administration did not allow to adequately estimate the distribution volume (V), it was fixed to 28.5 L as reported[14]. The structural PD model was an indirect turnover model with inhibition of C-RP generation, as described below:

$dR/dt = k_{\text{in}} \times (1 - \frac{Cc}{Cc+IC50} \times e^{-k \times t} - k_{\text{out}} \times R)$

where R represents the response (i.e., C-RP concentration in plasma); dR/dt represents the changing rate of C-RP in plasma relative to time; Cc is meropenem plasma concentration; kin and k_{out} represent the production and degradation rate constant, respectively, of C-RP; IC50 represents the meropenem concentration causing the half-maximal rate of C-RP reduction; k is a time-dependent constant introduced to discriminate C-RP trends.

3.2.3 Model Evaluation

Evaluation of the PK/PD model was based on the following goodness-of-fit plots: individual prediction (IPRED) vs. observation, individual weighted residuals (IWRES) vs. IPRED. A prediction-corrected visual predictive checks (pcVPC) showing the time course of the 10^{th}, 50^{th}, and 90^{th} percentiles of the observation and the corresponding 90% prediction intervals were calculated from 10,000 Monte Carlo samples. A PK or PD model is considered adequate if the 10^{th}, 50^{th}, and 90^{th} percentiles of observed data are inside the simulated prediction intervals. Model appropriateness was assessed by comparing the objective function values (OFV) and the Akaike information criteria (AIC) among tested models. A reduction of at least 3.84 points of the OFV along with a reduction of the AIC were used for model selection. Standard errors (SE) and percentage of relative standard errors (%RSE) of parameters were calculated from the Fisher information matrix. One thousand nonparametric bootstrap iterations with resampling of each population parameter were simulated with the "Rsmlx" package of R.

3.2.4 Monte Carlo Simulation and Probability of Target Attainment

Monte Carlo simulations based on the final PK/PD model were performed in Simulix® (version 2021R1, Lixoft, Antony, France). A total of 3 simulated clinical scenarios were created in order to obtain C-RP concentration-vs-time profiles after the administration of the meropenem dosages recommended for empirical treatment of FN in onco-hematological patients, namely 1g q8h by CI, 1g q6h by CI, and 1.25g q6h by CI in patients with eGFR classes of 50-89 mL/min/1.73m^2, 90-129 mL/min/1.73m^2, and >130 mL/min/1.73m^2 [8]. The probability of target attainment (PTA) was defined as proportion of patients having 25%, 50%, and 75% reduction of C-RP levels from baseline in each simulated scenario at days 3, 5, and 7. Optimal PTA was considered>90%.

3.3 Results

3.3.1 Demographics and Clinical Data

A total of 141 patients (59.57% males, 84/141) were included in this PK/PD analysis, of which 82 were concomitant with anti-fungal and anti-Gram positive antibiotics and 52

were concomitant with antifungal (Figure 3.1). Median (min-max range) age, weight, and eGFR were 59 (19-81) years, 70 (42-118) kg, and 97 (17-195.6) mL/min/1.73m^2, respectively (Table 3.1). Acute myeloid leukemia was the most frequent hematologic malignancy in the population (91/141, 64.54% of patients). Microbiological isolates were identified in 46/141 patients. The medium (min-max range) duration of meropenem treatment was 10 (2-32) days. The median (min-max range) number of meropenem concentration and C-RP measurements per patient were 2 (1-7) and 12 (1-32), respectively. The median (min-max range) of C_{ss} and of C-RP at baseline were 11.4 (3.0-39.5) mg/L and 9.83 (4.99 to 17.35) mg/dL.

3.3.2 Population Pharmacokinetic/Pharmacodynamic Modeling

A total of 283 meropenem plasma C_{ss} and 1373 plasma C-RP measurements were included in the PK/PD models. A one-compartment model with zero-order administration and first-order elimination from the central compartment was developed and eGFR was included as a covariate on clearance in the final population PK model. The coefficient of determination (R^2) of the observed versus individual-predicted concentrations was 0.85 (Figure 3.2A). The population estimate of CL was 13.34 L/h with an inter-individual variability of 45%. No trends were observed in the distribution of the IWRES vs. IPRED (Figure 3.2C). The pcVPC showed good predictive performance of the population PK model as most of the concentrations were within the prediction intervals (Figure 3.3A).

The PK values of the population estimates and of the standard deviation of the random effects were included as fixed values in an indirect turnover PD model. The fit of the PK/PD model to C-RP data yielded an R^2 of 0.83 for the observed versus individual-predicted concentrations (Figure 3.2B). The pcVPC of the PK/PD model confirmed the adequacy of model predictions (Figure 3.3B). The parameter estimates of the PK/PD model are summarized in Table 3.2. Model parameters were estimated with good precision as RSE% was less than 30% for most of them.

3.3.3 Monte Carlo Simulation

The PTAs of C-RP reduction by 25%, 50%, and 75 over the first two weeks of treatment are shown in Figure 3.4. The doses of 1g q8h for the eGFR class of 50-89 mL/min/1.73m^2, 1q q6h for the eGFR class of 90-130 mL/min/1.73m^2 and of 1.25g q6h for the eGFR class of >130 mL/min/1.73m^2 started reducing C-RP after 47, 43 and 52 hours from starting therapy, respectively.

PTAs of C-RP reduction by 25% at day 3, 5 and 7 were of 37.94%, 53.34%, and 65.59%, respectively, for the regimens of 1g q8h, of 37.40%, 52.64%, and 64.87%, respectively, for the regimen of 1g q6 h and of 35.92%, 51.10%, and 63.64%, respectively, for the regimen of 1.25g q6h by CI (Figure 3.4A).

PTAs of C-RP reduction by 50% at day 3, 5 and 7 were of 23.93%, 42.04%, and 56.29%, respectively, for the regimens of 1g q8h, of 24.04%, 41.61%, and 55.57%, respectively, for the regimen of 1g q6h and of 22.45%, 39.90%, and 54.40%, respectively, for the regimen of 1.25g q6h by CI (Figure 3.4B).

PTAs of C-RP reduction by 75% at day 3, 5 and 7 were of 4.07%, 23.23%, and 39.97%, respectively, for the regimens of 1g q8h, of 3.97%, 23.28%, and 39.47%, respectively, for the regimen of 1g q6h and of 3.63%, 22.20%, and 37.54%, respectively, for the regimen of 1.25g q6h by CI (Figure 3.4C).

3.4 Discussion

In this study, the relationship between meropenem and C-RP in febrile neutropenic onco-hematological patients was assessed by a population PK-PD approach. The model-based simulation demonstrated the C-RP profile over 14 days further clarified the possibility of using C-RP as a response biomarker to meropenem treatment. To our knowledge, this is the first quantitative study that described the exposure-response relationship between meropenem and C-RP in onco-hematological patients and presents intriguing insights into the complexities of antibiotic therapy within this specific clinical context.

The PK model of meropenem was described by a one-compartment model since all meropenem concentrations were collected during 24h-CI administration. The influence of age, gender, weight, height, serum creatinine, eGFR, and type/site of infection on meropenem PK were evaluated. Considering meropenem is predominantly eliminated by the kidneys, eGFR was included as a covariate of meropenem total clearance as that in the previous study[8]. From a pathophysiological point of view, chronic inflammation induced intracellular fluid leakage and/or organ dysfunction in oncohematologic patients might alter the PK of meropenem, especially affecting antibiotic distribution. Meanwhile, most of our study patients provided only one steady-state measurement, which further challenges estimating of V mathematically. In our study, the V was therefore fixed (28.5 L) to stabilize the model fitting[14].

The population PK of meropenem has been broadly investigated by multiple studies, including three conducted among patients with hematological malignancies during intermittent infusion (n=2) and continuous infusion (n=1). Contejean et al. found that among 88 onco-hematological patients (median CLCr was 120 mL/min/1.73m^2) who received a meropenem dose of 1g to 2g by 30min to 1h infusion every 8h, the estimated CL and V were 12.3 L/h and 28.5 L, respectively[14]. Lee et al. reported that among 57 Korean onco-hematological patients (median CLCr was 121 mL/min) who were treated with 0.5g every 8h meropenem by intermittent infusion, the CL and V were 9.7 L/h and 14.6 L, respectively[15]. In another study conducted in 61 febrile neutropenic patients with hematologic malignancies (median CLCr was 107.3 mL/min/1.73m^2) who were administered with 2g to 4g 24-CI meropenem, the final estimates were 13.04 L/h for CL and 21.88 L for V[8]. Overall, our model showed a similar meropenem CL (13.34 L/h) with that reported in previous studies.

A turnover, full inhibition model was employed to describe C-RP response to meropenem therapy, indicating the generation of C-RP was inhibited by meropenem treatment. There is considerable C-RP variability in our study population. To capture variations of real-world data, we introduced a versatile parameter k to characterize the time-varying generation rate of C-RP. This parameter improved individual C-RP fitting significantly, despite the IIV being large (IIV=1.51). This model gave a typical IC50 estimate of 41.5 mg/L, making it difficult for physicians to determine the optimal meropenem dosing regimen. With referent to this value, the meropenem concentration that exerts

90% inhibitive C-RP generation effect would be extremely higher than the EUCAST suggested exposure (8-16 mg/L) calculated by a frequently used clinical breakpoint (2 mg/L) against Enterobacterales and Pseudomonas aeruginosa. Despite that meropenem exhibits a wide therapeutic window and benefits of using meropenem typically outweigh the potential risks when it is prescribed appropriately, dose increasement can still lead to risk of adverse effect or promote resistance development[16], [17]. This indicates that the IC50 estimated by the PK/PD model might be unplausible and unreliable in clinical practice.

Model-based Monte Carlo simulations and PTA analysis presented the target attainment over time among patients undergoing 3 frequently used dose regimens (Figure 3.4). Based on the estimated IC50 value, none of the simulated scenarios achieved the predefined optimal PTA within the first week. Findings were similar at the timepoint of 2 weeks, indicating that under this assumption none of these dose regimens were of sufficient magnitude to be considered clinically optimal and warrant a desirable treatment outcome. Considering the unplausible high IC50 of meropenem and slow response of C-RP, C-RP seems not to be a good biomarker to meropenem treatment in oncohematologic patients.

Possible explanations, in our opinion, include first, the stimulation of C-RP production in our study population was not unique. The level of C-RP can be elevated in various conditions of inflammation, not only limited to bacterial infections-, but also including surgery-, tissue injury-, and certain cancer-induced inflammation[18]–[20]. Baseline C-RP levels are also vary depending on age, sex or so. Besides infections, in oncohematologic patients, disease-related and/or treatment-induced inflammation are potential explanations of C-RP elevation. For example, hematologic malignancy induced paraneoplastic syndromes and bone marrow dysfunction can cause systematic chronic inflammation[21]. A certain type of hematologic malignancy, e.g., leukemia cells, can infiltrate organs and tissues[22], [23], leading to inflammation and elevated C-RP levels as well.

Second, meropenem is mostly prescribed empirical and it is not the only anti-infection agent used. Treatment of FN is almost always empiric in oncohematologic patients, prescribing the appropriate type and dose of anti-infection agent with microbiological evidence was unfeasible in most cases[24]. In our study population, 2/3 (89/134) were undergoing empiric meropenem treatment, meaning that we did not know prior if the pathogen was susceptible to meropenem or was the meropenem adequately exposed. Moreover, fungal and Gram-positive pathogen infection related C-RP elevation is a considerable confounding of precision meropenem therapy. In this population the concomitant use of antifungal and anti-Gram-positive prophylaxis was very common[24], namely meropenem is not the only agents that acting on C-RP.

Third, immune system state is another aspect affecting C-RP generation/degredation. As we all know, host defense is a crucial manifestation of the immune system's function in body homeostasis maintenance[25], [26]. An infection-induced inflammatory environment, e.g., reflected by the elevated C-RP, could alert/activate the healthy immune system, which is a prerequisite to the adaptive immune response against pathogens[25], [27], [28]. However, oncohematologic therapy destroys the immune system, consequently leading to an immunocompromised state in onco-hematological patients. With a weakened immune system, signs, symptoms, and response of infection are typically attenuated. The time and ability of recovering from immunocompromised state diverse patient by patient, which indicates that the robustness of the immune system is inconsistent among patients and difficult to assess in our study population. In recent years, antibi-

otics have been reported to possibly interact/interfere with the host's immune system. Different authors showed that antibiotics might harm the immune-modulating effect by damaging the gut environment[29]. On the other hand, antibiotics and the immune system reinforce each other in maintaining body homeostasis. The sophisticated interaction between the immune system and meropenem in onco-hematological patients remains unclear, which might be a causative of IC50 variability/unplausibility. We tried to check the immune system status by counting white blood cells, then tested the association between IC50 and white blood cell count. However, no significant correlation was found from those data. To figure this issue out, a physiologically based pharmacokinetic or quantitative systems pharmacology might help in future studies.

To date, absolute level of C-RP alone is not conclusive evidence of patient's response to antibiotic therapy in oncohematologic patients. Fever is a common hematologic presentation. The value of body temperature in combination with other inflammatory markers has been explored in several studies. Consideration of body temperature and inflammatory markers significantly increased the diagnosis accuracy. Yet unfortunately we could not retrospectively retrieve real-time body temperature. Procalcitonin is another sensitive biomarker of bacterial infection, however, its value in oncohematologic patients was limited due to the low absolute levels ($<$0.2 ng/mL). Instead of checking the absolute value of C-RP, monitoring biomarker dynamics to predict the treatment outcome has been preferred in recent years. Povoa et al. presented the possibility of using C-RP kinetics to identify patients' (n=935) outcomes after community-acquired bloodstream infection[30], suggesting that the C-RP dynamic may provide earlier warning of intervention. This approach may be worthwhile in our subsequent studies.

Some limitations can be raised in this study. First, estimated instead of measured renal function would perhaps lead to unexplained variability in PK modeling. Second, this retrospective study may be biased by patient selection and group settings, e.g., the number of meropenem or C-RP assessments per patient, length of treatment duration, the number of patients within each renal function class, and the C-RP trend, were imbalanced among patients and simulated scenarios, respectively. Whereas, from another side of view the complex instances reflecting a real-world population is a valuable strength of this study. Last but not least, lack of data relating to immune system hindered our understanding in how the immune system interacts with pathogens by generating C-RP.

In conclusion, the present study investigated the utility of C-RP as a biomarker response to meropenem treatment in onco-hematological patients. The model-based simulation revealed that the decrease of C-RP in onco-hematological patients treated with meropenem for FN is slow during the first two weeks of therapy. C-RP does not represent a reliable biomarker of quick response to meropenem therapy. Possible factors affecting C-RP may include the type and state of the underlying hematological disease. Further studies are needed to assess the role of C-RP in relation to the type of hematological malignancy for guiding antimicrobial therapy.

Table 3.1: Population demographics and clinical information.

Number of subjects (n)	141
Gender (n (%), [Female/Male],)	57/84 (40.43%/59.57%)
Age (year, median (IQR))	59 (52-64)
Weight (kg, median (IQR))	70 (62-80)
Height (m, median (IQR))	1.70 (1.65-1.79)
CLCr* (mL/min/1.73m^2, median (IQR))	97 (80-109)
Underlying Disease (n, %)	
AML	91 (64.54%)
NHL	23 (16.31%)
ALL	9 (6.38%)
MM	6 (4.26%)
CML	3 (2.13%)
CLL	2 (1.42%)
Other#	7 (4.96%)
Dosage regimens start from	2g loading dose+ 4g daily dose
Treatment duration (day, median (IQR))	10 (7-13)
C_{ss} (mg/L, median (IQR))	11.4 (8.05-16.45)

* CLCr was calculated through the CDK-EPI formula.
# Other: pancytopenia; myelodysplastic syndrome; vexas syndrome.
Abbreviation: AML, acute myeloid leukemia; NHL, non-Hodgkin lymphoma; ALL, acute lymphoid leukemia; MM, Multiple Myeloma; CML, Chronic myeloid leukemia; CLL, Chronic lymphoid leukemia.

Table 3.2: Final estimates of the population PK/PD model.

Parameters	Final PK-PD model		Bootstrap*	
	Estimates	RSE (%)	median	5^{th} – 95^{th} percentiles
Fixed effects				
V (L)	28.5	-	-	-
CL (L/h)	4.99	15.4	4.86	3.95 - 7.23
β CL-CLCr	0.009	17.7	0.0093	0.0054 - 0.0115
R0 (mg/dL)	5.82	13.2	7.08	3.85 - 9.28
k_{out} (h^{-1})	0.02	4.86	0.02	0.02 – 0.02
IC50 (mg/L)	41.5	23.6	79	23.72 – 405.58
k_{in} ($mg/dL*h^{-1}$)	0.49	6.09	0.42	0.30 – 0.56
k (h^{-1})	0.0037	15.7	0.0035	0.0019 – 0.0050
Random effects				
ω for V	1.64	12.7	1.61	1.27 - 1.92
ω for CL	0.45	7.34	0.45	0.38 – 0.49
ω for R0	1.25	8.35	1.14	0.92 – 1.39
ω for k_{out}	0.21	22.4	0.20	0.13 – 0.36
ω for IC50	1.68	11.2	2.05	1.42 – 3.13
ω for k_{in}	0.47	10.2	0.48	0.36 – 0.65
ω for k	1.51	7.59	1.56	1.26 – 2.08
Residual variability				
b1	0.27	5.99	0.26	0.24 – 0.29
a2 (mg/dL)	0.11	24.6	0.10	0.02 – 0.22
b2	0.31	2.88	0.31	0.28 – 0.34

* Bootstrap results were based on 1000 simulations.
Abbreviations: RSE(%), relative standard error of the estimate; CL, clearance; V, the volume of distribution; R0, baseline C-RP level; k_{out}, the degradation rate constant of C-RP; IC50, half maximal inhibitory concentration of meropenem; k_{in}, the generation rate constant of C-RP; k, a constant related to C-RP production rate; IIV, interindividual variability; b1: proportional residual error for PK model; a2, constant residual error for PD model; b2, proportional residual error for PD model.

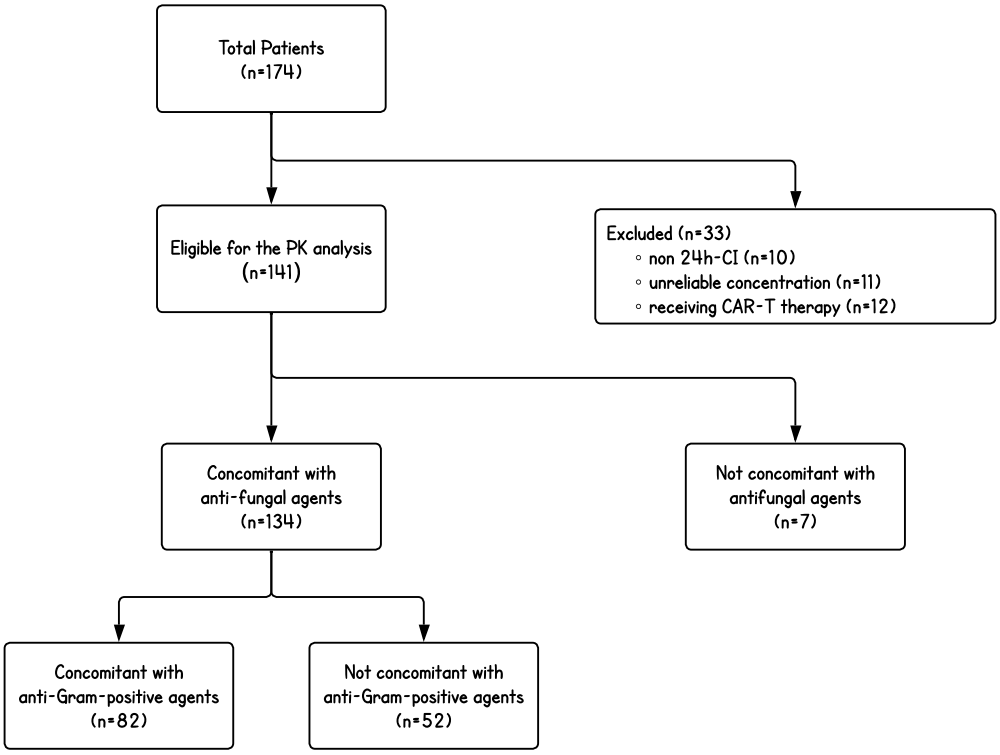

Figure 3.1: Flowchat of patients inclusion criteria in the study.

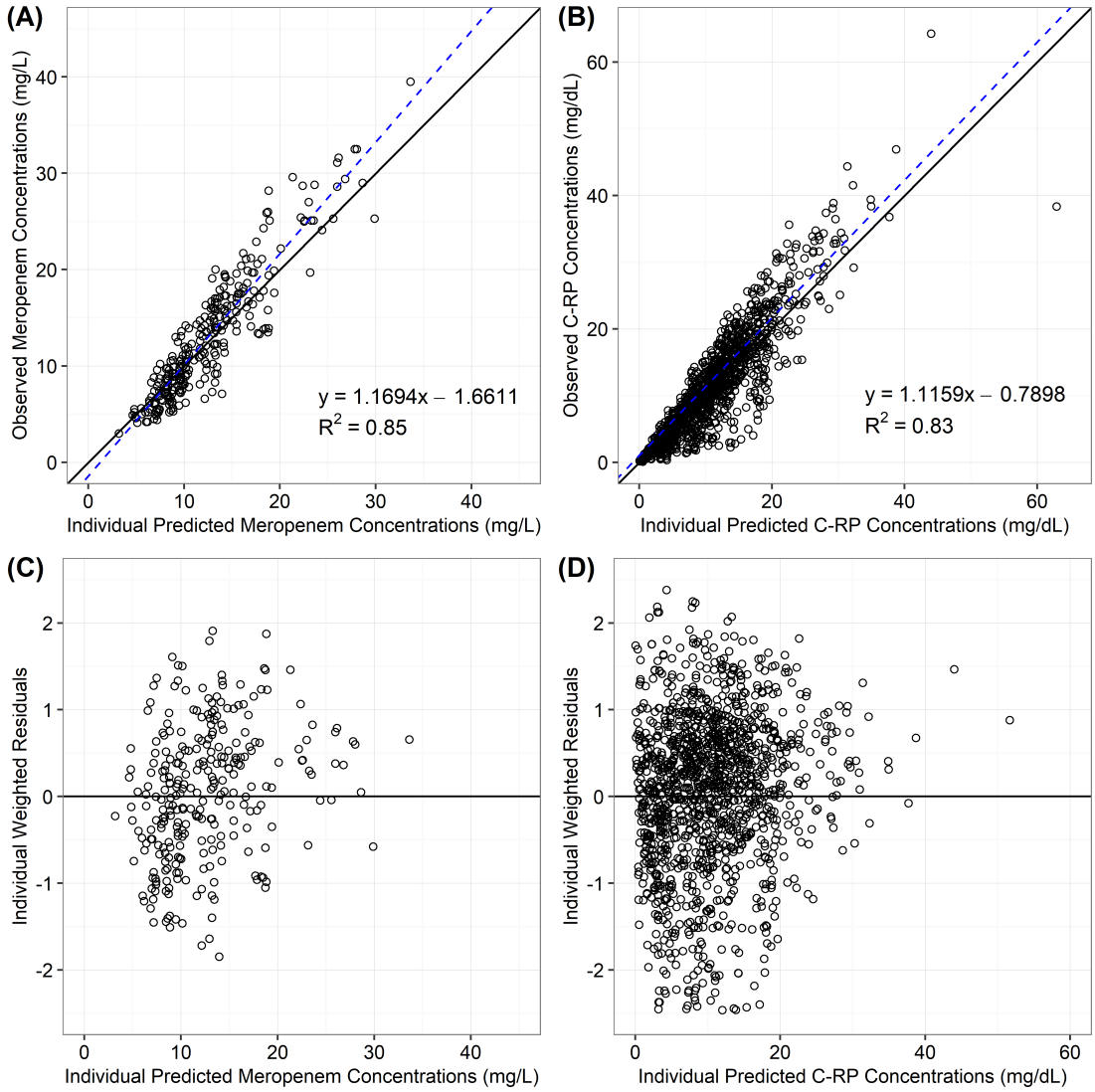

Figure 3.2: Diagnosis plot of the population PK/PD model. (A) Individual predictions of meropenem concentration (IPRED) vs. observed meropenem concentrations, the solid black line is the reference line of x=y while the dashed blue line is the linear regression between IPRED and meropenem observations; (B) Individual predictions of C-RP concentration (IPRED) vs. observed C-RP concentrations, the solid black line is the reference line of x=y while the dashed blue line is the linear regression between IPRED and C-RP observations; (C) Idividual weighted residuals (IWRES) vs. Individual predictions of meropenem concentration (IPRED), the solid black line is the reference line of y=0; (D) Individual weighted residuals (IWRES) vs. Individual predictions of C-RP concentration (IPRED), the solid black line is the reference line of y=0.

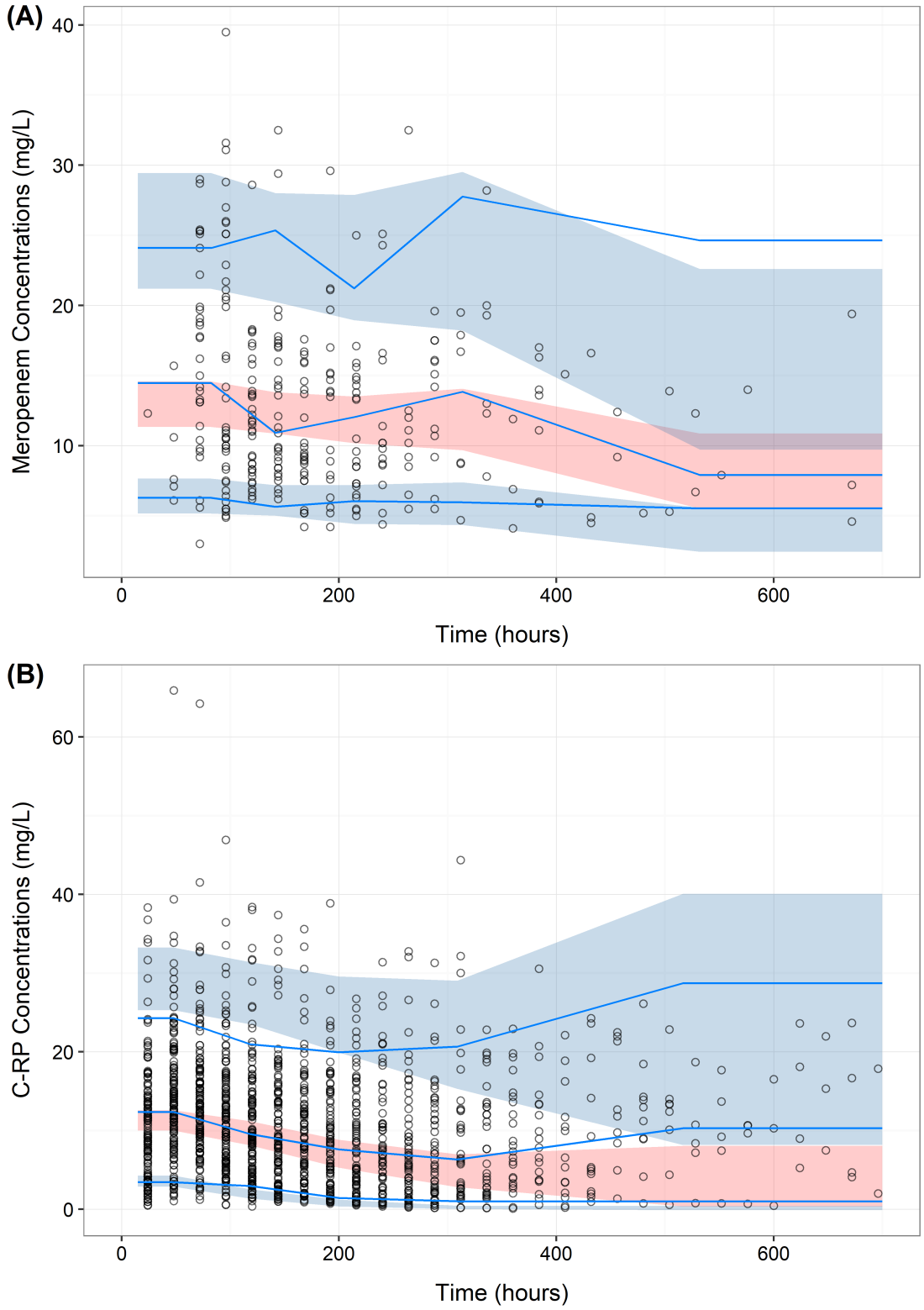

Figure 3.3: Prediction-corrected visual predictive checks (pcVPC) of the PK/PD model. Plot based on 10,000 Monte Carlo simulations. The solid blue lines represent the 10^{th}, 50^{th}, and 90^{th} percentiles of the observed data. The blue and pink shadows are simulation-based 90^{th} confidence intervals around the 10^{th}, 50^{th}, and 90^{th} percentiles of the observed data. The blue dots are the observed (A) meropenem concentrations and (B) C-RP concentrations.

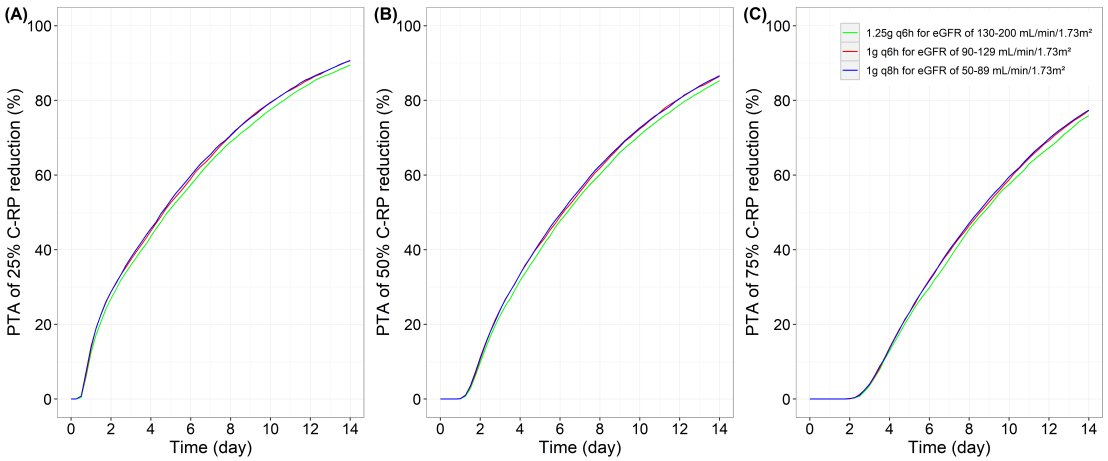

Figure 3.4: Monte Carlo simulations. Probability of attaining (A) 25%, (B) 50%, and (C) 75% C-RP reduction from baseline over time associated with the dosing regimen of 1g q8h, 1g q6h, and 1.25g q6h by CI for the eGFR classes of 50-89, 90-129 and >130 mL/min/1.73m^2, respectively.

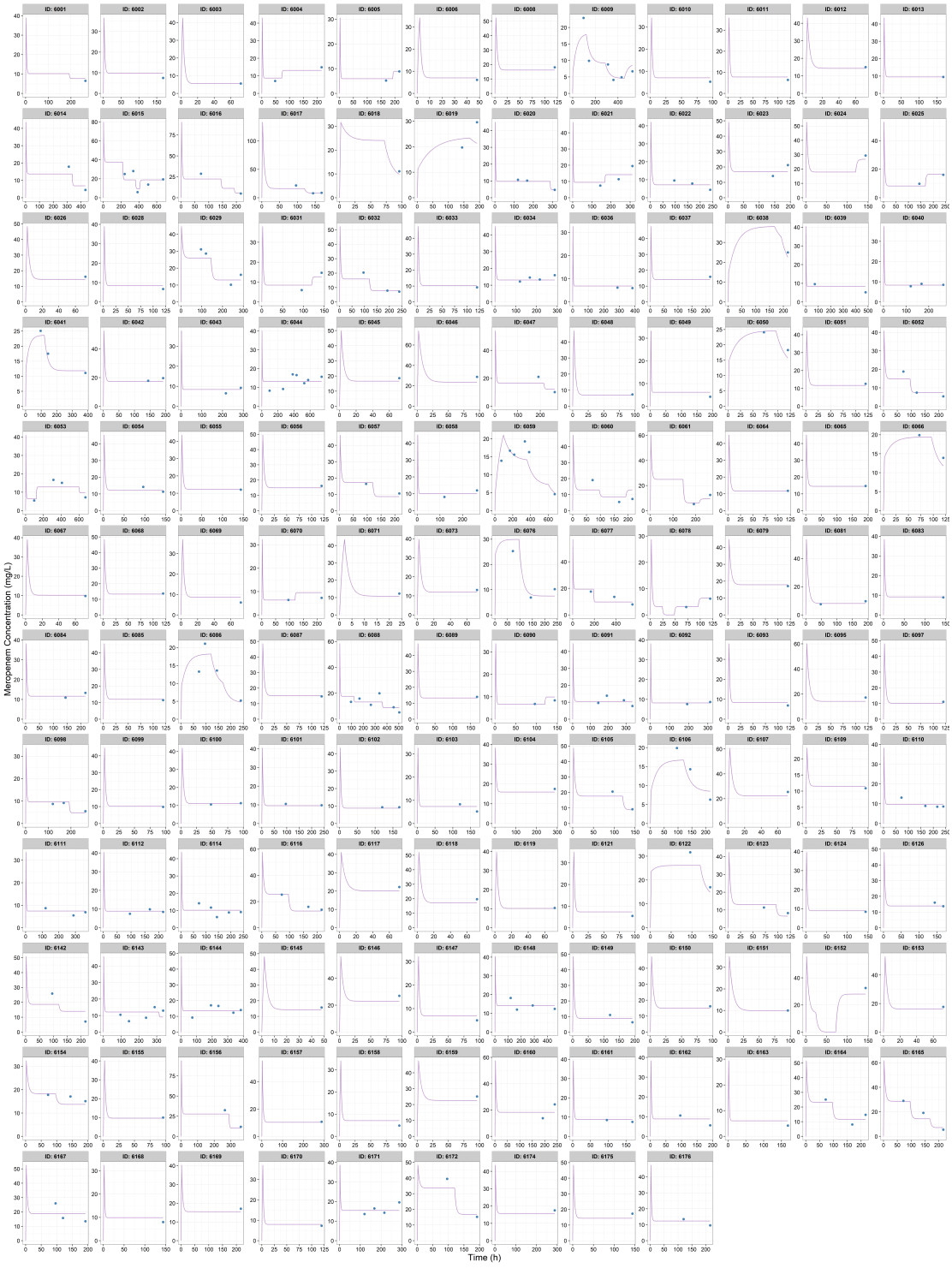

Figure S3.1: Individual predictions and observations of meropenem concentration. The blue dots are the observed individual meropenem concentrations; the solid purple lines are the individual predictions.

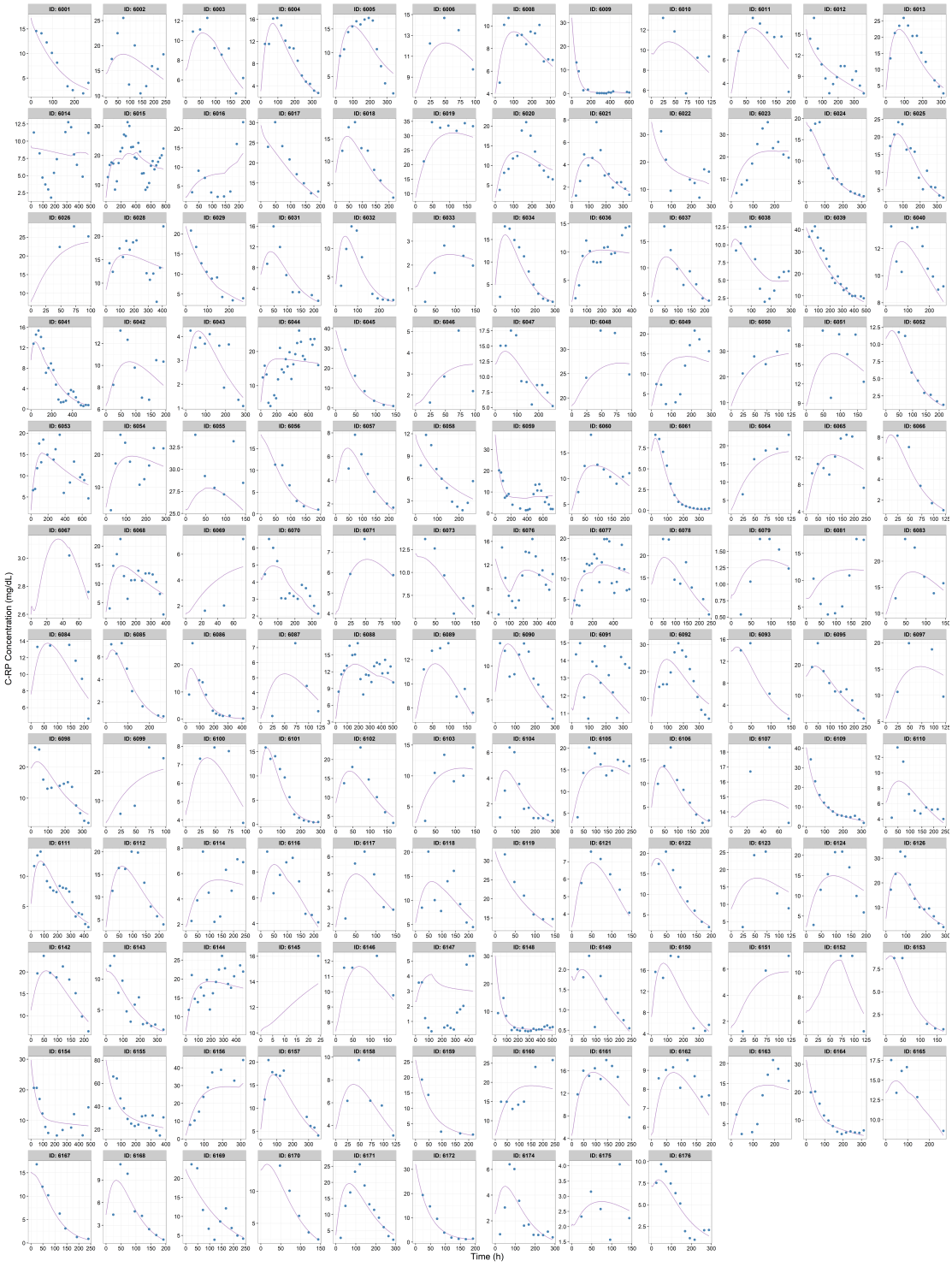

Figure S3.2: Individual predictions and observations of C-RP concentration. The blue dots are the observed individual C-RP concentrations; the solid purple lines are the individual predictions.

Part B: C-Reactive Protein as Predictor for Outcomes of Beta-Lactam Therapies in Oncohematologic Patients

Abstract

Background: Oncohematologic patients are recognized for a high risk of developing life-threatening infections. However, good infection management in this population remains a big challenge due to difficulties in obtaining microbiological data. This study aimed to explore the role of C-reactive protein (C-RP) in predicting beta-lactam therapeutic outcomes in oncohematologic patients.

Methods: This retrospective study included adult oncohematologic patients who received 24h-continuous infusion piperacillin/tazobactam or meropenem for treatment and/or prevention of infection. We employed the Cox proportional hazard (Cox PH) model to conduct a survival analysis, in which the treatment failure was defined as the endpoint. Clinical outcomes of antibiotic therapy were assessed at the end of treatment. Demographic information and clinical measurements were collected from medical history and examined as independent clinical outcome predictors. Model-based simulation was performed to demonstrate the clinical cure rate of beta-lactams.

Results: Among 142 patients, steady-state concentrations of both antibiotics were not able to discriminate clinical outcomes. Besides, high antibiotic exposure did not lead to a faster/larger C-RP reduction. Survival analysis showed that the Cox PH model comprised relative change of C-RP at day 5 after treatment versus baseline, age, and baseline C-RP level could compute the clinical outcomes roughly, despite the model uncertainty being high (85%). With a median age and baseline C-RP level of our study population, model-based simulation suggested that a 12.5-fold increase in C-RP at day 5 versus baseline indicated an approximate 50% clinical cure rate. Moreover, an increase in age and/or baseline C-RP levels also indicated a high hazard of undesirable outcomes.

Conclusion: Our study suggested that C-RP did not show good predictive ability within the first week of treatment due to high uncertainty. Physical examination and/or other biomarkers might be required to consolidate this model.

Keywords: C-reactive protein, Beta-lactam, Clinical Outcome, Cox PH model, Hematologic Malignancy.

3.5 Introduction

Infectious complications after chemo- and/or immuno-treatment increase the mortality of oncohematologic patients due to treatment-induced immunocompromise[1]. Nearly 50% of the infection-related deaths are attributed to Gram-negative bacteria, for instance, *Escherichia coli*, *Klebsiella spp*, and *Pseudomonas aeruginosa*[2]–[4]. Early initiation of appropriate antibiotics with the guidance of minimum inhibitory concentrations (MIC) of specific pathogens mentioned above can prevent life-threatening infections very well. However, in most oncohematologic patients, pathogen type and corresponding MIC are not always available in time. It means that physicians are forced to blindly or empirically prescribe antibiotics without clear evidence-based guidelines within the first several days, even weeks. This issue remains a tough clinical challenge of good infection management in oncohematologic patients.

One way to overcome this issue is to promptly and adequately adopt broad-spectrum

antibiotics, e.g., beta-lactams such as piperacillin/tazobactam or meropenem as escalation therapy[5]. Despite the broad-spectrum activity and good clinical performance of beta-lactams, physicians should remain prudent in clinical practice. Antibiotic abuse and/or long-term use could result in antimicrobial resistance worldwide. Besides, dosing strategy individualization is also difficult in empirical treatment because evaluating antibiotic efficacy may take weeks. There is a compelling need for biomarkers/techniques that can support early clinical decision-making in infection management.

C-reactive protein (C-RP) is considered a biomarker of infection. It is synthesized by hepatocytes during the acute phase of host defense to inflammation, thus promptly reflecting the host response[6]. Physicians frequently use it to assess the infection process/severity and guide antibiotic treatment[7]–[9]. Many studies have reported C-RP's predictive ability of complications or treatment outcomes in diverse populations[10]–[15]. Aulin et al systematically summarized biomarker-guided dosing strategies in clinical practice[16]. According to this study, the absolute C-RP level at admission does not show a robust link with clinical treatment outcome, while the C-RP dynamic somewhat reflects the host response to antibiotic therapy[9], [17]–[19]. This phenomenon has not been validated in oncohematologic patients yet, despite, in principle, the host response biomarker being a promising tool to predict antibiotic efficacy quantitatively. To achieve optimal efficacy and avoid toxicity/resistance, the intermediary role of C-RP deserves to be fully studied for characterizing the indirect interaction between antibiotic exposure and clinical treatment outcome in oncohematologic patients.

This study aimed to clarify the relationship between antibiotic exposure, biomarker dynamics, and antibiotic treatment outcomes in patients with hematological malignancies. We set out to (1) check the discriminate ability of antibiotic exposure to clinical outcomes, (2) describe the effect of antibiotics on the C-RP dynamic, and (3) characterize the association between C-RP and antibiotic treatment outcomes.

3.6 Materials and Methods

3.6.1 Study Design

This retrospective study was conducted among adult oncohematologic patients who were admitted to the Division of Hematology of IRCCS Azienda Ospedaliero Universitaria di Bologna, Italy during January 2021 and March 2022 as approved by the hospital ethical committee (No. 308/2021/Oss/AOUBo). Eligible patients were administered with 24h continuous infusion (CI) either piperacillin/tazobactam or meropenem as a second-line single-agent therapy for the treatment of febrile neutropenia (FN) or suspected infection. Both piperacillin/tazobactam and meropenem were treated upon reference to hospital treatment guidelines. They were initiated with a 2h quick loading dose (8g/1g for piperacillin/tazobactam, 2g for meropenem, respectively) followed by a 24h-CI maintenance dose (16g/2g for piperacillin/tazobactam, 4g for meropenem, respectively). After achievinahe steady state, each patient underwent therapeutic drug monitoring (TDM) guided dose adjustment. The targeted steady-state concentration (C_{ss}) of piperacillin/tazobactam and meropenem were 32-64 mg/L and 8-16 mg/L, respectively, which corresponded to 4-8 folds higher than pathogen MIC for 100% of the dosing interval (100% $fT>_{4\text{-}8\ folds}MIC$) of the European Society of Clinical Microbiol-

ogy and Infectious Diseases (EUCAST) clinical breakpoints of 8 mg/L and 2 mg/L, respectively.

The demographic and clinical data including age, weight, height, gender, creatine clearance (CLCr), C-RP, albumin, procalcitonin (PCT), C_{ss}, type of hematologic disease, and treatment duration were retrieved from medical history. Seven days after antibiotic initiation, patients underwent a physical examination to check the state of FN, which was defined as a single temperature higher than 38.3℃ or of no less than 38.0℃ lasting for 1h and corresponding with an absolute neutrophil count of lower than 500 cells/mm^3 of lower than 1000 cells/mm^3 with a predictive trend to below 500 cells/mm^3. Complete relief of febrile neutropenic symptoms along with negative microbiological culture after treatment was considered an optimal clinical outcome. At the end of treatment, two independent clinicians crossly assessed the clinical outcomes (failure/success) of antibiotic treatment. Patients with missing demographic information, missing clinical measurements for $\geq$3 consecutive days, and unplausible C_{ss} data were excluded from this study.

3.6.2 Data Analysis

We prepared the dataset and performed the analysis with software R (version 4.1.3, R-project.org). Continuous and categorical variables were presented as medians (25^{th} - 75^{th}, IQR) and numbers (%). The Cox proportional hazard (Cox PH) model was employed to conduct survival analysis, in which undesirable antibiotic treatment outcome was set as the primary endpoint. The following methods were described to explore the relationship between antibiotic exposure, biomarkers, and clinical outcomes.

(1) Antibiotic exposure ~ Clinical outcomes: The association between antibiotic exposure to clinical outcomes was checked by a robust boxplot and a Cox PH model. Only the last C_{ss} measurement of each patient remained in the boxplot to avoid unexpected exposure bias. Uni- and multivariable Cox PH analysis were utilized to determine the effects of antibiotic exposure alone and along with age on clinical outcomes.

(2) Antibiotic exposure ~ Biomarkers: The effect of antibiotic exposure on C-RP dynamic, i.e., relative/absolute change of C-RP versus baseline and area under the curve (AUC) of C-RP, was assessed in our study. To accurately reflect the antibiotic exposure, we calculated the temporal average antibiotic concentration from baseline to a given day i by equation 1. The relative/absolute change of C-RP and AUC of C-RP at a certain day i versus baseline were calculated by the equations of 2-4, respectively. Pearson correlations between C-RP dynamic and mean C_{ss} of the same day i were calculated and then shown by a heatmap.

Equation 1: mean $\text{Css}_\text{i} = \frac{\sum_{day=1}^{day=i} Css_i}{i} (mg/L)$

Equation 2: relative change of $\text{C-RP}_\text{i} = \frac{C\text{-}RP_i - C\text{-}RP_{baseline}}{C\text{-}RP_{baseline}}$ $(fold)$

Equation 3: absolute change of $\text{C-RP}_\text{i} = C\text{-}RP_i - C\text{-}RP_{baseline}$ (mg/dL)

Equation 4: daily AUC of $\text{C-RP}_\text{i} = \frac{AUC_{1 \to i} \ of \ C\text{-}RP}{i}$ $(\frac{mg}{dL} \times day)$

(3) Biomarker ~ Clinical outcomes: Uni-variate Cox PH models were established to select potential predictive factors, after which multivariable models were developed by including those selected factors. The Cox PH model with a lower Akaike Information Criterion (AIC) and higher R-square between observation/prediction was preferred. R-square represented proportion variance explained by the predictive factors. The close the er R-square was to 1, the closer the predicted values were to the observed value. The predicted mortality rate with confidence interval over biomarker distribution was calculated by the following equation, in which the x was the selected covariate.

Equation 5: $h(t, x) = h0 \times exp(\beta \times x)$

3.7 Results

3.7.1 Demographic and Clinical Data

A total of 142 adult patients were included, comprising 76 (57.89% male, 44/76) and 66 (68.18% male, 45/66) patients in piperacillin/tazobactam and meropenem cohorts, respectively. Their median age, weight, height, and treatment duration were summarized in Table 3.3 and Figure S3.3. Acute myeloid leukemia was the most frequent hematological malignancy in the population. Microbiological isolates were identified in 10/142 patients. The median (IQR) C_{ss} of piperacillin/tazobactam and meropenem were 47.25 (33.3-67.8) mg/L and 10.7 (7.18-16.7) mg/L, respectively. Median (IQR) C-RP level at baseline was 9.65 (5.66-15.18) mg/dL. The individual C-RP profiles were presented in Figure S3.4, in which we did not find a unified trend pattern by visual perspective.

3.7.2 Antibiotic Exposure Could Not Discriminate Clinical Outcomes

Among these two cohorts, there were 77.88% of piperacillin/tazobactam and 68.75% of meropenem measurements above their corresponding clinical susceptible breakpoints. Statistical test of antibiotic exposures and clinical therapeutic outcomes was examined, indicating that C_{ss} did not show adequate ability (p=0.15 in piperacillin/tazobactam group, p=0.11 in the meropenem group) to discriminate those patients who had an optimistic outcome from those who did not (Figure 3.5). The uni- and multivariable Cox PH model showed similar results (Table 3.4). The coefficient of C_{ss}, without/with age as a covariate, to the clinical outcome in the piperacillin group were both 0.024; this value was 0.097 and 0.096 in the meropenem group. The R-square of those Cox PH model was all no bigger than 0.0234.

3.7.3 Higher Antibiotic Exposure Does Not Lead to A Faster/Larger C-RP Reduction

The distribution of relative and absolute change of C-RP under antibiotic treatment were similar in both piperacillin/tazobactam and meropenem groups (Figure S3.5). Most patients' relative change of C-RP located between -5 to 5 folds and absolute change of

C-RP between ± 20 mg/dL. Weak positive correlations between antibiotic concentration and C-RP changes were observed, the strongest correlation was 0.27 in the piperacillin group between absolute C-RP change and mean C_{ss} at day 7 (Figure 3.6, panel A). Antibiotic concentration increase did not persistently inhibit the daily AUC for any comparison, and no consistent changes in AUC were seen across groups (Figure 3.6, panel B).

3.7.4 Relative Change of C-RP at Day 5, 6, and 7 Predicted Outcomes Better Than Other Assessed Factors

Multivariable Cox PH models comprise age, baseline C-RP level, and one more factor, i.e., daily measured C-RP or absolute/relative change of C-RP, were tested. Those models demonstrated that daily measured C-RP was the most significant factor to predict clinical outcomes among the data we tested (Table S3.1, p-value=1.59E-09). Considering that data on longitudinal C-RP change at a certain day i versus baseline might be more pragmatic to guide clinical decision-making, we summarized the fitting performances (% R-square) of diverse Cox PH models in chronological order and then compared the predictive ability of those daily C-RP derived factors with daily C-RP. Relative change of C-RP from day 5 to day 7 better predicted antibiotic clinical outcome than the absolute change of C-RP and that of earlier days, despite that all R-square were low and none of those models developed by relative or absolute change of C-RP were comparable with daily C-RP model (Figure 3.7). Table S3.1 presented similar results. Cox PH models using relative change of C-RP at day 5, 6, and 7 versus baseline in combination with age and C-RP level at admission predicted antibiotic therapeutic outcome with lower AIC and significant p-value (<0.01).

3.7.5 Model-based Simulation for Typical Populations

Balancing the time of starting infection management and model performance (Figure 3.7, Table S3.1), the model established by the relative change of C-RP at day 5 versus baseline, age, and baseline C-RP level was selected as the final model. We then generated a hypothetical dataset with the median values of our study population and enlarged relative change of C-RP at day 5 versus baseline for clinical cure rate prediction. The real population-based prediction was also done to assess the new dataset and model performance. Figure 3.8 showed that the majority relative change of C-RP at day 5 versus baseline located between -2 and 5. Within this range, the regenerated dataset represented the real population well. Meanwhile, an increase in relative change of C-RP at day 5 forecasting a plausible low clinical cure rate, 12.5 of the relative change of C-RP at day 5 corresponding to approximately 50% probability of clinical cure. Besides, a huge variability was observed when a relative change of C-RP at day 5 versus baseline was higher than 5 (Figure 3.8).

Age and baseline C-RP level were two other predictive factors in our model. Figure 3.9 demonstrated the predicted clinical cure rate stratified by baseline C-RP level and age. Higher baseline C-RP levels and older age were risk factors for low clinical cure rates. According to our prediction, for patients of the same age and relative C-RP change, high-level baseline C-RP harmed the clinical cure rate. This difference was not large

when the relative change of C-RP at day 5 versus baseline was less than 5 or greater than 17.5. But within 5 to 17.5, different baseline C-RP values, e.g., 5 mg/dL and 15 mg/dL, may cause a difference of more than 10% in the predicted mortality rate. Another significant risk factor was age. Similar to the baseline C-RP level, a growth of 30 years (e.g., from 45 to 75 years) was associated with an approximate 25% clinical cure rate decrease when assuming other predictors kept the same.

3.8 Discussion

This study evaluated C-RP in predicting antibiotic therapeutic outcomes in a retrospective cohort of oncohaematologic patients who received 24h-CI piperacillin/tazobactam or meropenem. A Cox PH model was established with relative change of C-RP at 5 days versus baseline, age, and baseline level of C-RP, indicating that in our study population a 12.5-fold increase in C-RP at day 5 corresponded with a 50% clinical cure rate. This model gave an overview of the clinical cure rate over C-RP relative change, while it did not accurately predict antibiotic therapeutic outcomes due to the high uncertainty. To our knowledge, this is the first study to quantitatively characterize the predictive ability of C-RP in patients with hematologic malignancies. Despite the imperfect performance of C-RP, this research provided new insight/framework into good infection management.

Among 142 patients, microbiological isolates and corresponding MICs were detected before starting antibiotic therapy in 10 patients. Except for 2 dead patients, the rest 8 all benefited from antibiotic therapy. In patients whose microbiological isolates were temporally undetectable, the treatment failure rate was around 26% (34/132). Although the antibiotic treatment in these 132 patients was guided by TDM based on EUCAST clinical breakpoint, the clinical cure rate was still lower than MIC guided treatment. This phenomenon suggested that a unified clinical breakpoint cannot always cater to individual requirements well. Considering the diversity of MICs, some patients might still be under dosed or not being treated with the appropriate type of antibiotic.

We subsequently checked the antibiotic exposure in patients who showed a good response to antibiotic treatment and who did not. The results, both shown in an intuitive boxplot (Figure 3.5) and the Cox pH model (Table 3.4), did not suggest any statistical differences in antibiotic exposure between patients who had a desirable outcome and who did not. A small positive correlation (0.0243 in piperacillin/tazobactam cohort, and 0.0967 in meropenem cohort) was observed between C_{ss} and clinical outcome. This result might surprisingly challenge our experience in antibiotic management because it indicated literally that higher risk of treatment failure is associated with higher antibiotic exposure. However, we found that the median estimated glomerular filtration rate (eGFR) was 96 mL/min/1.73m^2 and 105 mL/min/1.73m^2 in patients who had an undesirable and desirable outcome, respectively. In clinical practice, meropenem and piperacillin/tazobactam were initiated in all patients with a loading dose followed by a low maintenance dose if eGFR $<$60 mL/min/1.73m^2 or a high maintenance dose if eGFR $\geq$60 mL/min/1.73m^2. It is therefore not a surprise that patients with small eGFR exhibit higher antibiotic exposure when receiving the same dose.

Besides antibiotic exposure, age has been reported to be associated with an increased risk of antibiotic escalation and antibiotic treatment failure due to comorbidities or

poor functional status[20], [21]. Generally, elder patients are more likely to have serious underlying disease and their physical state is more difficult to recover from infections, which might bias the ability of antibiotic exposure to predict clinical outcomes. To exclude the confounding of age, a Cox PH model comprising age and C_{ss} was built next. Including age into Cox PH model did not improve the predictive ability of antibiotic exposure to clinical outcomes (Table 3.4). Therefore, we could confirm that adjust dosing strategy empirically with EUCAST breakpoint is not efficient enough in our study patients.

There are several studies explored the predictive ability of C-RP[10], [11], [22]–[24]. Yet the role of C-RP remains controversial. Kenny RA et al. first reported in 1985 that the elevation of absolute serum C-RP might be a biomarker of acute infection[25]. However, a single measurement of C-RP at the infection initiation or a certain day might lead to a wrong diagnosis of disease severity, subsequently delaying appropriate antibiotic treatment. In our studied population, the C-RP level at admission could reflect infection severity but not well predict antibiotic treatment outcomes alone. In recent years, an increasing number of studies have confirmed that the velocity of C-RP is a possible biomarker of infection diagnosis[26]–[28]. Povoa et al. demonstrated the possibility of using C-RP kinetics to identify patients' (n=935) outcomes after community-acquired bloodstream infection[29]. This study reported that both markedly greater relative and absolute changes of C-RP were observed in patients still alive on day 4 after the first treatment, which corresponded to our results on day 5. The plasma albumin on day 1 was also assessed by Povoa to show its ability to predict short- to long-term mortality. However, considering that neither the albumin was outside the normal level in our population, nor it was a significant predictive factor in the Cox PH model (p=0.71), plasma albumin was not included in our final model.

To make our study more clinically informative, instead of using daily measured C-RP itself, we explored the ability of daily changes in C-RP after initiating antibiotic therapy to predict clinical outcomes by the Cox PH model. Balancing the model performance and timeliness, model comprising age, baseline C-RP, and the relative change of C-RP at day 5 versus baseline was selected as the final model (AIC=371.44, p-value<0.01). The predicted clinical cure rate was relatively accurate when a relative change of C-RP at day 5 ranged between -2 to 5. This good prediction can be attributed to abundant data. However, with an increase in relative change of C-RP at day 5, sparse data lead to less-accurate predictions (75% confidence interval>0.85). Besides the uneven C-RP relative change distribution, the non-specificity of C-RP to bacterial infection might also be a possible reason for inaccurate prediction. Inflammation, all-cause infection, and tissue damage could stimulate prompt C-RP synthesis as well[30], [31]. Given that these causes are often insidious and difficult to quantify by simple physical examination, they may interfere with the predicted outcome, reducing the accuracy.

Thus far, we assessed the role of C-RP as a biomarker in predicting antibiotic treatment outcomes. Besides biomarkers, physical exam is another powerful tool in infection management. Relief of febrile neutropenic symptoms is one signal of infection recovery in our study population because trends of temperature and absolute neutrophil count normalization heralding immune function normalization. To balance the medical cost-effective, this physical examination was conducted on the 7^{th} day after antibiotic treatment for the first time to assess the febrile neutropenic symptoms severity/state. Same workflow and methodology was applied to this new predictors. This work revealed that tendencies of febrile neutropenic symptoms resolution (yes/no) had a significant impact in

predicting antibiotic treatment outcomes (p-value<0.01), and was integrated into the Cox PH model. Model-based prediction suggested that once a tendency of neutropenic symptoms resolution was caught, this patient has a probability greater than 90% of recovering from infections (Figure S3.6, panel B) since the relative change of C-RP higher than 20 was rarely observed. One major drawback of this model is time. Current anti-infection guidelines usually recommend an assessment around 4 days after antibiotic administration to support further decision-making, whereas neutrophil recovery usually takes longer, which limits the clinical application of this predictor.

This study has several limitations. First, the small number of patients who had undesirable clinical outcome (25.35%, 36/142) limits the conclusion of this study. Second, we could not perfect discriminate patients' death reason. For example, infection or hematological malignancies could both result in patients' death. Although physicians assessed the status of infection at the time of death, the possibility of confounding the cause of death still exists. Third, we were unable to include body temperature in the study due to missing data, although it is a vital indicator of immune system recovery.

In conclusion, our results suggested that although a relative change of C-RP over time may be somewhat predictive of antibiotic treatment outcomes in patients with hematological malignancies, we should remain prudent and doubt the accuracy of using this less robust biomarker in our study population. In any case, despite the imperfect performance of our current Cox PH model, we believe that future point-of-care biomarkers tests should still be recommended and might benefit empirical antibiotic treatment to some extent when traditional PK/PD targets are not available. The combination use of biomarkers and/or physical examination would also be a promising strategy in the future.

Table 3.3: Demographic data and hematological characteristics.

	Piperacillin/ Tazobactam	**Meropenem**
Number of subjects (n)	76	66
Sex (n (%), [Female/Male],)	32/44 (42.11%/57.89%)	21/45 (31.82%/68.18%)
Age (year, median (IQR))	58 (44.50-66.25)	61 (48.75-69)
Weight (kg, median (IQR))	70.5 (60.525-83.75)	71.8 (64-80)
Height (m, median (IQR))	1.7 (1.63-1.79)	1.7 (1.65-1.78)
CLCr* (mL/min/1.73m^2, median (IQR))	102 (77-116)	95.5 (73.25-109)
Underlying Disease (n, %)		
AML	30 (39.47%)	43 (65.15%)
ALL	11 (14.47%)	6 (9.09%)
NHL	17 (22.37%)	13 (19.70%)
HL	6 (7.89%)	0 (0.00%)
MM	6 (7.89%)	0 (0.00%)
Other#	6 (7.89%)	4 (6.06%)
Dose regimens start from	9g/1g loading dose, 18g/2g maintenance dose	2g loading dose, 4g maintenance dose
Treatment duration (day, median (IQR))	8.5 (7-12)	13 (9-17)
C_{ss} (mg/L, median (IQR))	47.25 (33.30-67.8)	10.70 (7.18-16.7)

* CLCr was calculated through the CDK-EPI formula.
# Other: Chronic myeloid leukemia (CML) and Chronic lymphoid leukemia (CLL).
Abbreviation: AML, acute myeloid leukemia; ALL, acute lymphoid leukemia; NHL, non-Hodgkin lymphoma; HL, Hodgkin lymphoma; MM, multiple myeloma.

Table 3.4: Regression coefficients of exposure without/with age to clinical outcome, derived from Cox PH model.

		Piperacillin/Tazobactam			**Meropenem**		
		coefficient	p-value	R^2	coefficient	p-value	R^2
C_{ss} ~ Outcome	C_{ss}	0.0243	0.2016	0.0150	0.0967	0.0716	0.0234
C_{ss}+Age ~ Outcome	C_{ss}	0.0240	0.2082	0.0154	0.0962	0.0887	0.0234
	Age	-0.0066	0.8520		0.0012	0.9764	

Table S3.1: Regression outcomes of C-RP and C-RP dynamics to outcome

Predictive Factor	**AIC**	**p-value**
Relative Change of C-RP at day2	454.79	8.92E-01
Relative Change of C-RP at day3	440.13	7.15E-01
Relative Change of C-RP at day4	439.78	4.61E-01
Relative Change of C-RP at day5	371.44	5.22E-06
Relative Change of C-RP at day6	343.02	5.72E-07
Relative Change of C-RP at day7	313.16	1.10E-06
Absolute Change of C-RP at day2	451.08	3.77E-02
Absolute Change of C-RP at day3	440.27	9.37E-01
Absolute Change of C-RP at day4	440.10	6.74E-01
Absolute Change of C-RP at day5	378.61	3.36E-02
Absolute Change of C-RP at day6	351.58	2.85E-02
Absolute Change of C-RP at day7	318.60	4.06E-04
Daily C-RP	427.99	1.59E-09

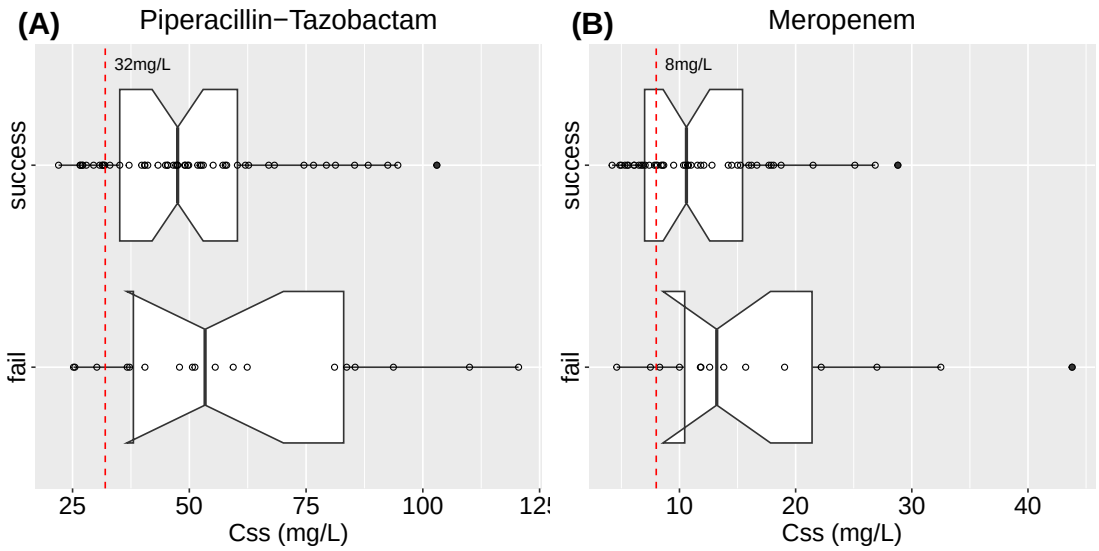

Figure 3.5: Antibiotic exposures of (A) piperacillin/tazobactam and (B) meropenem in patients who succeed or failed the treatment. Red dashed lines are the 4-fold of EUCAST breakpoints against *Enterobacterales* and *Pseudomonas aeruginosa* of piperacillin/tazobactam (4×8mg/L) and meropenem (4×2mg/L), respectively. The dots are the observed piperacillin or meropenem concentrations. Clinical outcomes were assessed by physical examination at the end of treatment.

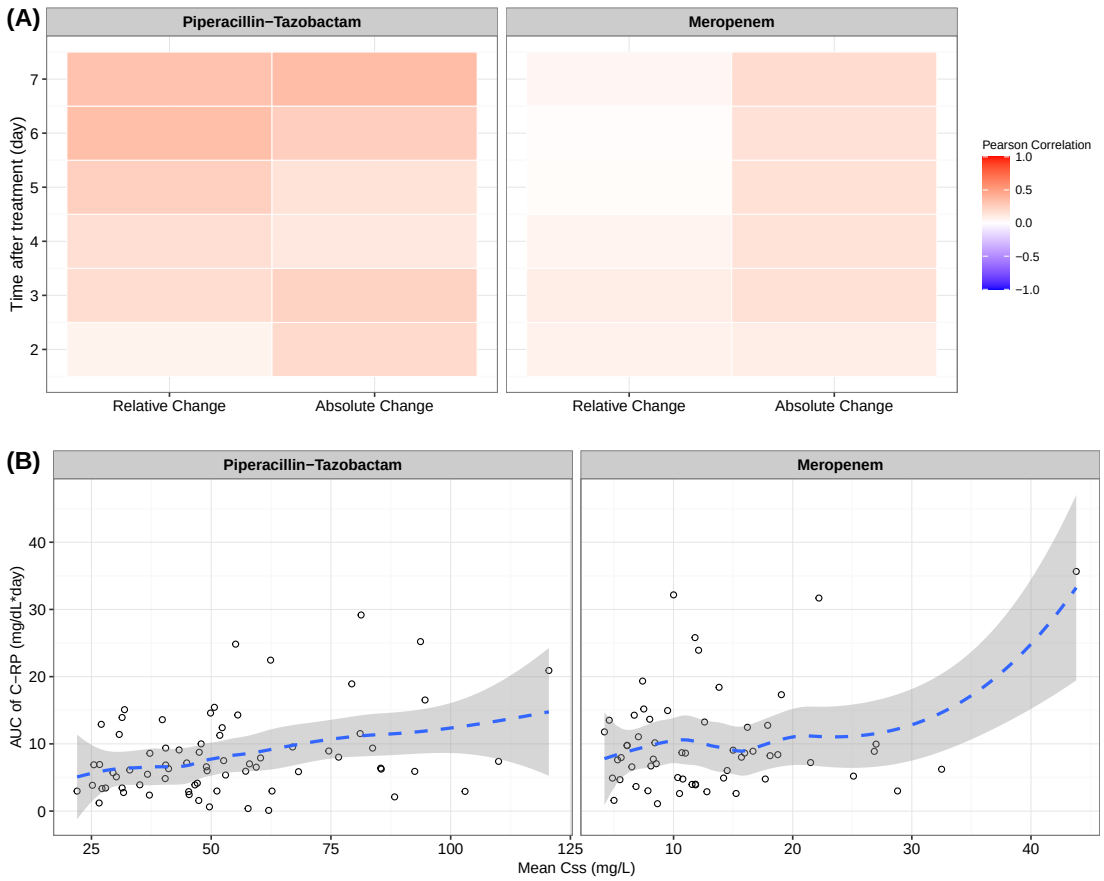

Figure 3.6: The effect of antibiotic exposure on C-RP dynamic. (A) The correlation between mean steady-state concentration (C_{ss}) and relative change of C-RP over time; (B) The association between mean C_{ss} and daily area under the curve (AUC) of C-RP. In panel A, the mean C_{ss} at a certain time point was calculated by all reliable observations before that time point. In panel B, the dots are the observed meropenem C_{ss}; the blue dashed line represents the smooth regression between meropenem C_{ss} and daily normalized AUC of C-RP; the grey shadow is the 90Cth confidence interval around the smooth regression.

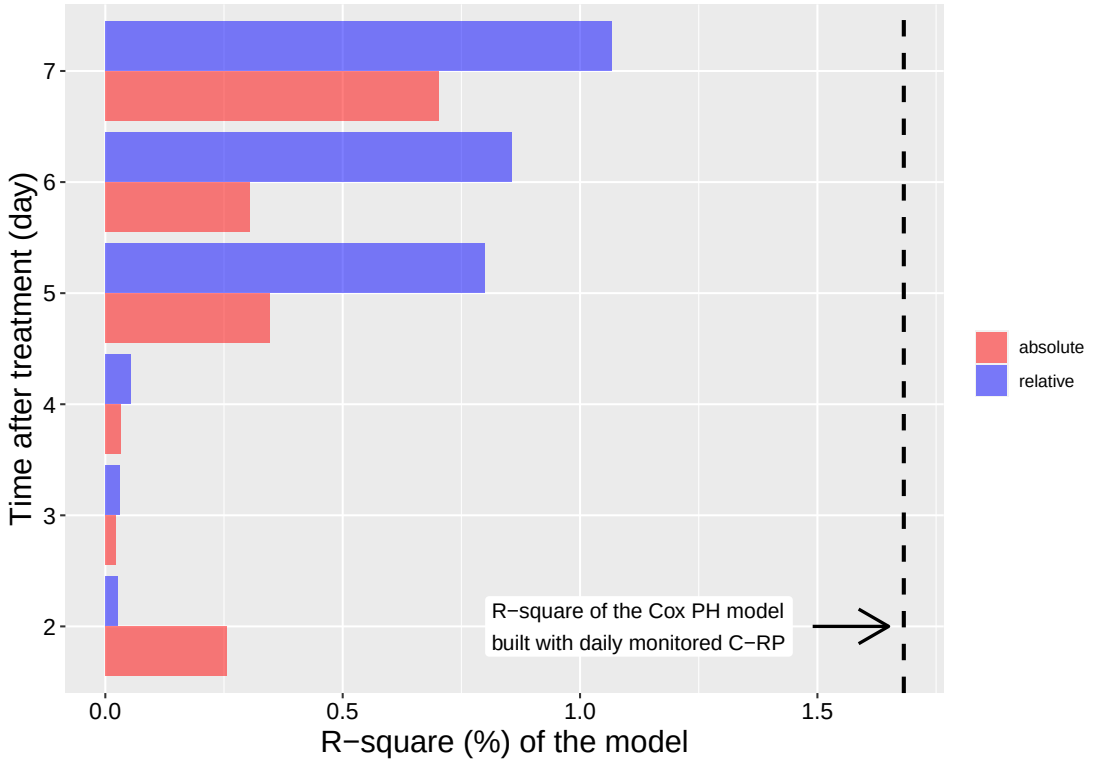

Figure 3.7: Comparison of R-square (%) for Cox PH models established by diverse relative or absolute changes of C-RP. The Black dashed line is the R-square (%) of the most informative model which was built by sequential daily monitored C-RP.

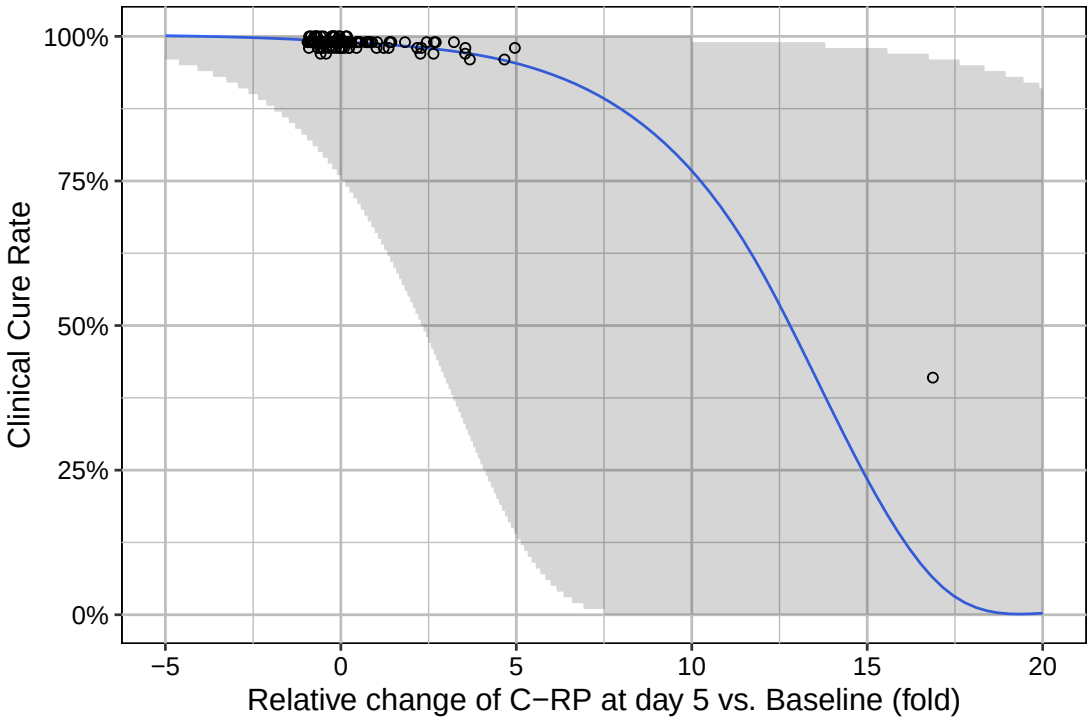

Figure 3.8: Predicted clinical cure rate over C-RP increase at day 5. The blue line is the survival rate predicted by using the enlarged typical dataset (median age and baseline C-RP values); the grey shadow is the 75^{th} confidence interval of the survival rate based on the enlarged typical dataset; the black dots are the individual survival rate predicted by using the observed patients.

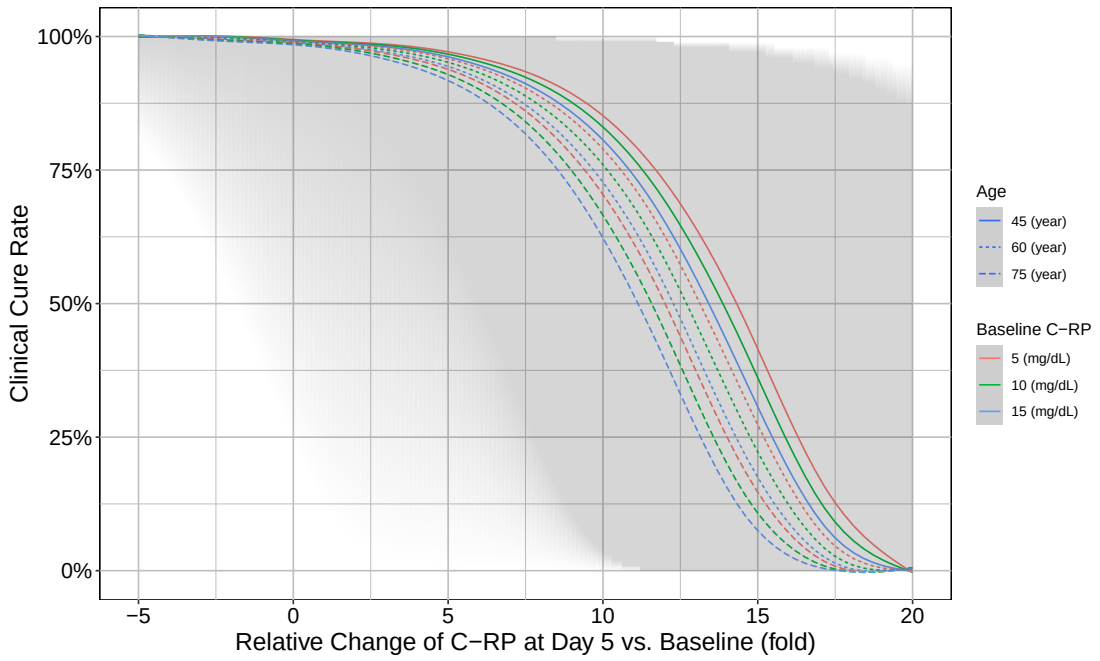

Figure 3.9: Predicted clinical cure rate over C-RP increase at day 5, stratified by age and baseline C-RP levels. For each predicted scenario, the age and baseline C-RP level are both fixed. The lines (solid/long-dashed/short-dashed) are the predicted mortality with the hypothetical datasets, which comprised of low/medium/high age and baseline C-RP, respectively; the grey shadow is the 75^{th} confidence interval of the survival rate based on the typical datasets.

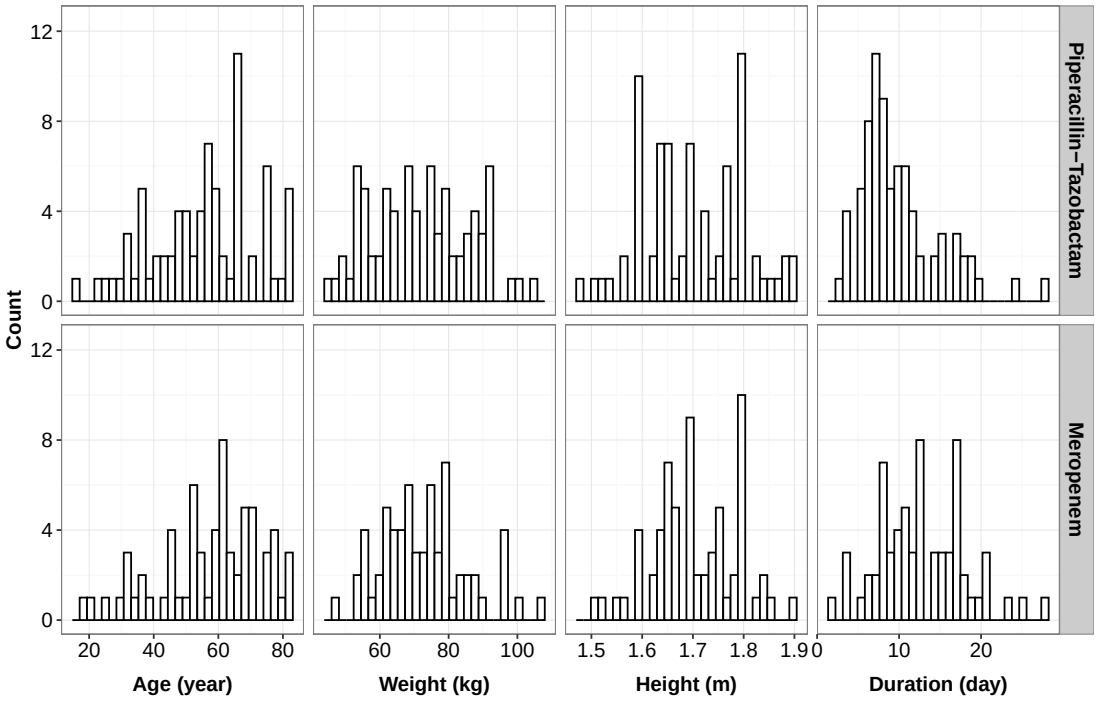

Figure S3.3: Demographic and treatment duration distribution.

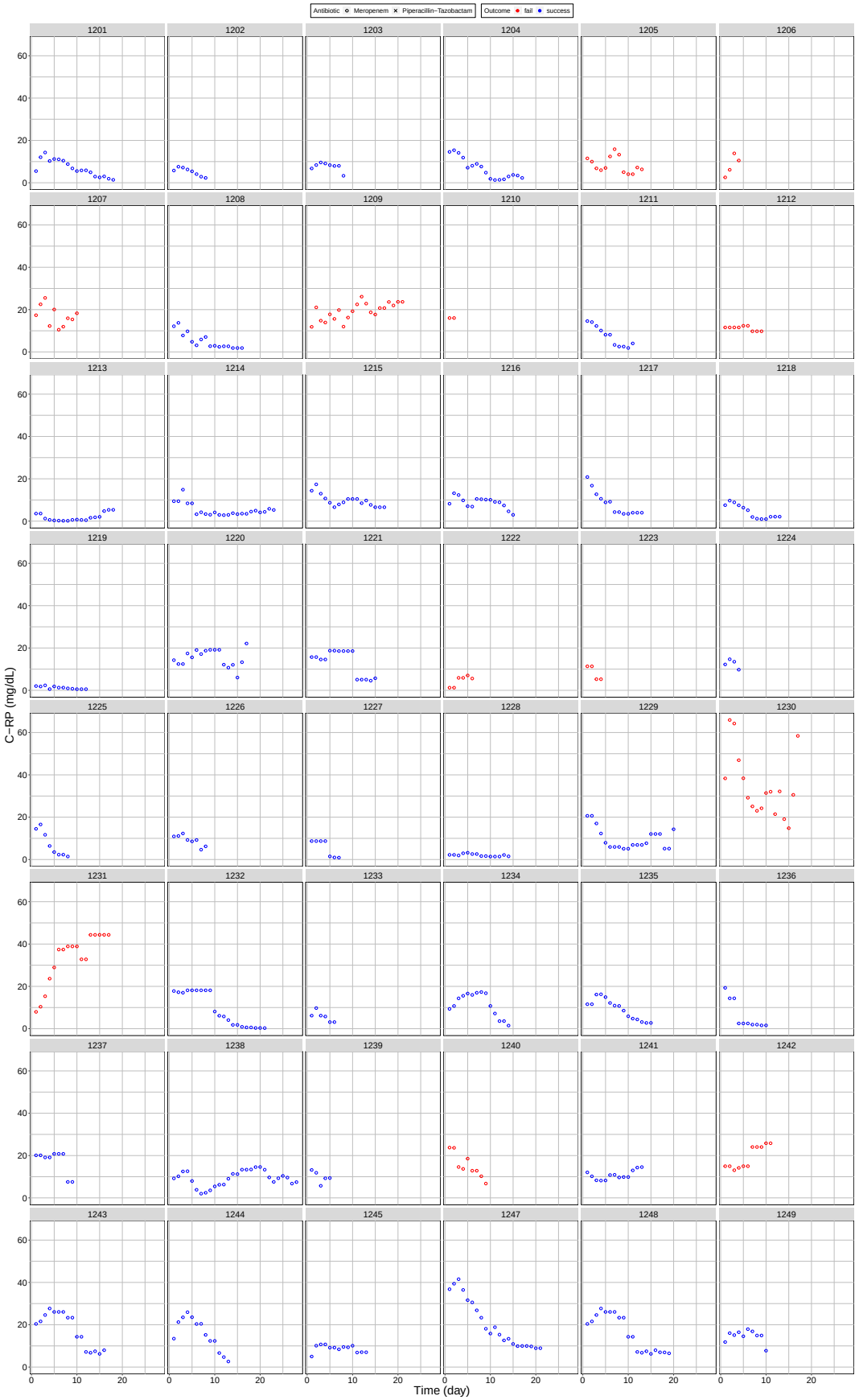
Antibiotic Meropenem Piperacillin−Tazobactam
Outcome fail success
1201
1202
1203
1204
1205
1206
1207
1208
1209
1210
1211
1212
1213
1214
1215
1216
1217
1218
1219
1220
1221
1222
1223
1224
1225
1226
1227
1228
1229
1230
1231
1232
1233
1234
1235
1236
1237
1238
1239
1240
1241
1242
1243
1244
1245
1247
1248
1249
C−RP (mg/dL)
Time (day)

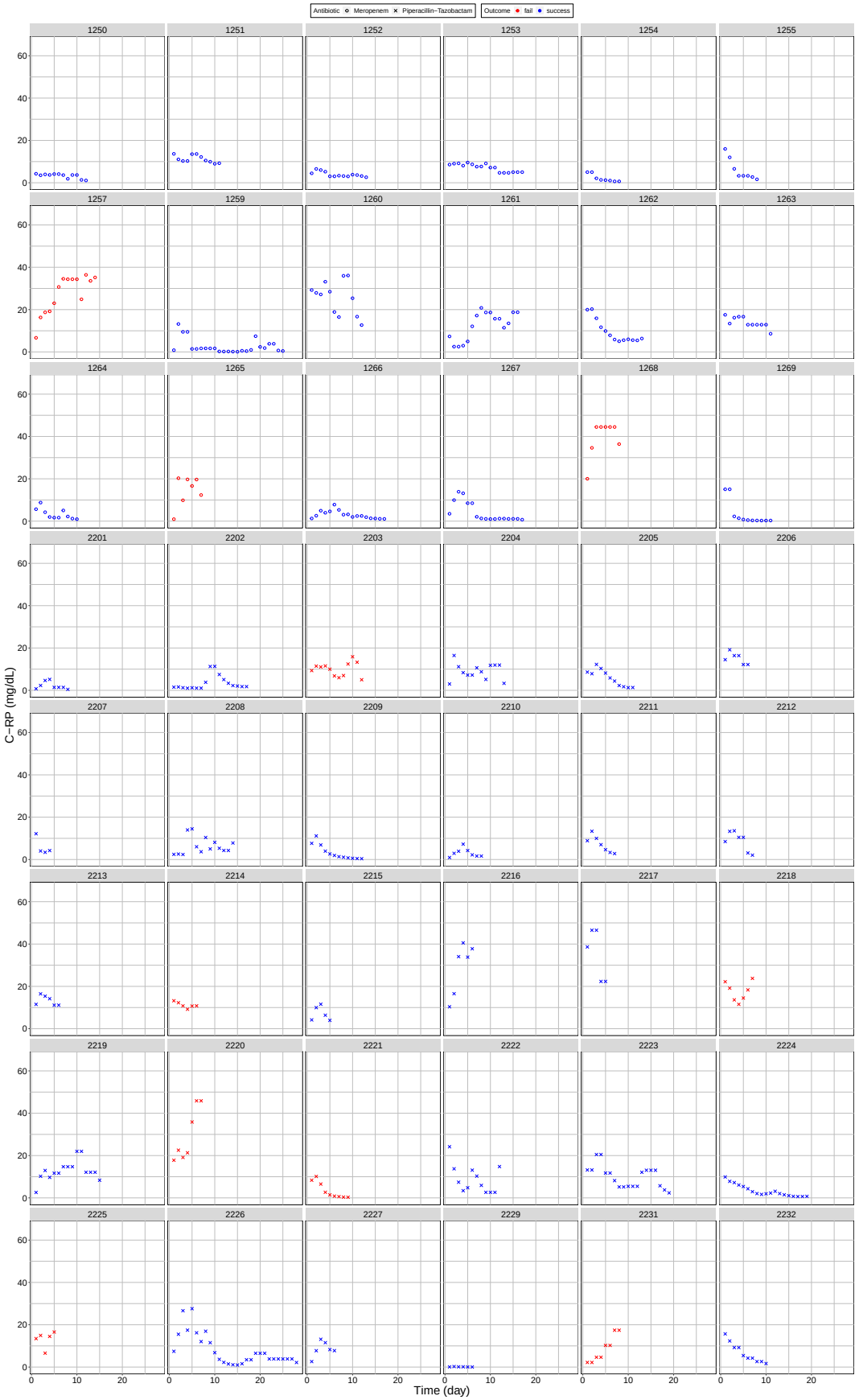
Antibiotic Meropenem Piperacillin−Tazobactam
Outcome fail success
1250
1251
1252
1253
1254
1255
1257
1259
1260
1261
1262
1263
1264
1265
1266
1267
1268
1269
2201
2202
2203
2204
2205
2206
2207
2208
2209
2210
2211
2212
2213
2214
2215
2216
2217
2218
2219
2220
2221
2222
2223
2224
2225
2226
2227
2229
2231
2232
C−RP (mg/dL)
Time (day)

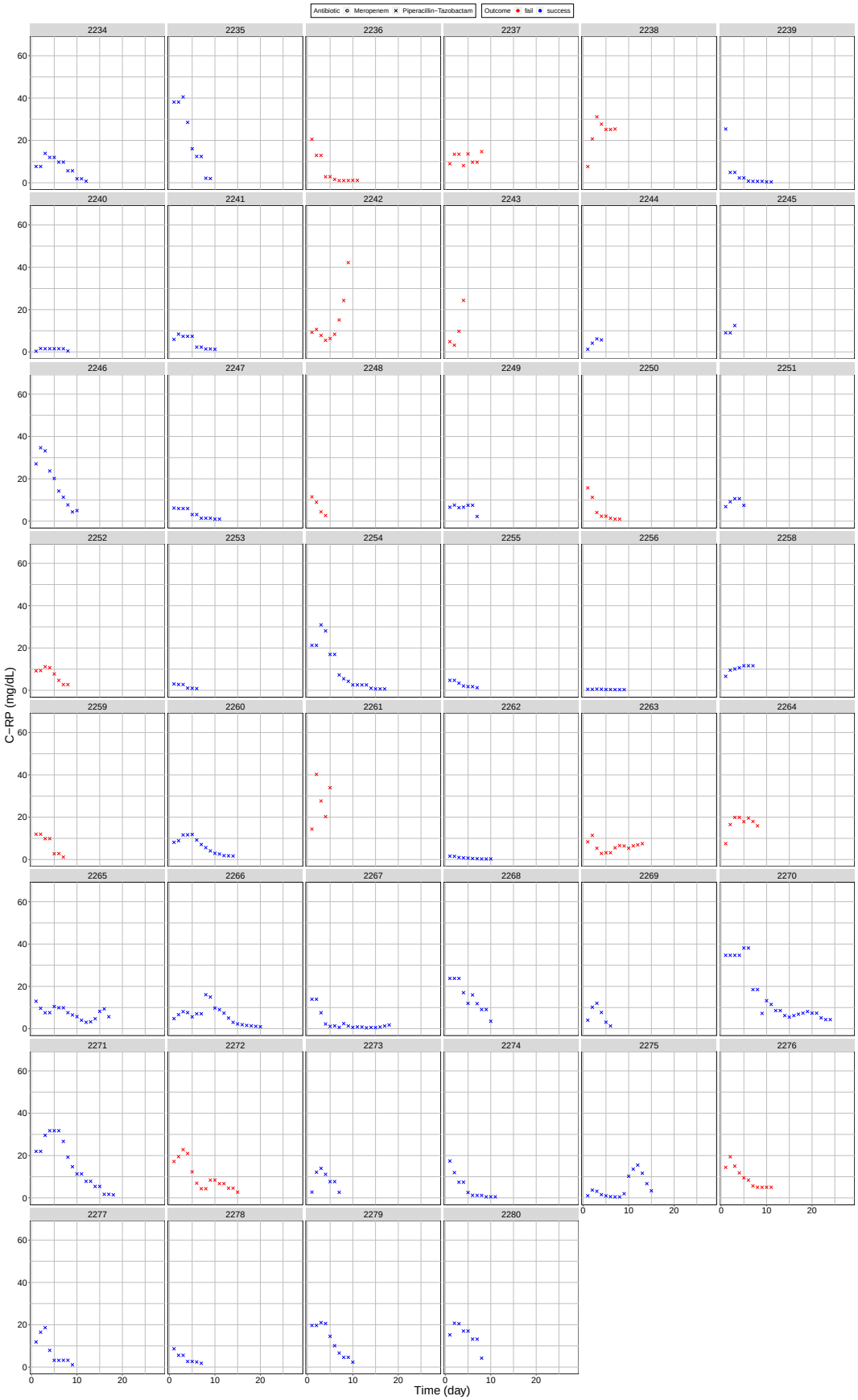

Figure S3.4: Individual C-RP profiles.

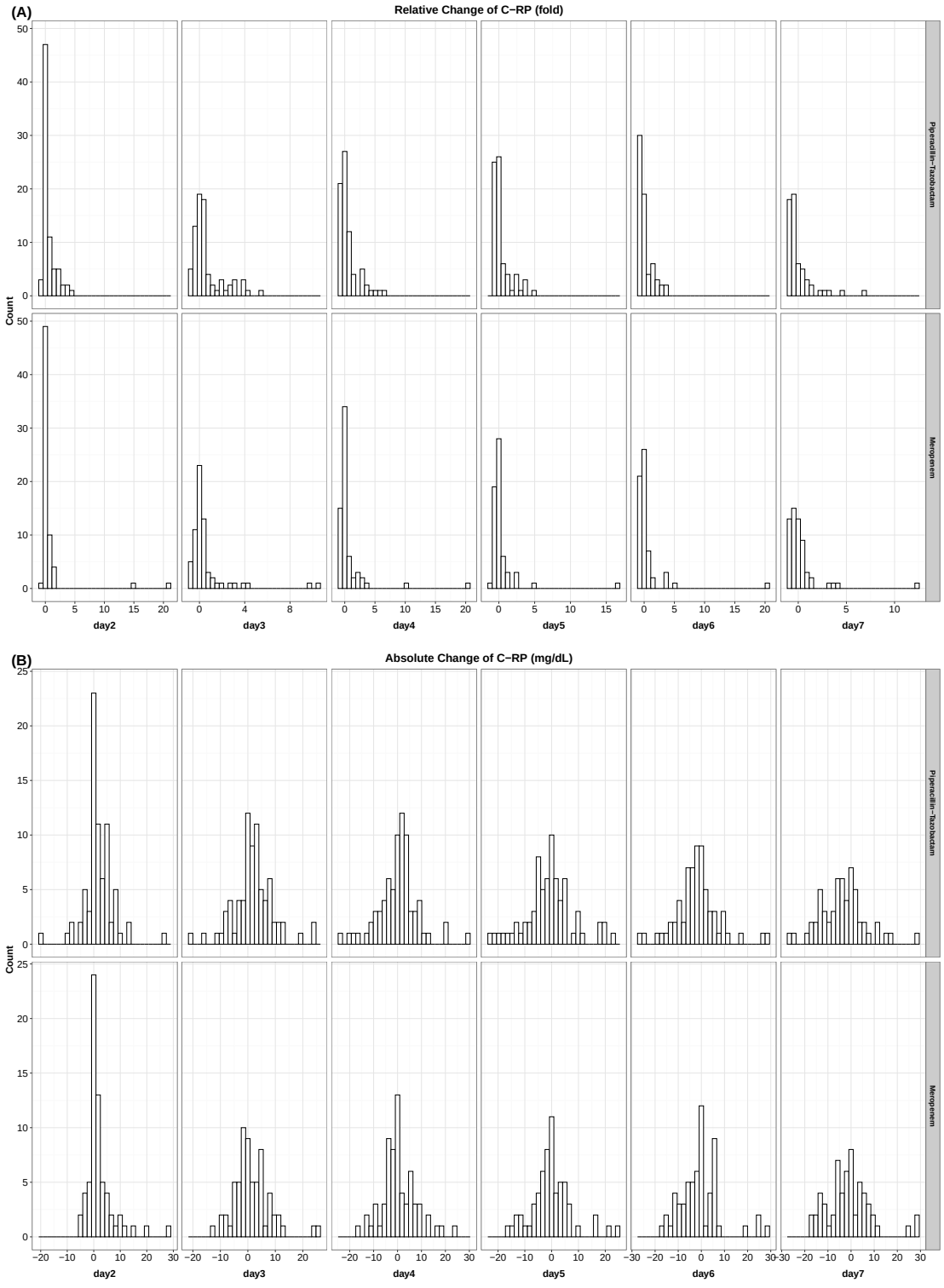

Figure S3.5: The distributions of (A) relative change of C-RP and (B) absolute change of C-RP.

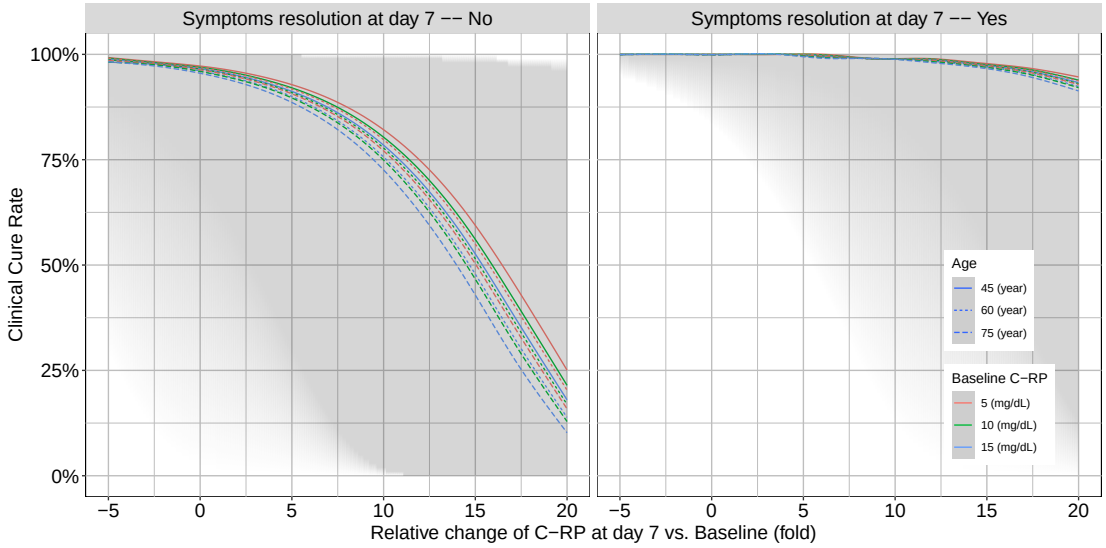

Figure S3.6: Predicted clinical cure rate over relative C-RP increase at day 7 versus baseline, stratified by age, baseline C-RP levels and symptoms resolution at day 7. The lines (solid/long-dashed/short-dashed) are the survival rate predicted by using the hypothetical dataset with low/medium/high age and baseline C-RP; the grey shadow is the 75^{th} confidence interval of the survival rate based on the typical datasets.

Bibliography

[1] O. Blennow and P. Ljungman, "Infections in Hematology Patients," Concise Guide to Hematology, p. 503, doi: 10.1007/978-3-319-97873-4_38.

[2] C. L. Holmes, M. T. Anderson, H. L. T. Mobley, and M. A. Bachman, "Pathogenesis of Gram-Negative Bacteremia," Clin Microbiol Rev, vol. 34, no. 2, pp. e00234-20, Jun. 2021, doi: 10.1128/CMR.00234-20.

[3] V. Mulanovich and D. P. Kontoyiannis, "Acute myeloid leukemia and the infectious diseases consultant," Leukemia & Lymphoma, vol. 59, no. 6, pp. 1284–1291, Jun. 2018, doi: 10.1080/10428194.2017.1365861.

[4] M. von Lilienfeld-Toal and G. Maschmeyer, "Challenges in Infectious Diseases for Haematologists," ORT, vol. 41, no. 6, pp. 406–410, 2018, doi: 10.1159/000487439.

[5] "Clinical Practice Guideline for the Use of Antimicrobial Agents in Neutropenic Patients with Cancer: 2010 Update by the Infectious Diseases Society of America — Clinical Infectious Diseases — Oxford Academic." Accessed: Oct. 09, 2023. [Online]. Available: https://academic.oup.com/cid/article/52/4/e56/382256?login=true

[6] I. M. Rajab, P. C. Hart, and L. A. Potempa, "How C-Reactive Protein Structural Isoforms With Distinctive Bioactivities Affect Disease Progression," Front Immunol, vol. 11, p. 2126, Sep. 2020, doi: 10.3389/fimmu.2020.02126.

[7] X. An et al., "C-reactive protein testing to guide antibiotic prescribing for COPD exacerbations: A protocol for systematic review and meta-analysis," Medicine, vol. 99, no. 29, Jul. 2020, doi: 10.1097/MD.0000000000021152.

[8] R. Keshet, B. Boursi, R. Maoz, M. Shnell, and H. Guzner-Gur, "Diagnostic and prognostic significance of serum C-reactive protein levels in patients admitted to the department of medicine," Am J Med Sci, vol. 337, no. 4, pp. 248–255, Apr. 2009, doi: 10.1097/MAJ.0b013e31818af6de.

[9] P. Póvoa, A. M. Teixeira-Pinto, and A. H. Carneiro, "C-reactive protein, an early marker of community-acquired sepsis resolution: a multi-center prospective observational study," Critical Care, vol. 15, no. 4, p. R169, 2011, doi: 10.1186/cc10313.

[10] M. Holzknecht et al., "C-reactive protein velocity predicts microvascular pathology after acute ST-elevation myocardial infarction," Int J Cardiol, vol. 338, pp. 30–36, Sep. 2021, doi: 10.1016/j.ijcard.2021.06.023.

[11] A. Banai et al., "Association between C-Reactive Protein Velocity and Left Ventricular Function in Patients with ST-Elevated Myocardial Infarction," J Clin Med, vol. 11, no. 2, p. 401, Jan. 2022, doi: 10.3390/jcm11020401.

[12] F. Liu et al., "Prognostic value of interleukin-6, C-reactive protein, and procalcitonin in patients with COVID-19," J Clin Virol, vol. 127, p. 104370, Jun. 2020, doi: 10.1016/j.jcv.2020.104370.

[13] E. Nahum, G. Livni, O. Schiller, S. Bitan, S. Ashkenazi, and O. Dagan, "Role of C-reactive protein velocity in the diagnosis of early bacterial infections in children after cardiac surgery," J Intensive Care Med, vol. 27, no. 3, pp. 191–196, 2012, doi: 10.1177/0885066610396642.

[14] G. Wang et al., "C-Reactive Protein Level May Predict the Risk of COVID-19 Aggravation," Open Forum Infect Dis, vol. 7, no. 5, p. ofaa153, May 2020, doi: 10.1093/ofid/ofaa153.

[15] D. Zahler et al., "C-reactive protein velocity and the risk of acute kidney injury among ST elevation myocardial infarction patients undergoing primary percutaneous intervention," J Nephrol, vol. 32, no. 3, pp. 437–443, Jun. 2019, doi: 10.1007/s40620-019-00594-2.

[16] L. B. S. Aulin, D. W. de Lange, M. A. A. Saleh, P. H. van der Graaf, S. Völler, and J. G. C. van Hasselt, "Biomarker-Guided Individualization of Antibiotic Therapy," Clinical Pharmacology and Therapeutics, vol. 110, no. 2, p. 346, Aug. 2021, doi: 10.1002/cpt.2194.

[17] P. Póvoa et al., "Biomarkers kinetics in the assessment of ventilator-associated pneumonia response to antibiotics - results from the BioVAP study," Journal of Critical Care, vol. 41, pp. 91–97, Oct. 2017, doi: 10.1016/j.jcrc.2017.05.007.

[18] S. X and V. Jl, "The time course of blood C-reactive protein concentrations in relation to the response to initial antimicrobial therapy in patients with sepsis," Infection, vol. 36, no. 3, Jun. 2008, doi: 10.1007/s15010-007-7077-9.

[19] L. T, S. R, D. E, R. A, T. Pj, and R. J, "C-reactive protein correlates with bacterial load and appropriate antibiotic therapy in suspected ventilator-associated pneumonia," Critical care medicine, vol. 36, no. 1, Jan. 2008, doi: 10.1097/01.CCM.0000297886.32564.CF.

[20] D. Viasus, J. A. Núñez-Ramos, S. A. Viloria, and J. Carratalà, "Pharmacotherapy for community-acquired pneumonia in the elderly," Expert Opinion on Pharmacotherapy, vol. 18, no. 10, pp. 957–964, Jul. 2017, doi: 10.1080/14656566.2017.1340940.

[21] T. Avni et al., "Participation of Elderly Adults in Randomized Controlled Trials Addressing Antibiotic Treatment of Pneumonia," Journal of the American Geriatrics Society, vol. 63, no. 2, pp. 233–243, 2015, doi: 10.1111/jgs.13250.

[22] P. Póvoa et al., "Pilot study evaluating C-reactive protein levels in the assessment of response to treatment of severe bloodstream infection," Clin Infect Dis, vol. 40, no. 12, pp. 1855–1857, Jun. 2005, doi: 10.1086/430382.

[23] D. Zahler et al., "C-Reactive Protein Velocity and the Risk of New Onset Atrial Fibrillation among ST Elevation Myocardial Infarction Patients," Isr Med Assoc J, vol. 23, no. 3, pp. 169–173, Mar. 2021.

[24] C.-C. Lee, M.-Y. Hong, N.-Y. Lee, P.-L. Chen, C.-M. Chang, and W.-C. Ko, "Pitfalls in using serum C-reactive protein to predict bacteremia in febrile adults in the ED," Am J Emerg Med, vol. 30, no. 4, pp. 562–569, May 2012, doi: 10.1016/j.ajem.2011.02.012.

[25] R. A. Kenny et al., "A COMPARISON OF THE ERYTHROCYTE SEDIMENTATION RATE AND SERUM C-REACTIVE PROTEIN CONCENTRATION IN ELDERLY PATIENTS," Age Ageing, vol. 14, no. 1, pp. 15–20, 1985, doi: 10.1093/ageing/14.1.15.

[26] T. Levinson and A. Wasserman, "C-Reactive Protein Velocity (CRPv) as a New Biomarker for the Early Detection of Acute Infection/Inflammation," Int J Mol Sci, vol. 23, no. 15, p. 8100, Jul. 2022, doi: 10.3390/ijms23158100.

[27] I. Porfyridis, G. Georgiadis, P. Vogazianos, G. Mitis, and A. Georgiou, "C-Reactive Protein, Procalcitonin, Clinical Pulmonary Infection Score, and Pneumonia Severity Scores in Nursing Home Acquired Pneumonia," Respiratory Care, vol. 59, no. 4, pp. 574–581, Apr. 2014, doi: 10.4187/respcare.02741.

[28] A. Nouvenne et al., "The association of serum procalcitonin and high-sensitivity C-reactive protein with pneumonia in elderly multimorbid patients with respiratory symptoms: retrospective cohort study," BMC Geriatr, vol. 16, p. 16, Jan. 2016, doi: 10.1186/s12877-016-0192-7.

[29] P. Póvoa et al., "C-reactive protein and albumin kinetics after antibiotic therapy in community-acquired bloodstream infection," International Journal of Infectious Diseases, vol. 95, pp. 50–58, Jun. 2020, doi: 10.1016/j.ijid.2020.03.063.

[30] S. Black, I. Kushner, and D. Samols, "C-reactive Protein*," Journal of Biological Chemistry, vol. 279, no. 47, pp. 48487–48490, Nov. 2004, doi: 10.1074/jbc.R400025200.

[31] S. T. Abrams et al., "Human CRP defends against the toxicity of circulating histones," J Immunol, vol. 191, no. 5, pp. 2495–2502, Sep. 2013, doi: 10.4049/jimmunol.1203181.

Chapter 4

Data-Driven Model Selection for Model-Informed Precision Dosing: A Machine Learning Case Study with Vancomycin

4.1 Background

In the context of therapeutic drug monitoring (TDM)-guided dose optimization, selecting an appropriate pharmacokinetic (PK) model is pivotal, particularly for antibiotics that have narrow therapeutic windows like vancomycin[1]. Accurate PK modeling enables precise dosing regimens, ensuring therapeutic efficacy while minimizing the risk of adverse effects. However, the diversity in patient demographics, underlying conditions, and concomitant medications necessitates a rigorous evaluation of PK models to identify the most robust and clinically applicable option.

Vancomycin is a vital antibiotic for treating infections caused by gram-positive bacteria. It has complex pharmacokinetic properties and can be toxic due to its concentration-dependent bactericidal activity. To ensure effective treatment while minimizing the risks of over-dosing, optimizing its dosages is essential. A model-informed and TDM-guided approach is crucial for achieving this goal, especially in cases where patient demographics and disease states vary. Machine learning (ML) techniques can be useful in this context[2].

In this study, we employ an ML approach to systematically evaluate and compare different published vancomycin PK models[3]–[5] which are built into a TDM software Insight Rx®. By leveraging advanced computational techniques, we aim to develop an ML model to predict optimal population PK model selection based on patient characteristics available before the first TDM sample. This research hopefully addresses a critical gap in optimizing vancomycin dosing strategies, ultimately enhancing patient outcomes and mitigating the emergence of antibiotic resistance.

4.2 Material and Methods

The flowchart of data cleaning and model building is shown in Figure 4.1.

4.2.1 Data Preparation

Vancomycin data were collected from a range of US hospitals that use Insight Rx® software for TDM-guided dose optimization. This dataset included demographic information (i.e., age, gender, height, and weight), clinical characteristics (i.e., observed vancomycin concentrations, creatinine, comorbidities, and concomitant therapy), outcomes (i.e., predicted vancomycin concentrations based on 3 selected models[3]–[5], respectively), and other tag information (i.e., dosing time, sampling time, vancomycin dose, length of infusion, hospital ID, and patient ID).

Raw dataset was cleaned first following the rules: (1) only kept the first TDM observation for each patient, (2) filtered out unrealistic TDM observations (i.e., >100 mg/L), (3) filtered out the patients with missing covariates value, (4) filtered out the patients with unrealistic covariates value (i.e., age<18years or >105years, height<30cm or >220cm, weight<30kg or >400kg, creatine<0mg/dL or >20mg/dL, vancomycin dose<100mg or >6000mg, length of infusion>1440min).

Engineered features were then added to the cleaned dataset to compile the final dataset. Those features including (1) Estimated Glomerular Filtration Rate (eGFR) calculated by CKD-EPI and CG formula, respectively; (2) Body Surface Area (BSA); (3) Body Mass Index (BMI); (4) Individual z-scores of age, height, weight, creatine, eGFR, BSA, and BMI to our own study population and the 3 selected models population. Z-score was calculated via the equation of

$$\text{Equation 1: z\_score} = \frac{\text{Covariate}_{\text{Individual}} - \text{Covariate}_{\text{PopulationMean}}}{\text{Covariate}_{\text{PopulationSD}}};$$

(5) Binary tags of age, height, weight, creatine, eGFR, and BMI (i.e., "young" for age <35 years and "old" for >70 years; "short" for height <135 cm and "tall" for >200 cm; "wt_underweight" for weight <40 kg and "wt_overweight" for >100 kg; "cr_low" for creatine <0.5 mg/dL and "cr_high" for >4 mg/dL; "eGFR_low" for eGFR <20 mL/min/1.73m^2 and "eGFR_high" for >150 mL/min/1.73m^2; "bmi_underweight" for BMI <18 kg/m^2 and "bmi_overweight" for >30 kg/m^2); (6) Best model (i.e., the model predicted a lowest |observation-individual prediction| value was defined as the best model).

4.2.2 Model Building

This cleaned final dataset with engineered features was randomly partitioned into 3 subsets: training (70%), validation (15%), and testing (15%) for exploration. Models were trained on the training subset and evaluated on the validation subset using a range of performance metrics, including R-squared, mean absolute error (MAE), and mean squared error (MSE). The testing subset will be used only once for testing the final model. Considering that the huge amount of calculation will slow down the running speed, 10,000 observations were enrolled for initial model development and exploratory analysis in this case study.

The classification ML model and regression ML model were both tried with the goal of (1) predicting which model will be the best for a given patient and (2) predicting the lowest value of |observation-individual prediction| for a given patient, respectively. R package "xgboost" was employed in our study.

4.3 Results

4.3.1 Classification Model

The classification ML model demonstrated an overall predictive accuracy of 46%, indicating that, given the three candidate PK models, the classification ML model correctly predicted the optimal one in 46% of cases. Figure 4.2 illustrates the predictive profile of the 3 candidate PK models considered in this study. The graph depicts the accuracy of the machine learning model in correctly identifying the optimal PK model when it is indeed the correct choice. As depicted in Figure 4.2, when the true PK model was selected, the machine learning model demonstrated varying levels of accuracy in prediction. For Model buelga_2005, the machine learning algorithm correctly identified it

as the optimal choice with a frequency of 37.4%. Similarly, for Model goti_2018, the algorithm exhibited a correct prediction rate of 50%. Model thomson_2009, on the other hand, was identified correctly by the machine learning model in 36.4% of cases. Figure 4.3 presents the importance of patient features to PK model prediction. Age, BMI, eGFR calculated by the CG formula, and creatine were the 4 most important factors with an importance of approximately 10%.

4.3.2 Regression Model

The regression ML model gave an overview of the observed |observation - individual prediction| vs. predicted |observation-individual prediction| profile of the 3 PK models. This regression ML model performed similarly in the training subset (Figure 4.4, upper panels) and validation subset (Figure 4.4, lower panels) among the 3 PK models. The accuracy of prediction was less optimal when the observed |observation-individual prediction| values were above 10 mg/L, which usually manifests itself as an underestimation of the value. Similar to the classification ML model, BMI, eGFR calculated by the CG formula, creatine, and age were the 4 most important factors with an importance of about 10% (Figure 4.5).

4.4 Discussion

This study used the ML approach to determine the appropriate vancomycin population PK models for TDM-based dose optimization based on patient-specific features prior to the first blood sample collection.

A classification ML model was developed first to fit our data. This approach can provide a clear and categorical output, making it suitable for scenarios where distinct classes or categories are essential[6]. The final output of this approach is one most appropriate PK model for a given patient, making the results easier and more understandable, especially for physicians who do not have much prior knowledge about PK modeling. The prediction accuracy of this model was around 46%, a bit higher than random selecting 1 from the 3 PK models (≈33%), whereas still less than expected. Meanwhile, this approach was prone to predict goti_2018 as the most appropriate model no matter if it was indeed the best model or not (Figure 4.1).

One possible explanation of this phenomenon could be that the good performance of the classification model partially relies on the sample size balance among classes. In our training dataset, the proportion of model goti_2018 as the observed best model was 70.8%, which might bias the model training process. Meanwhile, this approach could not take the |observation-individual prediction| values into consideration, some information like outliers is therefore ignored.

The main stone of TDM-guided dose optimization is Bayesian updating, to which both the prior population model knowledge and individual observations contribute. What to do when existing population models are not good enough are (1) model averaging, i.e., weight predictions from various models[7], [8], or (2) flatten priors, i.e., listen more to the individual observations than the population models[9]. Regression ML model could

be useful for model averaging because this approach allows to rank the population PK models. Unlike the classification ML model, the regression ML model is more sensitive to outliers, that may improve the data fitting. We therefore tried to fit our data via a regression ML model in the next step.

Overall, the performance of regression ML models were similar and not bad among the 3 population PK models when the |observation-individual prediction| values were between 0-10 mg/L. The similarity may be due to the similar distributions of |observation-individual prediction| values among these 3 PK models. However, this regression ML model underestimated the |observation-individual prediction| values when they were above 10 mg/L. There are many possible explanations for the underestimation, among which insufficient training data and insufficient fitting may be the most plausible causative. Limited by the number of observations (n=10,000) included in this study, there were only 7000 TDM samples in the total training subset. Using a low complex model can lead to insufficient fitting. However, considering the similar performance between training and validation subsets, it might suggest that the final dataset might not have been handled appropriately. Refining the dataset quality by imputing raw/new values, feature scaling, or encoding categorical variables to reduce bias may be necessary works for next step.

Using a more complex model is another possibility to improve the fitting. Selecting the right R package and model for ML, whether for classification or regression tasks, depends on various factors including the specific algorithms you want to use, ease of use, data support, and the requirements of the specific task[10]. Simple regression ML models are usually well known for their speed and efficiency in handling large data with diverse features. However, those regression models cannot handle non-linear relationships and high-dimensional feature data very well, hurdling them to learn and represent highly intricate patterns. The deep neural network regression model may overcome those limitations and will be tried in the following study.

The integration of advanced ML techniques allowed us to harness the full potential of available data, resulting in more accurate dosage recommendations and facilitating personalized dosing strategies. In conclusion, our study provides valuable insights into the selection of the appropriate vancomycin PK models for integration into TDM software. This research contributes to the ongoing efforts to enhance antibiotic stewardship and ultimately improve patient care in the era of precision medicine. Future studies may focus on validating these findings in larger patient populations, exploring diverse ML approaches, including/updating more vancomycin population PK models, ranking those PK models, and exploring real-world clinical applications.

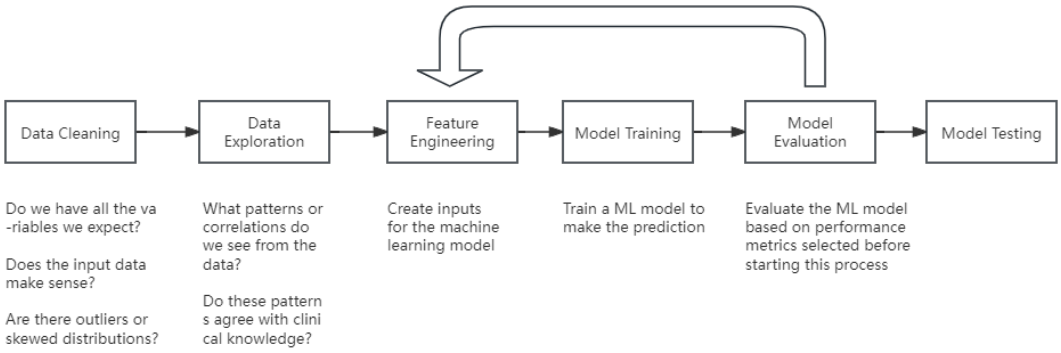

Figure 4.1: Work flow of data cleaning and machine learning model building

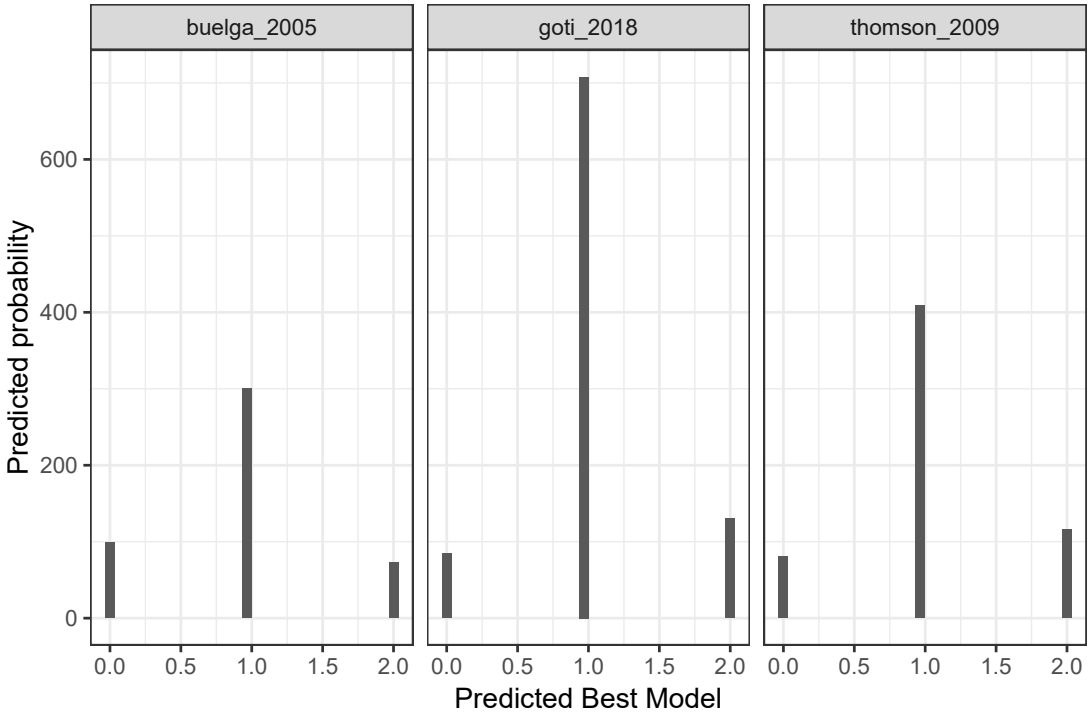

Figure 4.2: The performance of classification ML model. 0-buelga_2005; 1-goti_2018; 2-thomson_2009.

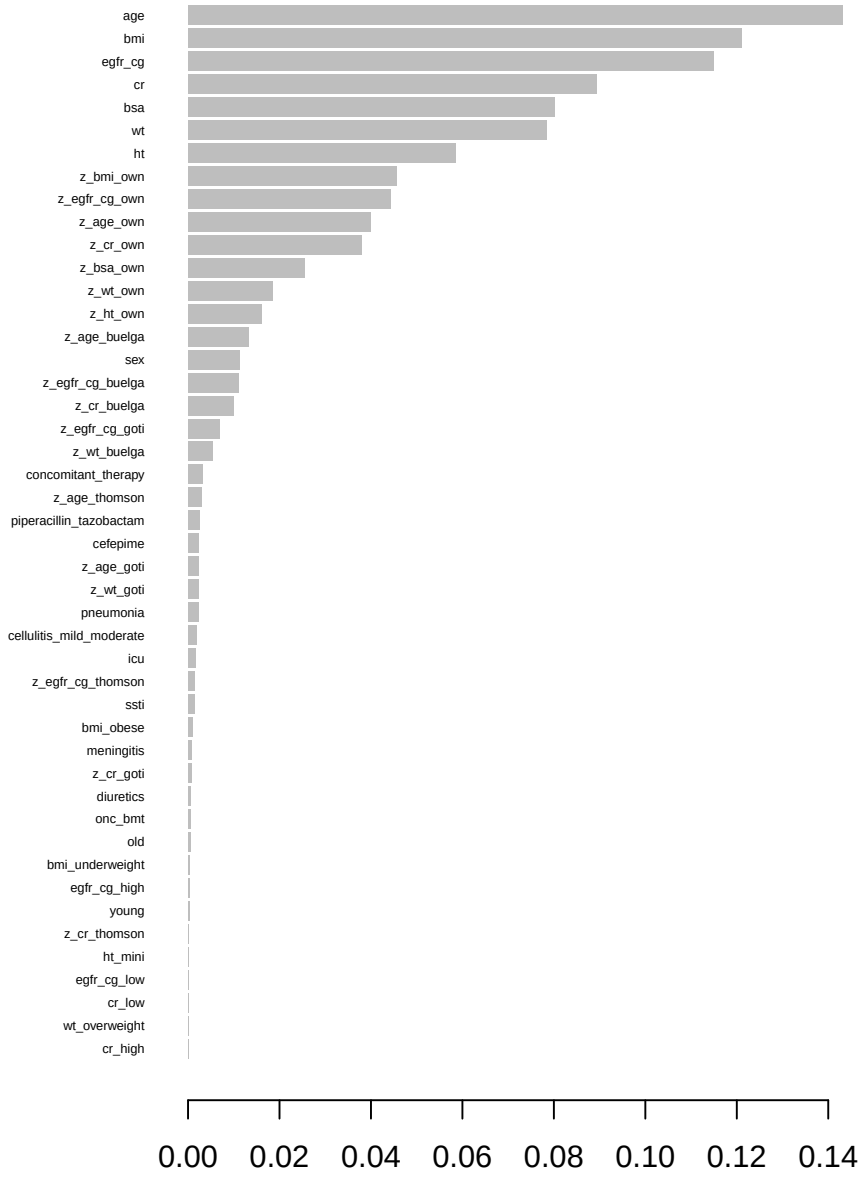

Figure 4.3: The importance of patients features

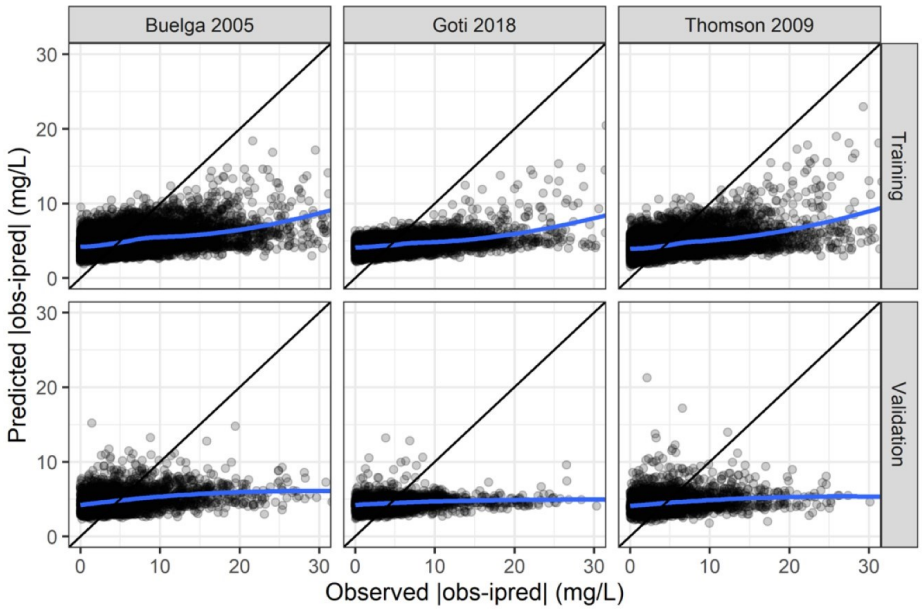

Figure 4.4: The performance of regression ML model

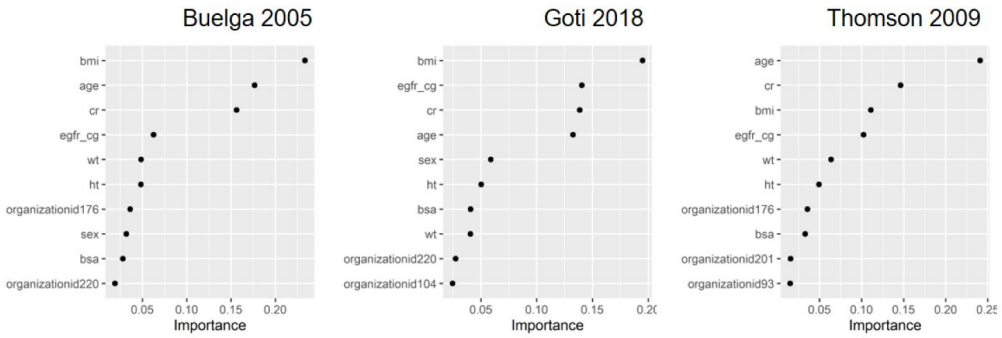

Figure 4.5: The importance of patients features

Bibliography

[1] J. P. Telles et al., "Optimization of Antimicrobial Stewardship Programs Using Therapeutic Drug Monitoring and Pharmacokinetics-Pharmacodynamics Protocols: A Cost-Benefit Review," Ther Drug Monit, vol. 45, no. 2, pp. 200–208, Apr. 2023, doi: 10.1097/FTD.0000000000001067.

[2] E. A. Poweleit, A. A. Vinks, and T. Mizuno, "Artificial Intelligence and Machine Learning Approaches to Facilitate Therapeutic Drug Management and Model-Informed Precision Dosing," Ther Drug Monit, vol. 45, no. 2, pp. 143–150, Apr. 2023, doi: 10.1097/FTD.0000000000001078.

[3] D. S. Buelga, M. del Mar Fernandez de Gatta, E. V. Herrera, A. Dominguez-Gil, and M. J. García, "Population pharmacokinetic analysis of vancomycin in patients with hematological malignancies," Antimicrob Agents Chemother, vol. 49, no. 12, pp. 4934–4941, Dec. 2005, doi: 10.1128/AAC.49.12.4934-4941.2005.

[4] V. Goti, A. Chaturvedula, M. J. Fossler, S. Mok, and J. T. Jacob, "Hospitalized Patients With and Without Hemodialysis Have Markedly Different Vancomycin Pharmacokinetics: A Population Pharmacokinetic Model-Based Analysis," Ther Drug Monit, vol. 40, no. 2, pp. 212–221, Apr. 2018, doi: 10.1097/FTD.0000000000000490.

[5] A. H. Thomson, C. E. Staatz, C. M. Tobin, M. Gall, and A. M. Lovering, "Development and evaluation of vancomycin dosage guidelines designed to achieve new target concentrations," J Antimicrob Chemother, vol. 63, no. 5, pp. 1050–1057, May 2009, doi: 10.1093/jac/dkp085.

[6] L. L. Vercio et al., "Supervised machine learning tools: a tutorial for clinicians," J. Neural Eng., vol. 17, no. 6, p. 062001, Nov. 2020, doi: 10.1088/1741-2552/abbff2.

[7] D. W. Uster et al., "A Model Averaging/Selection Approach Improves the Predictive Performance of Model-Informed Precision Dosing: Vancomycin as a Case Study," Clin Pharmacol Ther, vol. 109, no. 1, pp. 175–183, Jan. 2021, doi: 10.1002/cpt.2065.

[8] A. Chan, R. Peck, M. Gibbs, and M. van der Schaar, "Synthetic Model Combination: A new machine-learning method for pharmacometric model ensembling," CPT Pharmacometrics Syst Pharmacol, vol. 12, no. 7, pp. 953–962, Jul. 2023, doi: 10.1002/psp4.12965.

[9] J. H. Hughes and R. J. Keizer, "A hybrid machine learning/pharmacokinetic approach outperforms maximum a posteriori Bayesian estimation by selectively flattening model priors," CPT Pharmacometrics Syst Pharmacol, vol. 10, no. 10, pp. 1150–1160, Oct. 2021, doi: 10.1002/psp4.12684.

[10] J. E. Black, J. K. Kueper, and T. S. Williamson, "An introduction to machine learning for classification and prediction," Family Practice, vol. 40, no. 1, pp. 200–204, Feb. 2023, doi: 10.1093/fampra/cmac104.

Chapter 5

General Discussion and Summary

This multifaceted research initiative encompasses a comprehensive approach to precision antibiotic dosing in patients with hematologic malignancies, with a particular focus on beta-lactam antibiotics and the utilization of C-RP as a pivotal biomarker. The study unfolds in three distinct but interconnected parts, each designed to address specific challenges encountered in antibiotic therapy within this population. Chapter two provides crucial insights into the impact of CAR-T therapy on biomarker and antibiotic PK levels, facilitating refined infection management strategies for this specific patient population. Chapter three establishes a quantitative framework through PK-PD modeling, unraveling the intricate interplay between meropenem exposure, CRP dynamics, and clinical outcomes. Lastly, chapter four introduces an innovative approach utilizing machine learning to recommend precise vancomycin dose regimens, particularly in scenarios where conventional PK models encounter challenges.

The findings of this thesis underscore the critical importance of a personalized approach to antibiotic management in patients with hematological malignancies. By leveraging biomarkers and innovative computational techniques, clinicians can make more informed decisions, ensuring that patients receive the most effective and tailored treatment regimens. This research represents a significant step forward in the pursuit of precision medicine in the context of hematological malignancies and lays the foundation for further advancements in this critical area of healthcare.

Moving forward, future research endeavors could explore the integration of all three chapters' findings into a unified decision support system. Additionally, expanding the scope to incorporate a broader range of antibiotics and biomarkers, as well as validating the models in larger patient cohorts, could further enhance the applicability and impact of this research in clinical practice. Furthermore, considerations for regulatory approval and practical implementation should be addressed to facilitate the translation of these findings into routine patient care. This research paves the way for a more precise and effective approach to antibiotic therapy, ultimately benefiting patients with hematologic malignancies.

Appendices

Abbreviations

Short Form	Full Name
AIC	Akaike information criteria
AKI	Acute Kidney Injury
ALL	Acute Lymphoid Leukemia
AML	Acute Myeloid Leukemia
AUC	Area Under the Curve
BSI	Bloodstream Infection
CAR-T	Chimeric Antigen Receptor T Cell
CI	Continues Infusion
CKD-EPI	Chronic Kidney Disease Epidemiology Collaboration
CL	Clearance
CLCr	Creatine Clearance
CLL	Chronic Lymphoid Leukemia
Cmax	Peak Concentration
Cmin	Trough Concentration
CML	Chronic Myeloid Leukemia
Cox PH	Cox Proportional Hazard
C-RP	C-reactive Protein
CRS	Cytokine Release Syndrome
Css	Steady-state Concentration
CV	Coefficient of Variation
eGFR	estimated Glomerular Filtration Rate
EUCAST	European Committee on Antimicrobial Susceptibility Testing
FN	Febrile Neutropenia
HAP	Hospital-Acquired Pneumonia
IC50	Half-maximal Inhibitory Concentration
ICANS	Immune Effector Cell-Associated Neurologic Syndrome
IDSA	Infection Disease Society of America
IL-6	Interleukin-6
IL-8	Interleukin-8
IPRED	Individual predictions
IWRES	Individual Weighted Residuals
kin	Generation Constant
kout	Degradation Constant
LC-MS/MS	Liquid Chromatography Tandem Mass Spectrometry
LOQ	Limits of Quantification
MDR	Multi-drug Resistant
MIC	Minimum Inhibitory Concentration
MIPD	Model-informed precision dosing

Short Form	**Full Name**
ML	Machine Learning
MM	Multiple Myeloma
NHL	non-Hodgkin Lymphoma
OFV	Objective Function Valuess
pcVPC	prediction corrected Visual Predictive Checks
PD	Pharmacodynamics
PK	Pharmacokinetics
PTA	Probability of Target Attainment
RSE	Relative Standard Errors
SE	Standard Errors
TDM	Therapeutic Drug Monitoring
UTI	Urinary Tract Infection
V	Volume of Distribution